



CEOS Intercalibration of Ground-Based Spectrometers and Lidars

Final Report
Overview of Scientific Results

Version 3.1
May 2013

DOCUMENT PROPERTIES

Title	CEOS Intercalibration of Ground-Based Spectrometers and Lidars: Final Report
Reference	CEOS-IC-FR
Issue	3
Revision	1
Status	Final
Date of issue	01/05/2013
Document type	Report

	FUNCTION	NAME	DATE	SIGNATURE
LEAD AUTHOR	Project coordinator	M. Van Roozendael	01/05/2013	
CONTRIBUTING AUTHORS	Team Leaders	Ulf Köhler Gelsomina Pappalardo Esko Kyrö Alberto Redondas Folkard Wittrock Aldo Amodeo Gaia Pinardi		
REVIEWED BY	ESA project officer	Thorsten Fehr		
ISSUED BY	Project coordinator	Michel Van Roozendael		

DOCUMENT CHANGE RECORD

Issue	Revision	Date	Modified items	Observations
0.0	00	Nov. 2012	Template	Creation of document
1.0	00	Dec. 2012	All input integrated	Draft for internal review
2.0	00	Dec. 2012	Revised by all partners, Brewer part completed	Submitted for ESA review
3.0	00	Mar. 2013	Final version, after implementation of changes following ESA review	Final document

3.1	01	May 2013	Minor corrections added	Final (corrected)

Table of Content

Executive summary

The ESA CEOS Intercalibration project concentrated on important calibration activities addressing three key components of the ground-based network ground-truthing capacity in Europe, namely the Dobson/Brewer network of ozone spectrophotometers, the aerosol lidar EARLINET network and the UV-Vis MAXDOAS technique for air quality remote-sensing.

Dobson: Seven ESA-funded campaigns and four regular RDCC-E intercomparisons have been carried out since 2009 covering a wide range of atmospheric conditions and allowing to characterize the properties of the Dobson instrument and their differences to the Brewer spectrophotometer. It was found that the standard Dobson with its current calibration level (traced back to the World Primary Standard D083) measures about 1% lower ozone than the standard Brewer with somewhat larger but explainable differences at low sun, high ozone and high turbidity. A key outcome of the projet is that the Izaña site was found to be adequate for absolute calibrations of both types of spectrophotometers using the Langley Plot method. The resulting calibrations are comparable to those commonly performed at Mauna Loa using the World Primary Standard D083.

Brewer: Seven Brewer calibration campaigns and 65 calibrations were performed involving 40 instruments. Three types of campaigns were conducted: (1) absolute Langley calibrations at Izaña, (2) Nordic campaigns focusing on stray light effects and (3) routine calibration transfer at Arosa and Huelva. Due to restrictions on the maintenance of the WRT, the RBCC transferred its own calibration since 2011. The travelling reference stability has been checked before and after each campaign demonstrates a long term precision of 0.25%. The current status of the Brewer network is that all of the operative instruments are in the ±2% range, 80% within 1% range and 66% showing a perfect agreement of 0.5% after two years calibration period. The straylight effect was characterized during the campaigns and this was used to develop an instrumental model suitable for corrections. Furthermore the application of the Langley calibration to Dobson and Brewer together with the analysis of different absorption coefficients derived from the ACSO initiative gives encouraging results solving the Brewer-Dobson discrepancies when the Bremen cross sections are used. Further work is needed to extend these results including the study of the temperature dependence of the retrieved ozone.

UV-Vis MAXDOAS: The CINDI campaign has been very successful in achieving its observational and scientific objectives. A large data set of ground-based *in-situ* and remote sensing observations of NO_2, aerosol and other pollutants has been collected under various meteorological conditions and air pollution loads. Detailed analyses have been performed showing in particular that MAXDOAS NO_2 and O_4 DSCD measurements agree within 5–10% and HCHO measurements within 15%. Tropospheric NO_2 columns and surface concentrations derived from MAXDOAS agree within 15%, and within 25% with NO_2 lidar and in-situ NO_2 data. MAXDOAS AOD retrievals are in good agreement with AERONET and extinction profiles are consistent with ceilometer measurements. A major outcome of CINDI was to provide the necessary first steps towards harmonization of MAXDOAS measurements, and key recommendations for the building of ground-based networks suitable for the validation of future atmospheric Sentinels.

EARLINET: the European Aerosol Research Lidar NETwork, established in 2000, is the first coordinated lidar network for tropospheric aerosol study on the continental scale. It includes 27 lidar stations distributed over Europe. Six intercomparison measurement campaigns were carried out in between 2009 and 2012: EARLI09, ALI09, SOLI10, ROLI10, SPALI10 and AQUILI12. EARLI09 addressed the intercomparison of the five reference lidar systems from Hamburg, Munich, Potenza and Minsk allowing to establish a standardized calibration procedure. The following campaigns allowed to check the performances of most of the EARLINET systems. In total, 21 lidar systems (18 from EARLINET) have been successfully intercompared. Where necessary problems were analysed and adequate solutions found, resulting in a major consolidation of the network homogeneity.

Summary of activities in 2012

This document summarizes activities and achievements during the third part of the ESA CEOS Intercalibration project. The period covered by this report extends from February 2012 until October 2012.

Dobson activities

As part of the activities of the Regional Dobson Calibration Center for Europe (RDCC-E) three campaigns were organized in the third period of the project; one funded as a regular Dobson intercomparison by the DWD RDCC-budget, two of them funded by this project: MOHp 2012 (DWD funding), Arosa 2012 and Izaña 2012 (both funded by ESA). The continuation of refurbishment of Dobson No. 14 from Norway, the complete refurbishment of Italian Dobson No. 47 and the participation in three campaigns enabled to intensify and to deepen the knowledge and experience of the new Dobson operator and technician M. Heinen.

In addition the RDCC-E representative participated in the Quadrennial Ozone Symposium, in a meeting of International Ozone Commission (IO3C) and in the workshop of the WMO SAG (Scientific Advisory Group) for Ozone in Toronto from August 27 to September 5, 2012. Discussions and negotiations were started on the relocation of available Dobsons and their refurbishment incl. electronic upgradings. The upcoming issue concerning the closure of important ozone and climate monitoring stations and its consequences were intensively discussed. In addition the uncertain future of the global Dobson calibration system was addressed.

Brewer activities

During this reporting period the main activities of the RBCC-E are not directly related with the campaigns supported by the project. As is stated on the previous reports the Regional Brewer calibration Center transfer the calibration from the World Reference Triad in Toronto due the doubts about the maintenance of the World Triad the WMO scientific advisory group (WMO-SAG) authorized to RBCC-E to transfer his own calibration obtained by Langley. The efforts in this reporting period were concentrated in to obtain this absolute calibration and to transfer it to the campaigns. The second event is the publication of new absorption coefficients by the University of Bremen who have a large impact on the ozone calculation. The evaluation of how this new measurements affect to the Dobson and Brewer ozone calculation and the implications on the calibration transfer were analysed in this period.

Two campaigns were organized with the participation of the RBCC-E during the third period of the project: Arosa 2012 and the absolute calibration at Izaña 2012 both with the participation of the RDCC-E. The results of the Nordic campaigns, presented in the previous reports, were used to develop a Stray light correction algorithm. During the QOS-2012 the main findings of the project were presented in a four-poster and an oral presentation. Some of this poster and presentations are submitted for publication

UV-Vis MAXDOAS activities

During this last part of the CEOS ICal project, UV-Vis MAXDOAS activities concentrated on the campaign exploitation of the CINDI campaign data sets, with a focus on HCHO and aerosol retrievals. Already started during the previous reporting period, the HCHO DSCD intercomparison study has been continued and finalized resulting in a paper published in AMT. A comprehensive sensitivity study was performed to investigate the sensitivity of HCHO retrievals to changes in DOAS analysis settings and input data sets. The study highlighted the role of cross-correlation effects involving Ring effect, O_4, BrO and HCHO absorption cross-sections as well as the DOAS closure polynomial. Optimised retrieval settings were proposed to minimize such correlation effects. Furthermore, systematic and random uncertainties were estimated for typical observation conditions. The largest systematic errors were found to be related to the Ring effect and to the uncertainties in HCHO and O_3 absorption cross-sections. Overall, the systematic uncertainty on HCHO DSCD retrieval was found to be of the order of 20% with a weak dependence on the solar zenith angle. For scientific grade instruments (high throughput, low noise systems), the error budget is dominated by systematic error sources, while for noisier mini-DOAS type of instruments both systematic and random uncertainties contribute at the same level. One concludes that scientific grade instruments can provide high quality HCHO DCSD measurements at high temporal resolution (less than 30 minutes), while less sensitive mini-DOAS instruments can still be used to retrieve HCHO but with reduced temporal resolutions.

A second focus during this part of the project was on aerosol retrieval. Based on comparisons with coincident lidar measurements performed by RIVM during CINDI, it was found that the vertical structure of the boundary layer as retrieved from 4 MAX-DOAS instruments is in good qualitative agreement with backscatter profiles from Ceilometer data, especially for BIRA and IUPHD instruments. Likewise the AOD was found to be is in good agreement with sunphotometer measurements for most groups. Each of the algorithms and different approaches developed by the CINDI participants have their own advantages and shortcomings (in terms of vertical resolution, robustness, etc) and more work is definitely needed to converge towards a harmonised algorithm for MAXDOAS aerosol processing.

EARLINET calibration activities

Three measurement campaigns were planned, with three Italian lidar stations: Lecce, Napoli and L'Aquila, but only one was performed, because of system falilure. The AQUILI12 intercomparison measurement campaign was performed with the lidar system in L'Aquila. The intercomparison measurement campaigns allowed to compare the performances of the lidar system, applying the standard methodology used in the lidar system intercomparison and allowed to understand the reasons of failures and individuating the way to solve them. In addition, the automated and centralized calculus system was implemented and used in order to obtain and compare not only the pre-processed lidar range corrected signals, but only the optical products (aerosol and extinction backscatter coefficient) from the data measured during the several intercomparison campaigns.

1 Introduction

1.1 Scope of this document

This document is the second progress report of the CEOS Intercalibration of Ground-Based Spectrometers and Lidars project. It summarizes activities performed and results obtained from February 2012 until Octobre 2012.

1.2 Acronyms and abbreviations

ACSG	Atmospheric Composition Subgroup of the CEOS-WGCV
BAS	British Antarctic Survey
BIRA-IASB	Belgian Institute for Space Aeronomy
Cal/Val	Calibration and Validation
CEOS	Committee on Earth Observation Satellites
CNR-IMAA	Consiglio Nazionale delle Ricerche- Istituto di Metodologie per l'Analisi Ambientale
CNRS-SA	Service d'Aéronomie du CNRS
DMB	Daumont – Malicet – Brion (new ozone absorption coefficients)
DOAS	Differential Optical Absorption Spectroscopy
DWD	Deutscher Wetterdienst (German National Meteorological Service)
EARLINET	European Aerosol Research Lidar Network
EARLINET-ASOS	European Aerosol Research Lidar Network - Advanced Sustainable Observation System
ENVISAT	Environmental Satellite
EO	Earth Observation
EOS	(NASA's) Earth Observing System
ERS-2	European Remote Sensing Satellite-2
ESA	European Space Agency
ESRIN	European Space Research Institute
EUMETSAT	European Organisation for the Exploitation of Meteorological Satellites
FFT	Fast Fourier Transform
FP7	Seventh Framework Preogramme of the European Commission
FTIR	Fourier Transform Infrared Radiometer
GAW	Global Atmospheric Watch
GEO	Geostationary orbit
GEOSS	Global Earth Observation System of Systems
GMES	Global Monitoring of Environment and Security
GOME	Global Ozone Monitoring Experiment
IGACO	Integrated Global Atmospheric Chemistry Observations IGOS Theme
IGOS	The Integrated Global Observing Strategy
INTA	Instituto Nacional de Técnica Aeroespacial
IOS	International Ozone Services
IO3C	International Ozone Commission
IUP	Institute of Environmental Physics
KNMI	Royal Netherlands Meteorological Institute
MAXDOAS	Multi-Axis DOAS
METOP	Meteorological Operational satellite programme

MOHp	Meteorological Observatory Hohenpeissenberg
MPI	Max-Planck-Institute
Mu-range	Relative optical path of the sunlight through the ozone layer
NASA	National Aeronautics and Space Administration
NDACC	Network for the Detection of Atmospheric Composition Change
OMI	Ozone Monitoring Instrument
QA	Quality Assessment
RDCC-E	Regional Dobson Calibration Centre for Europe
RT	Radiative Transfer
SAG Ozone	Scientific Advisory Group for Ozone (WMO)
SCIAMACHY	SCanning Imaging Absorption spectroMeter for Atmospheric CartograpHY
SOO-HK	Solar and Ozone Observatory Hradec Kralove
SOW	Statement of Work
SZA	Solar Zenith Angle
TOMS	Total Ozone Mapping Spectrometer
WCWG	CEOS Working Group on Calibration and Validation
WDCC	World Dobson Calibration Centre
WMO	World Meteorological Office
WPDS	World Primary Dobson Spectrophotometer D083
WOUDC	World Ozone and Ultraviolet Data Center

1.3 Applicable documents

[AD1] CEOS Intercalibration of Ground-Based Spectrometers and Lidars, Proposal in response to ESRIN/RFQ/3-12340/08/I-EC (ref. this proposal).

[AD2] ESA/ESRIN Statement of Work, ref. SOW: CEOS Intercalibration of ground-based spectrometers and lidars, GMES-CLVL-EOPG-SW-08-0002.

[AD3] Draft Contract, Appendix 2 to ESRIN/RFQ/3-12340/08/I-EC

1.4 Reference Documents

[RD1] Vicarious Calibration and Geophysical Validation Functional Baseline, GMES-SPPA-EOPG-TN-06-0001.

[RD2] ENVISAT Calibration and Validation Plan, PO-PL-ESA-GS-1092.

[RD3] IGOS – Integrated Global Observing Strategy: Atmospheric Chemistry, http://ioc.unesco.org/igodpartners/atmosphere.htm

[RD4] CEOS – Working Group on Calibration and Validation: Satellite missions/ Atmospheric Chemistry, http://www.oma.be/NDSC_SatWG/Documents/SatelliteMissionsPlanning(30 Nov2007)_A4.pdf

2 Work achieved in 2012

2.1 Dobson and Brewer calibration activities

2.1.1 Activities of the Regional Dobson Calibration Center for Europe (RDCC-E) at Meteorological Observatory Hohenpeissenberg (MOHp)

In the third phase of the project two campaigns were performed, which were funded by ESA; one campaign was organized as official WMO RDCC-E intercomparison funded by DWD:

- Brewer Service 2012 and MOHp 2012 (Hohenpeissenberg, Germany, June 11 – 22): In May the annual, regular Brewer Service was performed and used as occasion to compare field and reference Dobsons (No. 104 and 064) and Brewers (No. 10 and 17). During MOHp 2012 three Dobsons from Greece, Czech Republic (secondary reference Dobson No. 074 from the RDCC-E partner observatory Hradec Kralove) and from Italy (completely refurbished before) had undergone a regular calibration service. In addition the traveling primary standard Dobson No. 065 from the WDCC at NOAA (Boulder, USA) was invited with an operator to perform the overdue calibration of the European regional standards Dobson No. 064 and D074 (normally every two years, the last calibration took place during the Irene 2009 campaign in South Africa) towards the calibration level of the world standard. These activities were funded by DWD.

- Arosa 2012 (Switzerland, July 16 to 27) was again a combined campaign for calibration of Dobsons in the European network (3 Dobsons from Switzerland) and for comparison of the reference Dobson and Brewer in Europe.

- Izaña 2012 was conducted from September 24 to October 12. The main objective was the joint absolute calibration after Langley of the regional standard Dobson No. 064 and the Spanish Brewer triad (RBCC-E) at the Izaña Observatory.

Another important activity was the participation in the Quadrennial Ozone Symposium, the meeting of the Internation Ozone Commission and the workshop of the WMO SAG for Ozone, which took place in Toronto from August 27 to September 5. The activities and results of this project were presented in two posters (Köhler et al, 2012a, Köhler et al. 2012b) to a great number of ozone and climate scientists. A suggestion was made by the RDCC-E to the IO3C and the WMO SAG for Ozone to extend the calibration cycle of field Dobsons from four to five years. It was decided, that an official proposal should be submitted to the IO3C. This extension should reduce the amount of work in times of shrinking financial and personnel resources. The results of the calibration campaigns during the past two decades and the upgrading of a considerable number of Dobsons allows this reduction of calibration frequency without any deterioration of the quality of the long-term data records in the Dobson network.

Several presentations and information during informal talks the problems of the monitoring network and of the Dobson calibration system were brought up. Financial cuts, reduction of staff, closure of facilities and/or retirement of experts will endanger the future activities.

The refurbishment of the Dobson No. 14 (electronically upgraded in 11/2011) was continued at MOHp, as some unexpected intrumental shortcomings were detected and had to be resolved. One Dobson (Italian Dobson No. 47) has got an electronical, optical and mechanical upgrading before its participation during MOHp2012. These activities and the three campaigns were successfully

used to increase the knowledge, capabilities and experience of the new Dobson operator and technician M. Heinen. Intense investigations of intrumental properties, however, have not been possible yet.

Results of Brewer Service and MOHp 2012

The regular Brewer service in May 2012 revealed a very good agreement of all participating instruments (Figure 1). This is in contrast to the results of former comparisons and also to the Arosa 2012 and Izaña 2012 findings afterwards. The principal difference between Dobsons and Brewers of about 1% (Dobson values lower) could not be seen in this comparison with the IOS Brewer No. 17, calibrated against the Canadian Brewer triad in Toronto. All instruments match within ±1 %.

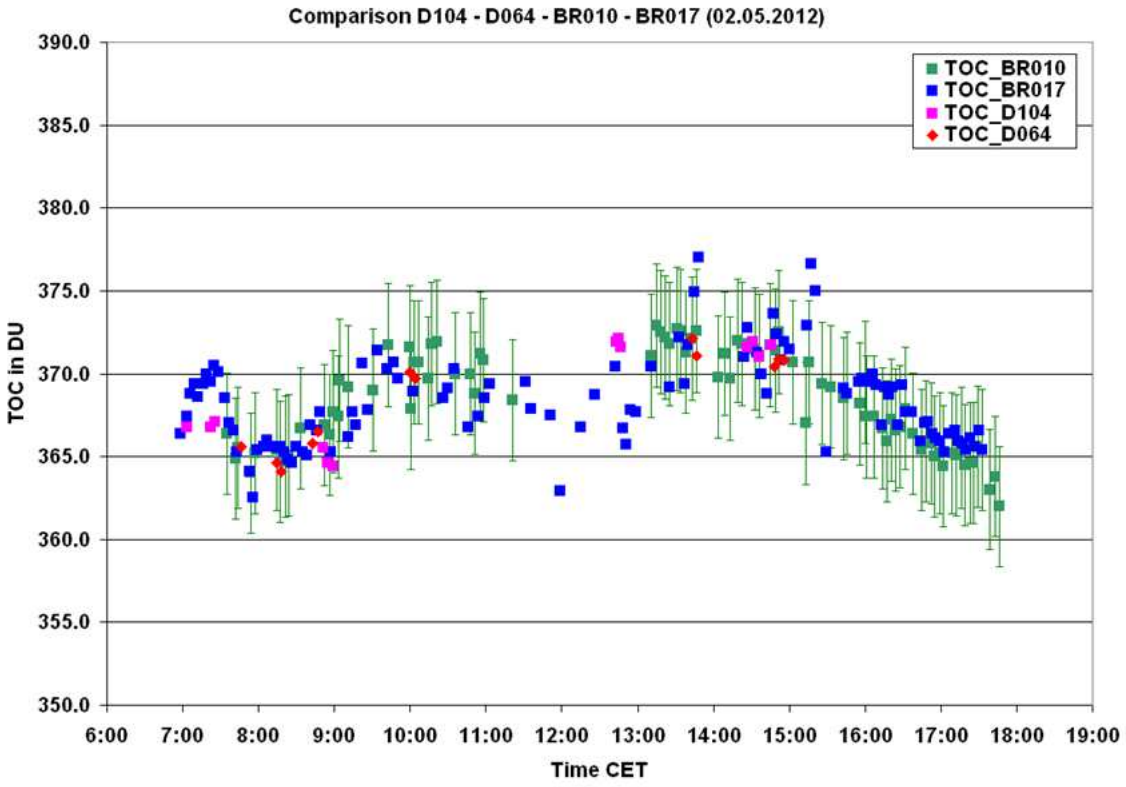

Figure 1: *Comparison of D104 (field instr.), D064 (reference), BR010 (field instr.) and BR017 (reference) on May 2, 2012. Green bars represent the ± 1%-difference.*

This leads to the conclusion, that the calibration level of the traveling standard BR017 has been changed since the last calibration service and the El Arenosillo campaign in 2011.

Beside the normal calibration service for the European field Dobsons the work package of MOHp 2012 comprises also the calibration of the regional standard Dobsons towards the primary standard. The regular intercomparison of these three standard Dobsons D064 (regional standard for Europe), D065 (traveling primary standard) and D074 (second regional standard for Europe) confirms the good agreement within the ±1 limit for well calibrated instruments. The small difference of less than 1% between D064 and D065 (Figure 2) is probably caused by the fact, that D064 is originally calibrated against the World Primary Standard D083 (NOAA) during Irene 2009, whereas the recent D065 comparison with D083 revealed a small difference in the same order, which was not corrected (as less than 1%).

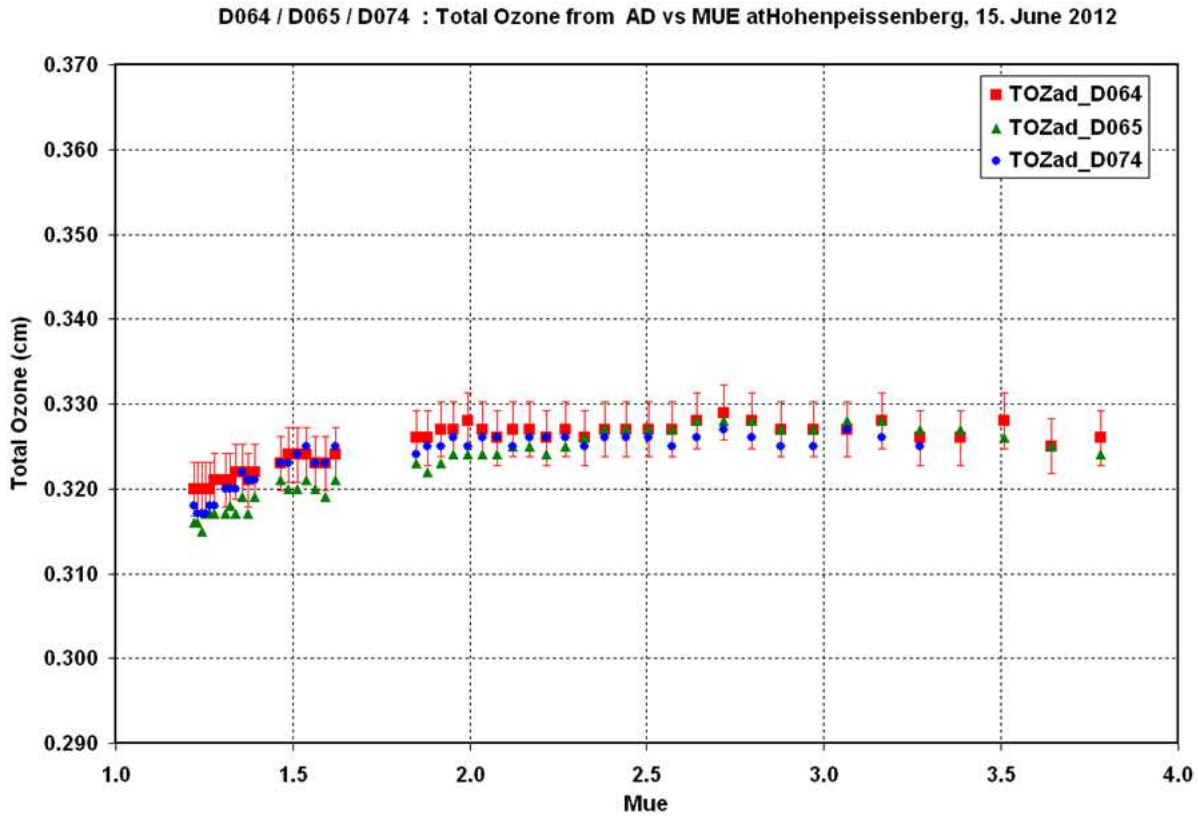

Figure 2: *Comparison of the standard Dobsons D064, D065 and D074 on June 15, 2012. Red bars represent the ± 1%-difference.*

In any case the recent comparisons between all the standard Dobsons confirm, that their calibration levels are consistent and comparable. Thus it is assured, that the transfer of the World Standard's calibration level at least into the European Dobson network has been successfully achieved during the past years or even decades. Figure 3 confirms, that the regional standard Dobson No. 64 at the RDCC-E Hohenpeissenberg has been a very stable instrument in the past three decades. Most of the initial calibrations showed a difference between the D064 and the standard instrument of less than 1%. The three absolute calibrations after the Langley method confirm this good and stable performance.

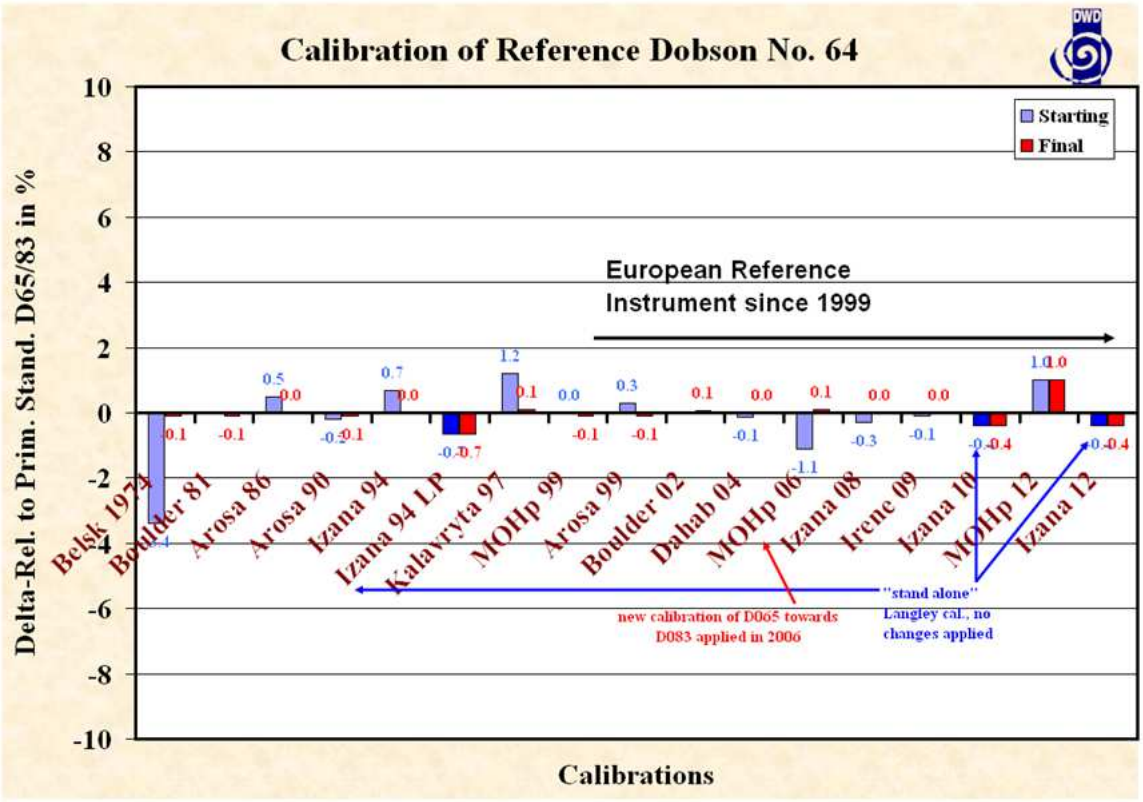

Figure 3: *Comparisons and absolute calibrations of the standard Dobsons D064 since 1974.*

Results of Arosa 2012

The combined Dobson-Brewer comparison campaign in Arosa in July had two Dobson-relevant objectives.

- Calibration service for the three Swiss Dobsons (regular RDCC-E task)
- Comparison between standard Dobson and standard Brewer (work package of the ESA-project)

Figure 4 summarizes the results of MOHp 2012 and Arosa 2012 for the Dobsons in the European ozone monitoring network, compared with Dobson No. 064. Only one Dobson from Italy exceeded the 1%-limit for a well calibrated Dobson. The reason for the 1 % difference of the Hohenpeissenberg standard Dobson D064 compared with the primary standard D065 (and the 0.7% difference of the D074 as well) is already explained in the section before.

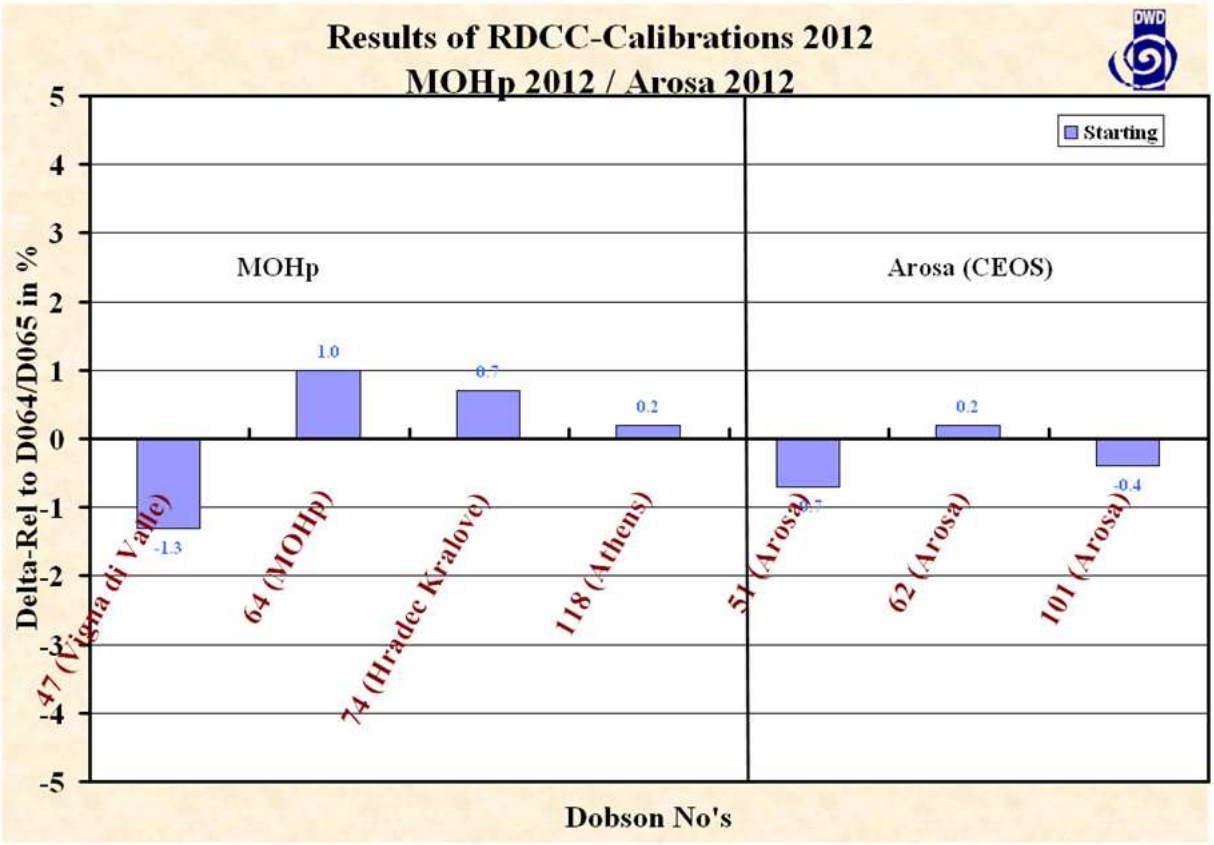

Figure 4: *Results of the regular European Dobson campaigns in 2012. Relative difference between field and standard Dobson at the beginning of a campaign (initial calibration).*

The results of the second goal, the comparison between standard Dobson No. 064 and standard Brewer No. 185, is shown in Figure 5, which confirms the findings of the ESA campaigns in the years before. A principal mean difference of approx. 1% (Dobson lower than Brewer) can be seen in almost all comparisons of the RDCC-E and RBCC-E standard instruments. Sometimes higher differences, as seen in Sodankylä, can be explained by the different temperature dependencies of the specific absorption coefficients and differences in the calculation of Mu.

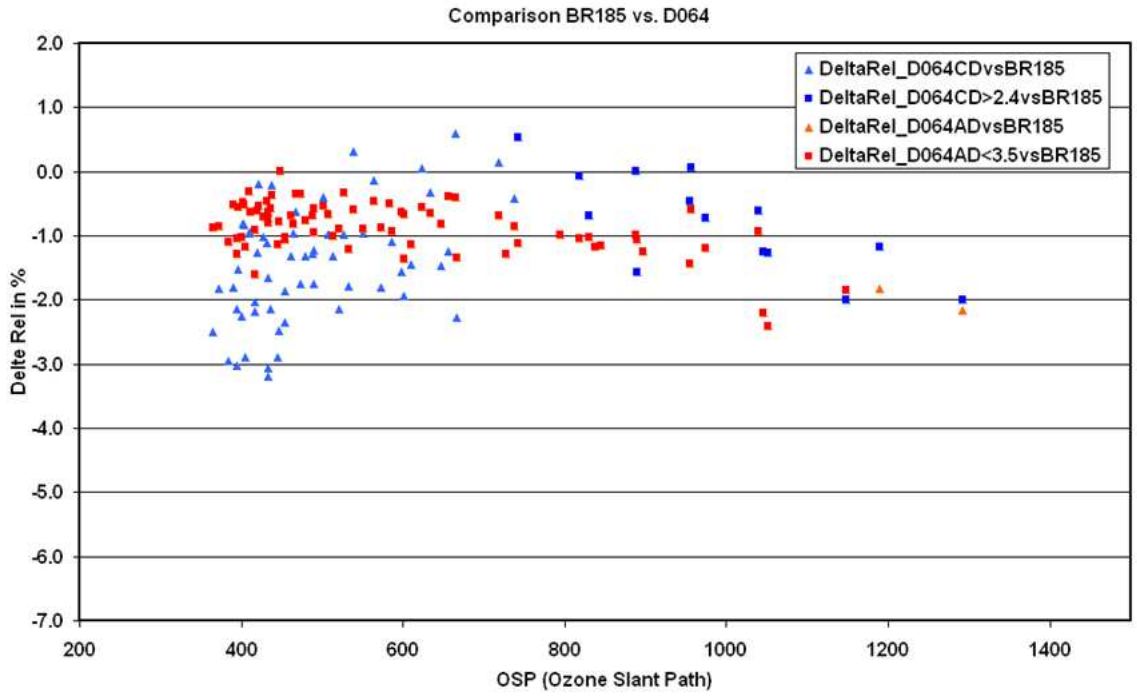

Figure 5: *Comparison of D064 (combined AD- and CD-wavelength pairs in different Mu-ranges) and BR185 during Arosa 2012, relative difference in % against Brewer values.*

Results of Izaña 2012

Absolute calibration campaigns after the Langley method were already carried out at the Izaña Observatory of the Spanish Meteorological Service AEMET on Tenerife in 2008 (together with the World Primary Standard D083 and the second Regional European Standard D074, Hradec Kralove, Czech Republic) and in 2010 (only with the Hohenpeissenberg Regional European Standard D064).

These campaigns unfortunately suffer from not optimal weather conditions and problems of the Dobson No. 064 with RFI (radio frequency interference) caused by the neary-by TV-antenna. The campaign in 2012, however, could be performed under much better conditions. Perfect atmospheric conditions (very clear, no diurnal variation in ozone) were found on four of 12 days and together with some more days with acceptable conditions approximately 700 out of 900 observation cycles could be used for the Langley method to determine the extraterrestrial constants of the Dobson No. 064.

Figure 6 shows the so-called Langly Plot for all appropriate measurements in the Mu-range between 1.2 and 2.4. The obtained ETC-correction of 0.38 for Nad, which represents the standard ozone observation in the double wavelength pairs A and D, stands for an average increase of the derived ozone value of about +0.6%. These results are similar to those of the two former campaigns at Izaña, although the conditions were not optimal.

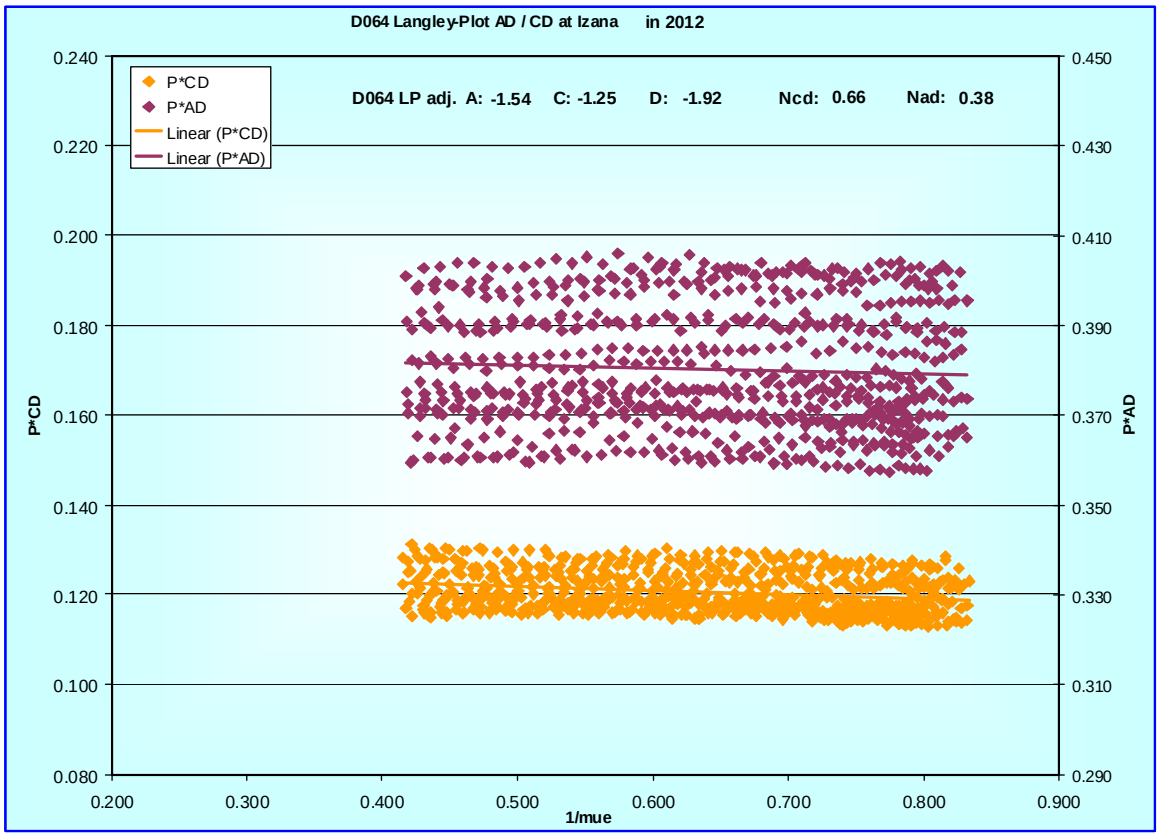

Figure 6: Comparison of D064 (combined AD- and CD-wavelength pairs in different Mu-ranges) and BR185 during Arosa 2012, relative difference in %.

The application of the Langley Plot-derived correction of +0.38 on the AD-observations can be seen in Figure 7. After the correction is applied the difference between Dobson and Brewer is reduced at least at higher sun. The straylight problems of the Dobson at lower sun is still significant, but could be improved, when the double CD wavelength pairs are used (not shown here). Private communication with Robert Evans from the WDCC at NOAA (Boulder, USA) confirms, that the Izaña results of the D064 absolute calibration are comparable with the D083 absolute calibration on Mauna Loa (Hawaii).

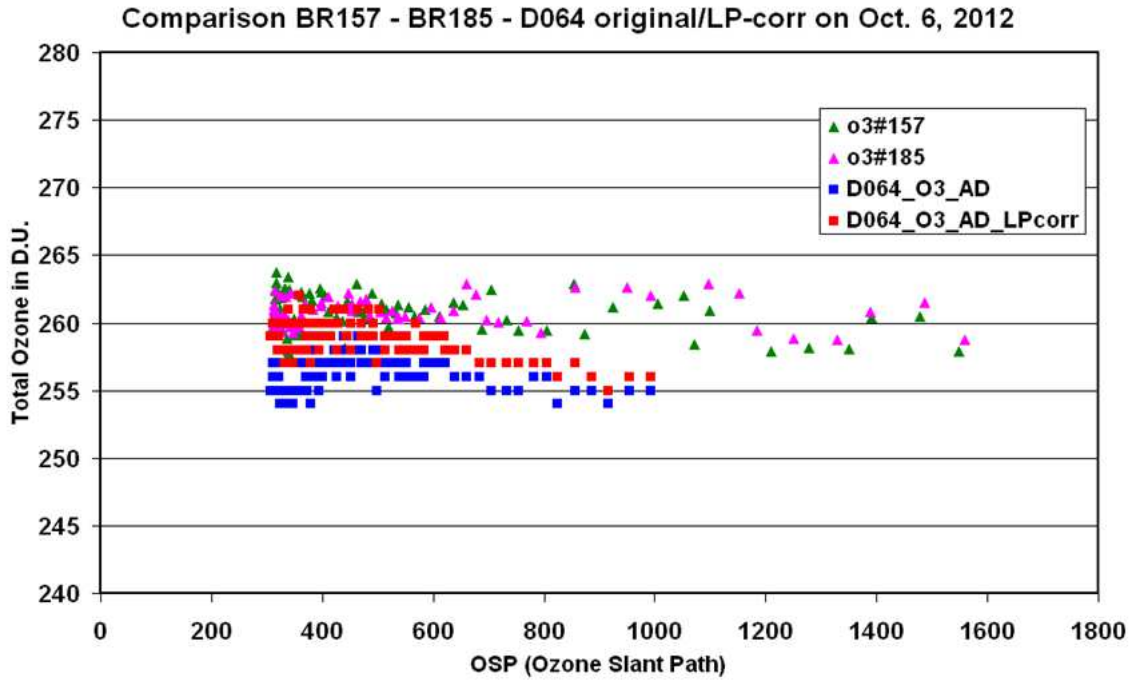

Figure 7: *Comparison of the standard Brewer instrument No. 157 and 185 with original and Langley Plot-corrected data of standard Dobson No. 064 at Izaña on October 6, 2012.*

2.1.2 Activities of the Regional Brewer Calibration Center for Europe (RBCC-E) at Izana and Nordic Brewer campaing activities (FMI)

The Brewer activities are divided in four sections; the first is dedicated to the reference triad maintenance and how we get the calibration and transfer the calibration to the campaigns. Second, we describe the calibration campaign at Arosa and the main results obtained. The third section is dedicated to the stray light, the developed model and the testing results using the 2011 campaigns data at Izaña and Sodänkylä. Finally we present the results of the Brewer-Dobson comparison at Arosa 2012 and the Langley campaign at Izaña with the application of the new ozone cross section calculations.

2.1.2.1 Calibration and Characterization of the RBCC-E Brewer triad

2.1.2.1.1 The link with the World Reference Triad. Absolute calibration.

The Regional Brewer Calibration Center for Europe (RBCC-E) was established at the Izaña Atmospheric Research Centre in 2003. It comprises three MkIII type Brewer spectrophotometers: a Regional Primary Reference (Brewers#157), a Regional Secondary Reference (Brewers#183) and a Regional Travelling Standard (Brewers#185). The calibration of the RBCC-E triad against the WBT was established through yearly comparison with the IOS travelling standard brewer #017 and checked with the Langley results at the station. In addition, during the calibration campaigns the RBCC-E travelling #185 is compared to other reference instruments. This reference instruments are: IOS travelling #017, the brewer #145 operated by Environment Canada (EC) and the Kipp & Zonen travelling reference #158. The two Canadians instruments IOS and EC provide a direct link to the world triad. The lasts "world travelling reference triad to European reference triad" calibration transfer were performed in September 2010 and July 2011 (Figure 8).

Since the beginning 2012, due to internal reorganization of AEMET, the technical maintenance of RBCC-E instruments will be performed by Kipp & Zonen, Brewer manufacturer, and the link will be directly with the world triad in Toronto or by common Langley campaigns at Mauna Loa or IZO. Due the EC situation and the lack of funds of AEMET, only the RBCC-E will transfer its own absolute (Langley) calibration.

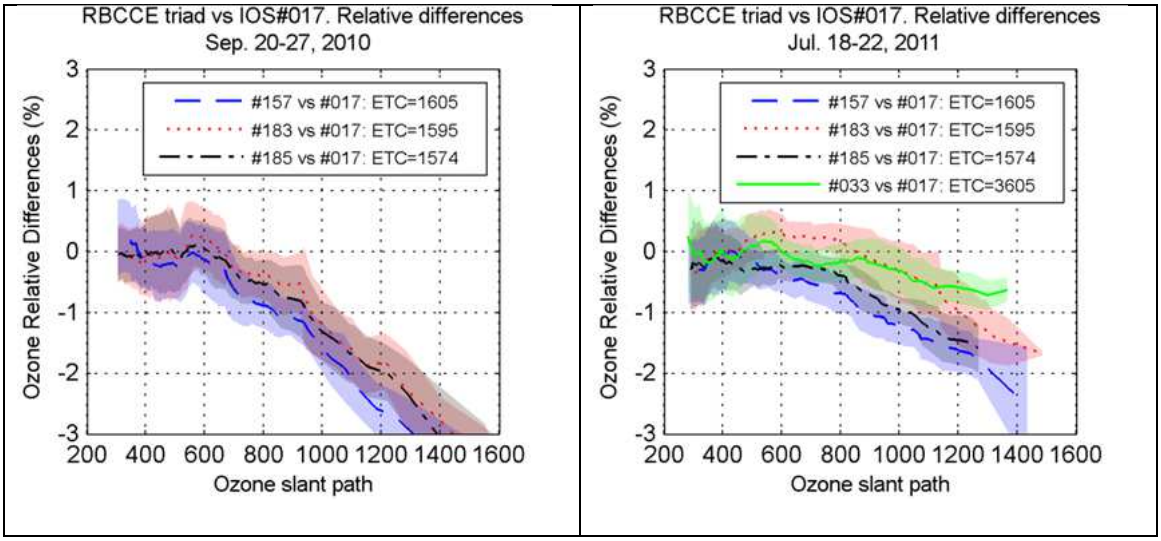

Figure 8: Comparison of the RBCC-E Brewer triad with respect to the travelling reference #017. It is showed ozone relative differences as a function of ozone slant path during the last two intercomparisons performed at Izaña in September 2010 (left, after Arosa 2010 intercomparison) and July 2011 (right, after El Arenosillo 2011 intercomparison). The agreement with the travelling is very good (less than .25%) in the ozone slant path range of 300-800 DU. Beyond 600 DU the stray light of #017 is pronounced and the comparison degrade reaching the 1% at 800 DU

In contrast to the Dobson spectrometer, the Langley methodology for the Brewer used by the World Reference Triad is not published. At RBCC-E we adapt the published Dobson methodology and the results were presented and discussed at several Brewer workshops (Redondas 2003, Redondas 2005, Ito et al, 2011). As we mention in the introduction, at the Arosa 2012 campaign we transfer the Langley calibration obtained at Izaña. Unfortunately, the Brewer #017 cannot participate to the campaign and we cannot compare our Langley calibration with the WRT. However, we can display a long-term comparison of the calibration transferred by IOS with the instrument #017 at Izaña, with the calibration obtained by Langley for the instrument #157. The agreement is quite good, always below 1% and usually less than 0.5% with no systematic differences. Is important to note that there isn't any change in the IOS transferred calibration since 2005, when the RBCC-E was established. A good example of how the Langley calibration can track properly instrumental changes is the case of Brewer 185. This instrument has suffered several modifications and adjustments after the Huelva campaign in June 2011. All this modifications can be clearly tracked with the Langley calibration record.

To assure the calibration of the triad, routinely calibrations are performed on a weekly basis at IZO and the frequency of instrumental tests performed at the calibration has been increased from yearly to monthly basis. On the other hand, the measurement schedule has been adapted to maximize the Langley observations, reducing the spectral UV and Umkehr measurement program. This routinely calibrations are reported on the RBCC-E web showing the temporal evolution of the instrumental performance (an example of such reports during 2012 year can be found

here). As a result of this maintenance and continuous calibration work we achieve long term agreement between the instruments of the triad with a precision of less than 0.25%.

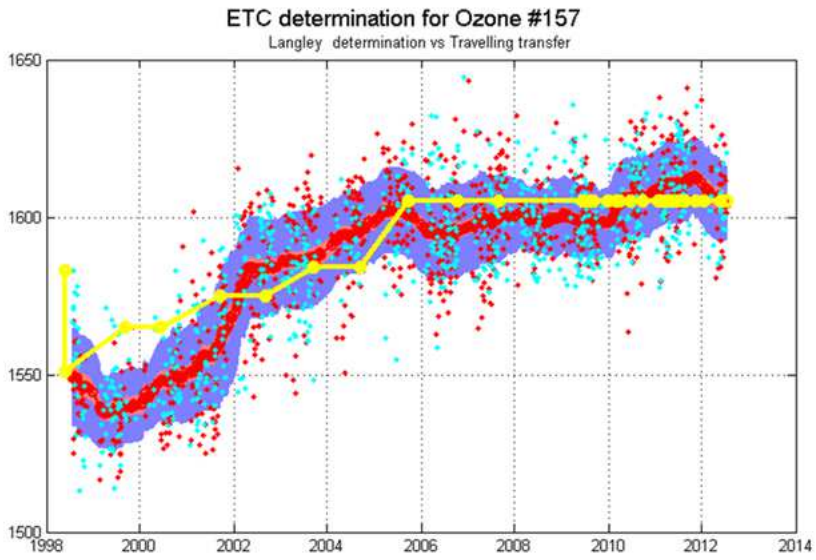

Figure 9: Long term comparison 1998-2012 of Extraterrestrial constant transferred from the travelling instrument #017 and the Langley obtained at Izaña for the reference instrument #157. The yellow line are the calibration transferred from #017 every year, the dots are the ETC for a particular Langley event (blue morning, red afternoon), the red line are the one month smooth ETC from the Langley and the red area the 95% confidence interval and the blue area the one standard deviation.

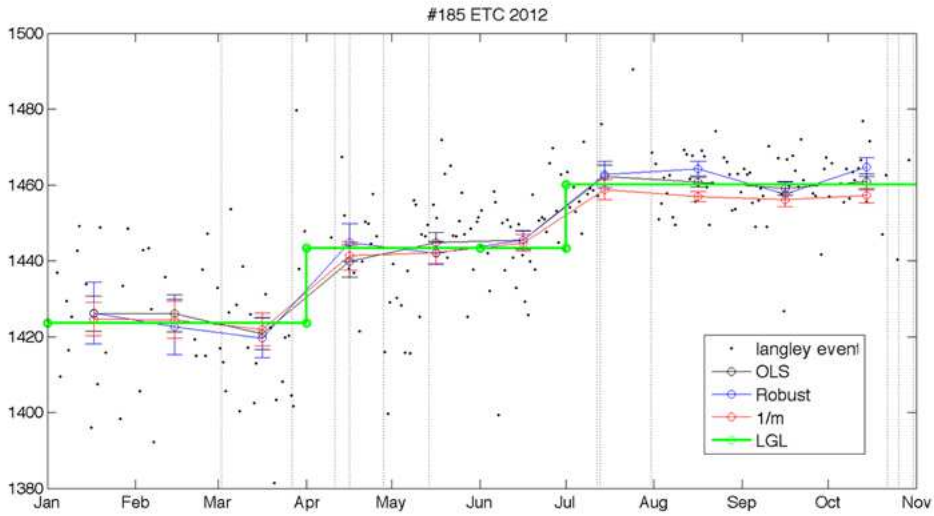

Figure 10: Langley analysis of the #185 during the 2012. The dots indicate the Langley events, the circles are the monthly mean with different regression methods: OLS ordinary least square, 1/m is the Dobson spectrometer regression and Robust is a robust estimation of the ETC. Finally the green line indicates the calibration adopted for this instrument.

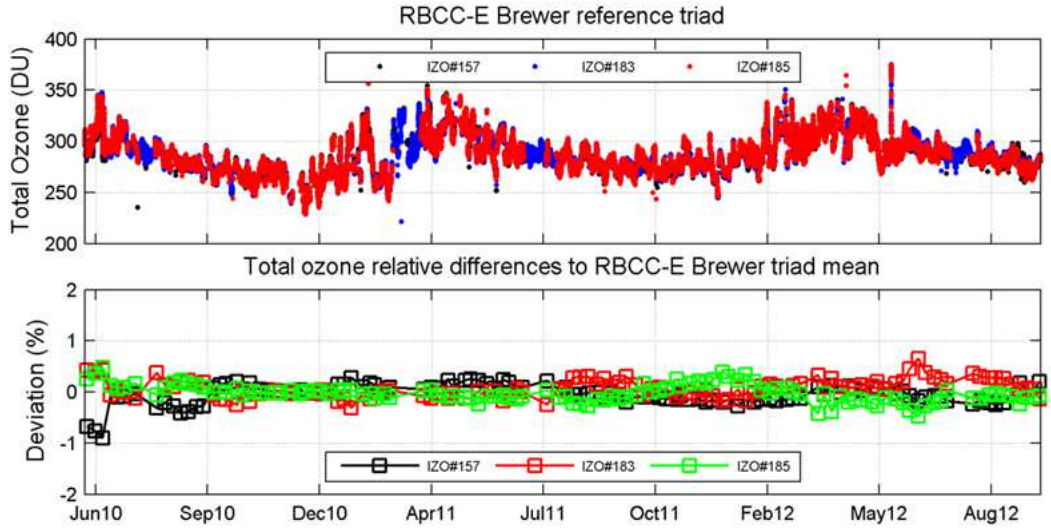

Figure 11: Long term weekly comparison of the RBCC-E triad, during the project.

2.1.2.1.2 The Travelling reference: calibration during the campaigns

The stability of the travelling standard is checked before and after the campaign by comparison with the other instruments of the triad, and, if possible, by performing a Langley analysis. All calibration reports are available from the Iberonesia webpage, http://www.iberonesia.net. Additionally, we provide also summaries of calibration results on the so called reference calibration checklists, a standard document developed during this project in cooperation with IOS and Kipp & Zonen. An example of this document is shown on Table 1.

Traveling Standard check list: Brewer#185	Description	Passed?		Value	Comments
		Y	N		
Calibration data	Intercomparison period			170-190/ 2012	
Reference of the traveling (Triad , RBCC-E,)	RBCC-E reference #185			RBCC-E	
Is traveling standard calibrated?		Y			IOS#017 (Jul/2011)
%diff. before travel	Ozone relative differences with respect to RBCC-E triad mean			-0.2+/-0.29	Days 175 to 190
%diff. after travel	Ozone relative differences with respect to RBCC-E triad mean			-0.1+/-0.25	Days 175 to 190
Instrument operation:					
HP/HG	Hp/Hg tests repeatable to within 0.2 steps	Y			
SH	SH shutter delay is correct				NAN

RS	Run/Stop test within +/- 0.003 from unity for illuminated slits and between 0.5 and 2 for the dark count	Y			
DT	Dead time is between 28 ns and 45 ns for multiple-board Brewers and between 16 ns and 25 ns for single-board Brewers		N	30/29	DT_{ref} 33 ns
SL R6	SL ratio R6 is within 5 units from calibration	Y		213/217	$R6_{ref}$ 218
SL R5	SL ratio R5 is within 10 units from calibration	Y			

Table 1: Travelling Reference Checklist

The travelling reference performance during this reporting period is shown in Figure 12 (the correspondent values are found in Table 2). Even despite the instrumental changes during 2012, the instrument do not change during the travel, and the comparison with the RBCC-E triad is lower than 0.2%. As we mentioned before the calibration scale for the Brewer 185 were obtained by Langley.

.

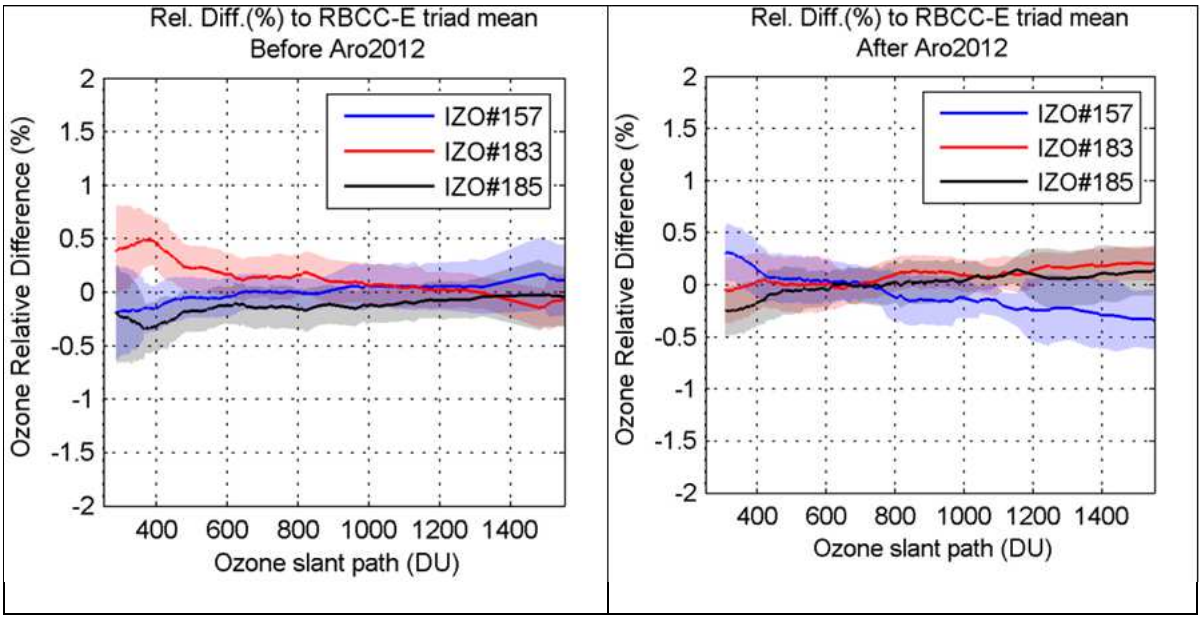

Figure 12: Near-simultaneous ozone ratios of RBCC-E standard Brewers (serial no. #157, #183 and #185) to the mean of all instruments are shown before (left) and after (right) Arosa 2012 intercomparison

	#157	#183	#185	Nobs
Before	-0.1 +/- 0.29	0.3 +/- 0.32	-0.2 +/- 0.29	467
After	0.1 +/- 0.30	0.0 +/- 0.27	-0.1 +/- 0.25	302

Table 2: Mean ozone relative difference (DU) and standard deviation of the RBCC-E Brewer reference triad against the mean of all instruments before and after Arosa2012 intercomparison campaign.

year	*month*	*smooth*	*OLS*	*Robust*	*1/m*
2011.	*12.*	*1425.*	*1425.*	*1429.*	*1424.*
2012.	*1.*	*1423.*	*1423.*	*1420.*	*1422.*
2012.	*2.*	*1424.*	*1428.*	*1423.*	*1425.*
2012.	*3.*	*1415.*	*1413.*	*1413.*	*1412.*
2012.	*4.*	*1442.*	*1446.*	*1447.*	*1446.*
2012.	*5.*	*1444.*	*1442.*	*1440.*	*1441.*
2012.	*6.*	*1446.*	*1447.*	*1447.*	*1446.*
2012.	*7.*	*1453.*	*1464.*	*1456.*	*1457.*

Table 3: Langley: Monthly mean Extraterrestrial constants for the brewer #185 obtained by Langley by four different regression methods (OLS ordinary Least Square, Robust and the Dobson regression 1/m

Figure 13: Brewer Instruments at Arosa 2012 #185 , #067, #158 and #066.

2.1.2.2 The Arosa calibration campaign

This seventh intercomparison campaign was a joint exercise of the Regional Dobson Calibration Center for Europe (RDCC-E) and the Regional Brewer Calibration Center for Europe (RBCC-E) in collaboration with the Arosa Lichtklimatisches Observatorium (LKO) of Meteo Swiss during the period July 16 to 27, 2012. Nine brewer instruments managed by 11 experts of five countries participated to the campaign (Table 4). The instruments were compared with the RBCC-E travelling reference Brewer#185 for ozone and with the QASUME unit for UV, European UV reference from the World Radiation Center (WRC). The maintenance of the instruments was performed by IOS (International Ozone Services). Brewer #017 do not participate in the campaign, and so, the data labelled as 017 on the plots were obtained by the optics of the #017 installed on the #072 instrument.

Institution	Name	Brewer	Country
IOS	Martin Stanek Volodya Savastiouk	#017-MKII	Canada
LKO	René Stübi, Herbert Schill, Werner Siegrist	#040-MKII #072-MKII #156-MKIII	Switzerland
AAB :	Henri Diemoz	#066-MKII	Italy
URO. University of Rome	Giuseppe R. Casale	#067-MKII	Italy
K&Z	Wim Roeterdink	#158-MKIII	Netherland
WRC	Julian Gröbner Gregor Huelsen	#163-MKIII	Switzerland
AEMET-IARC	Alberto Redondas Juan J. Rodriguez Virgilio Carreño Marta Sierra	#185-MKIII	Spain

Table 4: Participating instruments at the Arosa 2012 intercomparison campaign.

During this campaign we introduced several improvements.

- The Arosa campaign was the first campaign processed in real-time, a provisional calibration being provided to all the participating instruments at the end of the campaign. This calibration can be considered final for most of them. The calibration reports are available online.

- A calibration history of the instruments was introduced, for the instruments present on previous campaigns. This allows an easy recalculation of the previous observations.

- The measurement schedule of the campaign was optimised and even with not ideal conditions we obtain 340 observations with the reference with many instruments reach the 80% of the potential measurements (Figure 14).

- The initial comparison, using the instruments' original calibration constants, shows a very good agreement, with most of the instruments inside the 1% level (6 of 8, see Figure 15).

- After the maintenance the agreement is very good for all the instruments. On the stray light free region all the instruments are inside the 0.5% range (Figure 16).

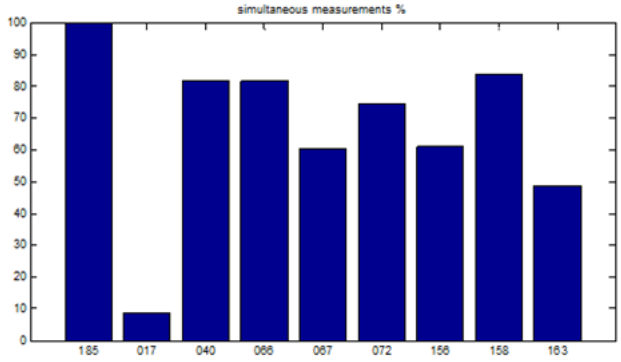

Figure 14: Percentage of simultaneous measurements of the different instruments of the campaign

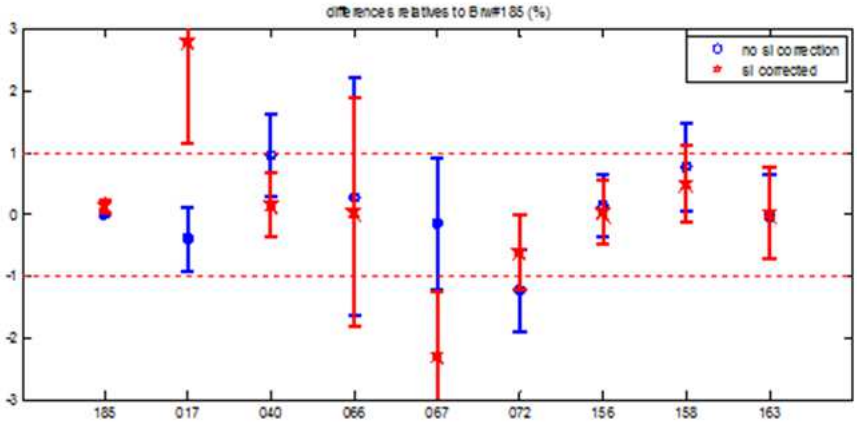

Figure 15: Ozone relative percentage differences of all Arosa 2012 participating instruments to RBCC-E travelling standard #185. Ozone measurements collected during the blind period have been reprocessed using the original calibration constants, with (red plots) and without (blue plots) SL correction. Error bars represent the standard deviation.With the application of the SL correction all the instruments agree within 1%.

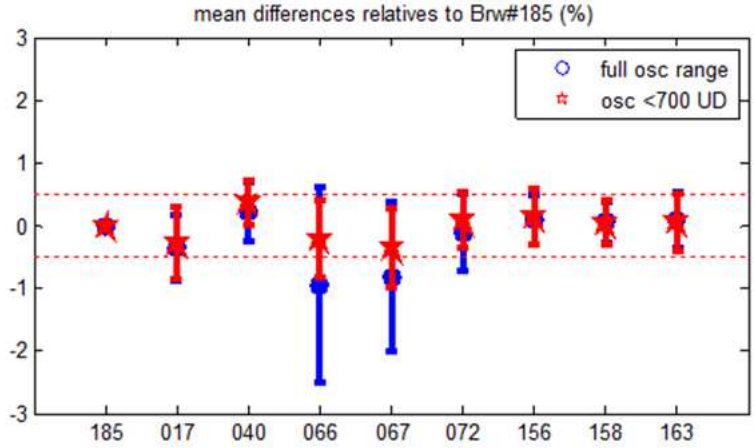

Figure 16:Total ozone final comparison, percentage ratio with the reference for all observations (blue) and only the stray light free range (Ozone Slant Column lower than 700 UD), all the instruments agree within +/- 0.5%. Note the pronounced stray light on the MK-IV #066 and #067.

2.1.2.3 Nordic Brewer campaign activities (the Arctic aspect of the ozone monitoring network)

Sodankylä campaign March 2011 and Izana campaign Oct-Nov 2011

Spectrometers are designed to isolate particular wavebands and suppress light of other wavelengths outside the band of interest. However, a small amount of light will always enter into the detector, not through the designed optical path, but through random scattering from the instrument optical components, housing and dust particles. Every spectrophotometer has stray light coming from outside the nominal measurement waveband. For Dobsons and single monochromator Brewers, which are basic instruments in the WMO ozone and UV monitoring network, the error introduced by stray light can be substantial, especially in the Arctic spring when the ozone slant path becomes very large due to large solar zenith angles and a thick ozone layer. To study this issue a long ozone slant path Intercomparison/Calibration campaign for Nordic Brewers and Dobsons was held at Sodankylä in March 8-24, 2011 and a follow-up campaign to extend calibrations to shorter ozone slant paths took place at Izaña observatory, Tenerife between October 28 and November 18, 2011.

During the active intercomparison periods, measurements were taken only when good conditions for sun or moon observations existed. Laboratory measurements using calibration lamps and Helium-Cadmium (HeCd) lasers were an essential part of both campaigns. The campaigns produced a high-quality database of total ozone and UV measurements and an accurate and up-to-date calibration and characterization of participating Brewers and Dobsons against the European standard instruments from RDCC-E and RBCC-E. We developed and present below a physics-based method to correct the stray light of single brewers using instrument characterization data and radiative transfer modelling. The method has been tested using independent data from the campaign. The key results have been presented in a poster at Quadrennial Ozone Symposium, in Toronto in August 2012, and also submitted for publication (Karppinen et al., 2012).

Data collected during the campaigns held at Sodankylä in Arctic spring conditions (March 2011) and at the subtropical Izaña observatory (November 2011) are considered, covering ozone slant paths from 360 to 2500 DU. The observations and the calibration checklist where the calibration results are summarized are available at the RBCC-E web page www.rbcc-e.org.

Brewer ozone retrieval

Brewer spectrophotometer total ozone retrieval is based on calculating weighted ratios of photon count rates resulting from the spectral intensities on four ozone wavelengths channels: F3 (λ3~310.0 nm), F4 (λ4~313.5 nm), F5 (λ5~316.8 nm) and F6 (λ6~320.0 nm). The weighting factors (powers) have been selected so as to minimize the effects of aerosols and SO2 (Kerr et.al., 1980). The double ratio, denoted as MS9 in the Brewer operating software, is calculated as

$$MS9 = 10^4 \times \log_{10}\left(\frac{F_5^{2.2} \times F_4^{0.5}}{F_6^{1.7} \times F_3}\right)$$

Total ozone column, MS11, is calculated from the MS9 through equation:

$$MS\,11 = \frac{MS\,9 - ETC}{\alpha\mu},$$

Where μ is the airmass factor and ETC and α are the weighted combinations of extraterrestrial and absorption coefficients, respectively. In principle, the absorption coefficient should be calculated

from a known absorption spectrum, currently Bass and Paur, (1995) and the extraterrestrial constant from a Langley plot. Often, however, these are transferred in intercomparison campaigns from well calibrated reference Brewers, in this work from the members of RBCC-E Brewer triad. Assuming individual count rate correction factors a_i for each channel, we arrive, after some arithmetic manipulation, at an additive correction β to double ratio MS9.

$$MS9_{ideal} = 10^4 \times \log_{10}\left(\frac{(a_5F_5)^{2.2} \times (a_4F_4)^{0.5}}{(a_6F_6)^{1.7} \times (a_3F_3)}\right)$$

$$= 10^4 \times \left[\log_{10}\left(\frac{F_5^{2.2} \times F_4^{0.5}}{F_6^{1.7} \times F_3}\right) + \log_{10}\left(\frac{a_5^{2.2} \times a_4^{0.5}}{a_6^{1.7} \times a_3}\right)\right]$$

$$= MS9_{single} + 10^4 \times \log_{10}\left(\frac{a_5^{2.2} \times a_4^{0.5}}{a_6^{1.7} \times a_3}\right) = MS9_{single} + \beta$$

To estimate β one need careful characterization of the instrument radiative transform code (in this case the *LibRadtran RT model*, freely available from the Internet). The most important issues in the instrument characterization are HeCd-laser measurement of the slit-functions and response functions of each channel. These measurements were made both in Sodankylä calibration laboratory and Izana calibration laboratory campaign during the said campaigns. In the following we demonstrate the method shortly with FMI single Brewer no. 037 measurements and calculations. After knowing the slit-functions and DS responses of B37 and an "ideal B37" with a triangle slit of the same half width as B37 it is possible to simulate the count rates Fi of above equation for both instruments and so estimate the correction factor β.

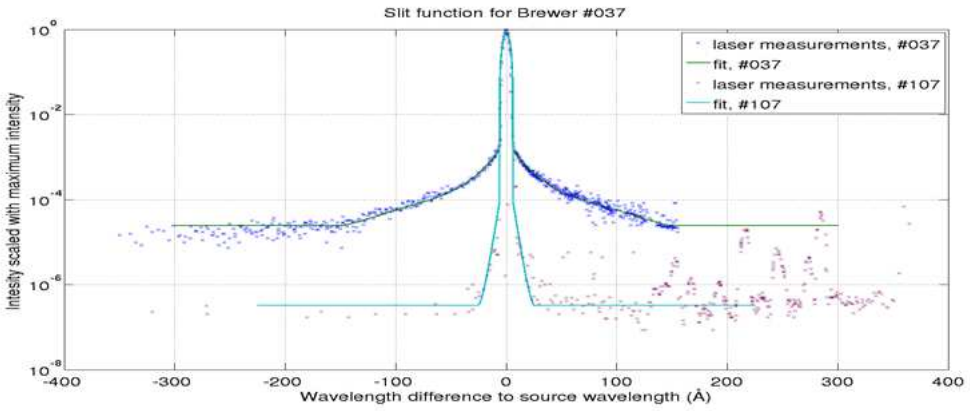

Figure 17. The slit functions of FMI Brewers B37 (single monochromator) and B107 (double monochromator) measured during Izana campaign demonstrate the straylight rejection difference between the two instrument types. However, in the calculations B107 was not used as a reference but an "ideal B37" with triangle slit function of same half width as real B37 but the straylight wings region zeroed were used.

.

Direct response

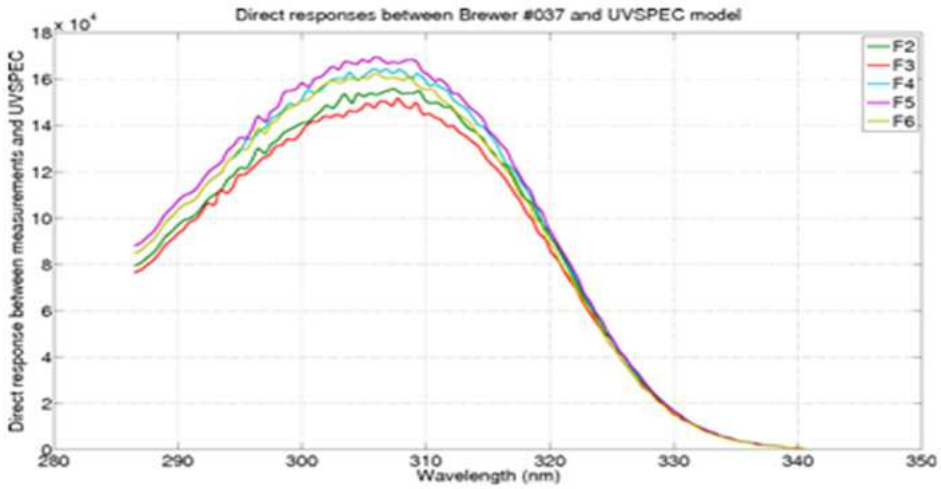

Direct response of each channel was not measured directly but obtained by first measuring the global response through the UV port at each channel and then simulating the (DS-Global) response difference with radiative transfer code.

Intensity ratios

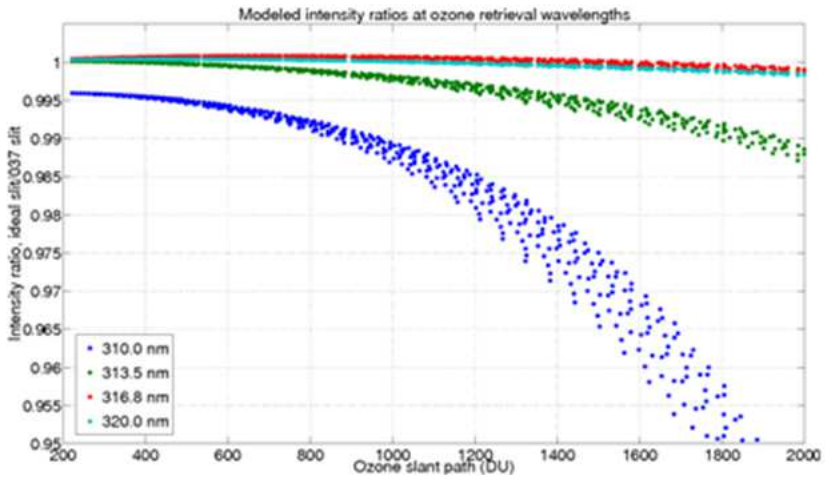

With known slit functions and DS responses it was then possible to calculate the intensity ratios between the "ideal B37" and real B37 for each of the ozone channels and hence obtain the additive correction β to MS9 shown below (Figure 18).

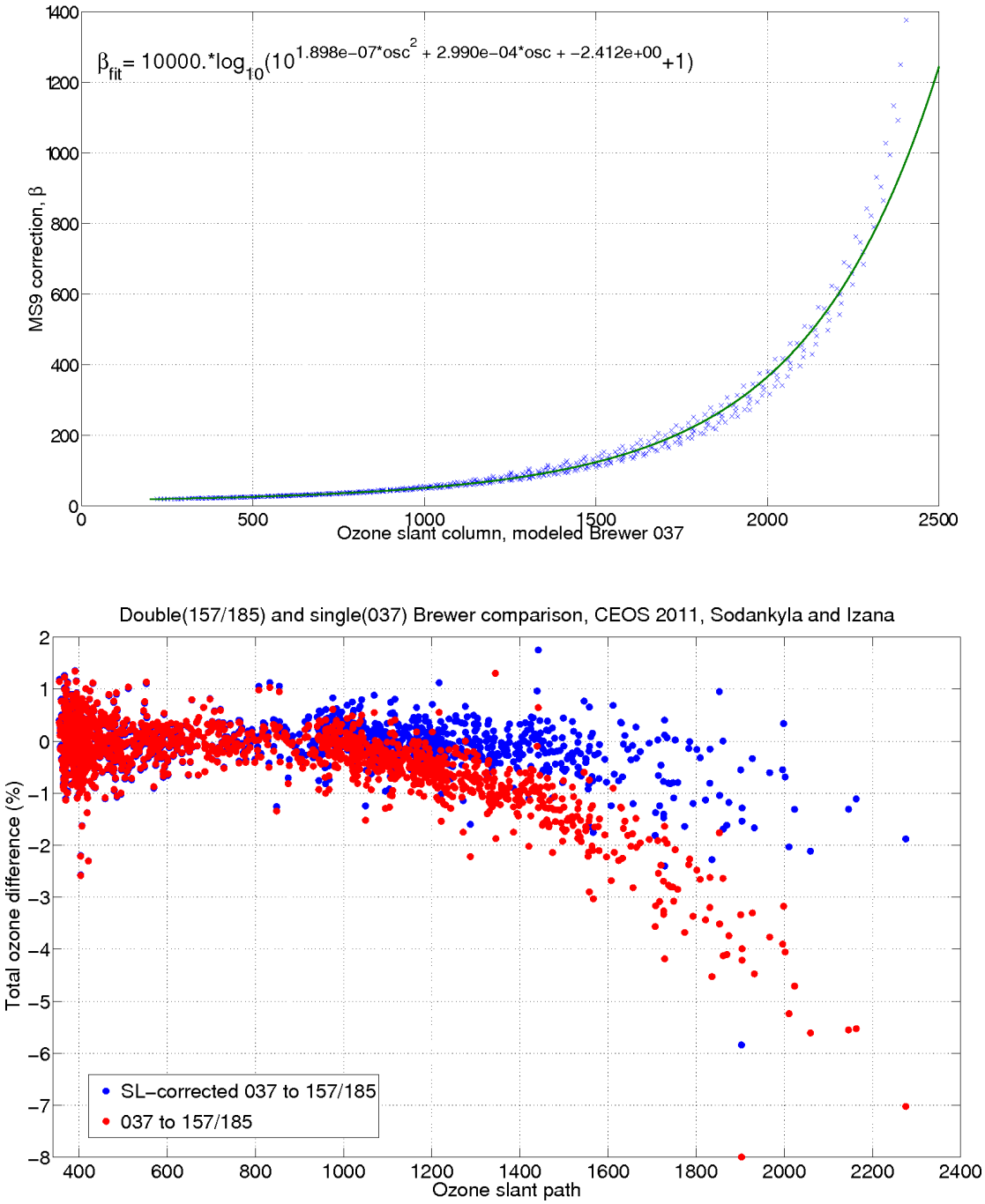

Figure 18: Upper plot) Correction coefficient β plotted as a function of ozone slant column and the corresponding exponential fit. Lower plot). Ratio between the Brewer no.37 and RBCC-E reference Brewer no.157 before (red) and after (Blue) stray light correction as a function of the ozone slant path. The method significantly improves the agreement in situation of large slant path.

Conclusions and suggested improvements

The early results look promising, but several questions require further study and development:

- The reconstructed DS responses for the ozone slits used for the model Brewer 037 are likely to differ from the real ones. In the continuation project the real DS responses for the ozone slits has to be measured.
- New measurements of slit-functions will be needed such that each slit will be measured separately in high resolution
- Comparison between the transfer method where the absorption coefficients are transferred from reference Brewer and the method where the absorption coefficient is calculated directly from the slit function and the ozone absorption spectrum belongs also to the future tasks.
- The new double Brewer 214 is going through testing and characterization measurements before lifting it on the roof beside Brewer 037. This tandem Brewer system is hoped to yield additional important data for evaluating/improving the correction system in long time operation.
- The biggest exercise for the future, however, is to put the system in real test with a large amount of data, applying the correction to the 25 year long Sodankylä ozone time series, and to study the effect of stray light error in late winter/spring ozone trends.

2.1.2.4 Brewer – Dobson Langley Calibration

The Brewer – Dobson Langley campaigns took place from 20 of September to 12 of October at the Izaña Observatory (IZO), with very good sky conditions. We obtained twelve good "Langley" days (Figure 19). The Langley days requires clear and stable atmospheric conditions. As shown, during these days the ultraviolet AOD, recorded at 340 nm by the CIMEL sun photometer, was below 0.05. The data set of this campaign is used to study the differences in Langley calibration between Brewer and Dobson.

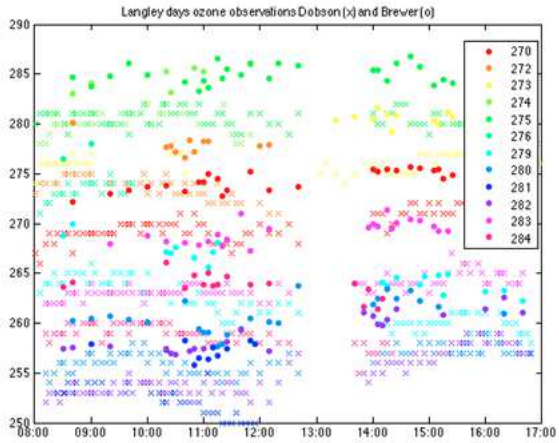

Figure 19: Individual Ozone simultaneous measurements recorded during the campaign by the Dobson (crosses) and Brewer (dots) during the campaign, the different days are represented by colour,

The comparison of Brewer and Dobson were in agreement with previous comparisons, with an underestimation of 1.5% of the Dobson respect to the Brewer (Figure 20). It's important to note that the reference for this calculation is the mean of Brewer and Dobson taken separately

$$ref(t) = \frac{\overline{Dobson}(t) + \overline{Brewer}(t)}{2}$$

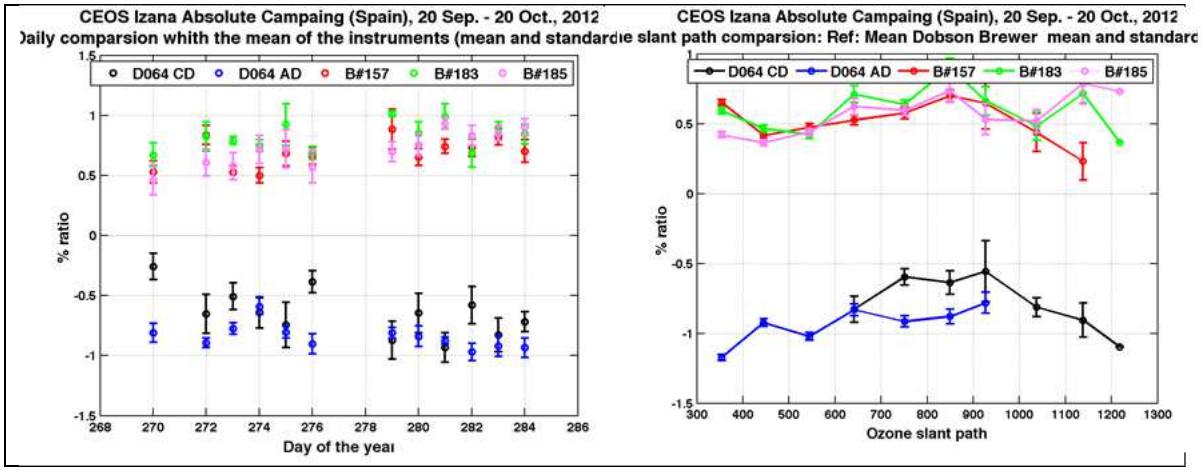

Figure 20: Daily mean (left) and Ozone slant path (right) total ozone Brewer and Dobson t comparison during the campaign. The percentage ration is represented: o3-ref/ref with the reference the mean of the three brewer instruments and the Dobson AD/CD pairs.

Despite the similarities on Dobson and Brewer algorithms, there are some differences concerning the Langley calibration of these instruments. In both instruments the ozone is calculated using the expression $O_3 = (F - ETC)/\mu\alpha$, where F is the Rayleigh corrected ratio of the measured UV intensities, μ is the airmass, α is the ozone absorption coefficient and ETC is the Extraterrestrial constant. With the requirement of constant ozone during the "Langley", the linear regression of the measured ratios on the air mass gives the ETC constant. In the case of the Dobson the ETC is included on F calculation Introducing an ETC correction ETC=ETCo+ETC and regressing $P = (F - ETC_o)/\mu$ by $1/\mu$ we obtain the required correction as the slope of the regression line. In the case of Brewer spectrophotometer the regression is performed for F over μ, and the ETC is the intercept of the resulting line. Both cases are illustrated in Figure 21.

As a part of the exercise, the RBCC-E also processes the Dobson Langley observations and compares the results with the data provided by the RDCC-E using near-simultaneous (within 5 minutes) data sets for Brewer and Dobson instruments. As expected, the results are comparable (Table 5) an estimation of the error were added to the RBCC-E evaluation; Table 6 shows a summary of the calculations. We performed some testing analysis using the Brewer observations: first we used the "Dobson" method, regressing the ratios on the inverse of ozone airmass, and then we compared the results with the results obtained using the "Brewer" method, which is regressing the ratios on air mass. Both methods yield to similar results, without any significant differences.

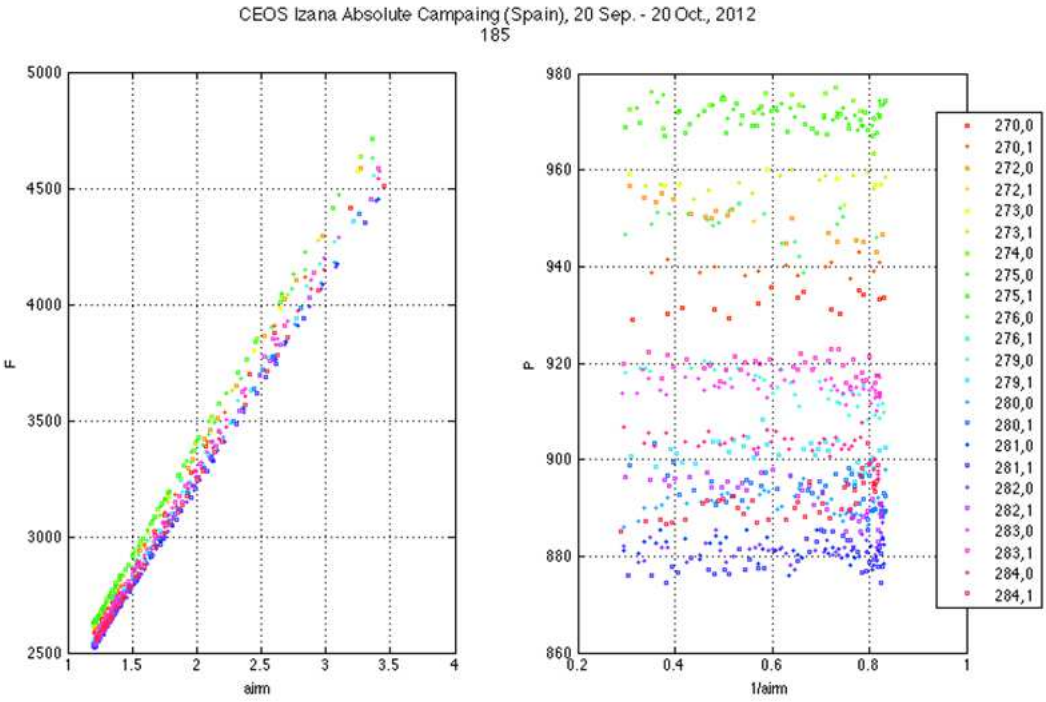

Figure 21: Langley plots for the Brewer 185 during the campaign. We show in the left panel the regression vs. mu and in the right panel the Dobson method P= F-ETC/nu vs. 1/mu

Day	CD	CD(*)	AD	AD(*)	C-D	C-D(*)	A-D	A-D(*)
270.25	0.96	0.99	-0.32	-0.31	0.60	0.63	0.25	0.25
270.75	0.08	0.08	1.08	1.08	0.44	0.44	0.59	0.54
272.25	1.23	1.25	0.10	0.10	0.83	0.88	0.68	0.68
273.25	0.70	0.70	-0.46	-0.46	0.31	0.31	0.02	0.12
273.75	0.05	0.09	0.50	0.50	0.47	0.46	-0.09	-0.09
274.25	1.59	1.59	-0.03	-0.03	1.21	1.21	0.56	0.56
275.25	0.96	0.96	-0.66	-0.66	0.57	0.57	-0.07	-0.07
275.75	-0.19	-0.19	0.21	0.21	0.19	0.19	-0.28	-0.40
276.25	1.39	1.39	-0.70	-0.70	1.01	1.01	-0.08	-0.08
279.25	1.28	1.28	0.96	0.96	0.90	0.90	1.51	1.55
279.75	-0.15	-0.15	0.33	0.33	0.21	0.21	-0.24	-0.24
280.25	1.33	1.33	0.16	0.16	0.96	0.96	0.74	0.74
280.75	0.32	0.34	0.90	0.90	0.67	0.69	0.35	0.38
281.25	1.11	1.11	0.78	0.78	0.74	0.74	1.36	1.36
282.25	0.74	0.74	-0.69	-0.69	0.35	0.36	-0.13	-0.13
282.75	0.38	0.38	1.65	1.65	0.76	0.76	1.07	1.07

Table 5 RBCC-E and RDCC-E (with an asterisk) calculations for the double pair Langley. Note the dispersion of the results even with almost perfect weather conditions

	C	D	A	CD	AD	C-D	A-D
RBCC-E	-1.26	-1.92	-1.54	0.76	0.22	0.66	0.38
Err	0.04	0.08	0.06	0.06	0.08	0.14	0.13
RDCC-E	-1.25	-1.92	-1.54	0.77	0.22	0.66	0.38

Table 6: Mean of the Langley calculations from RBCC-E with the associated error and RDCC-E.

In order to obtain a successful Langley calibration both the atmospheric conditions and the instrument have to be stable. The stability of the instruments can be confirmed by the internal checks, whereas the dispersion in the Langley results is attributed to atmospheric variability. Hopefully the average of several events removes this variability and so we can derive the calibration of the instrument. If the instruments do not change and the variability on the ETC results is mainly due to atmospheric conditions, then the changes in ETC detected by different instruments Brewer or Dobson must be related. This is the case during the campaign. We show in Figure 22 the corrections on ETC for different instruments during the campaign. In the case of the Brewer-Dobson the coefficient of Determination is 0.65, slightly better in the case of Brewer-Brewer (0.79).

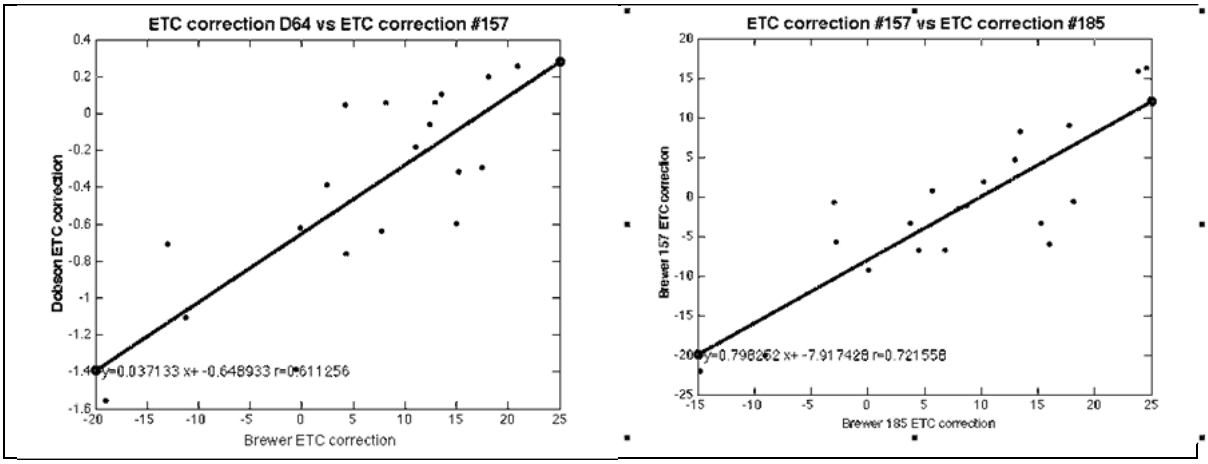

Figure 22: Correction to the ETC constant derived from the Langley plots for the Dobson 064 vs. Brewer 157 (Left panel) and Brewer 175 vs. Brewer 185 (right panel).

The Langley suggests significant changes on Brewer triad calibration; a 10 unit's ETC change on Brewer 157 and 183 mean a 0.6% change in ozone. Does these new constants change the Brewer-Dobson comparison? In the case of Brewer #183 the change in ETC was detected through the internal SL tests and thus applied to the ozone retrieval, so the ozone for this instrument does not change. For Brewer #157 the change in calibration constants is related with a change of the wavelength calibration associated to the internal mercury lamp replacement (Figure 23), According to this, the ozone absorption coefficient also change, although it is partially compensated by the change in the ETC. This is the reason why it was not detected through comparison of the RBCC-E triad. In summary, applying the new constants do not change significantly the ozone of the triad (0.2%) and therefore the comparison with the Dobson, but change the comparison between the Brewers of the triad (see Figure 24).

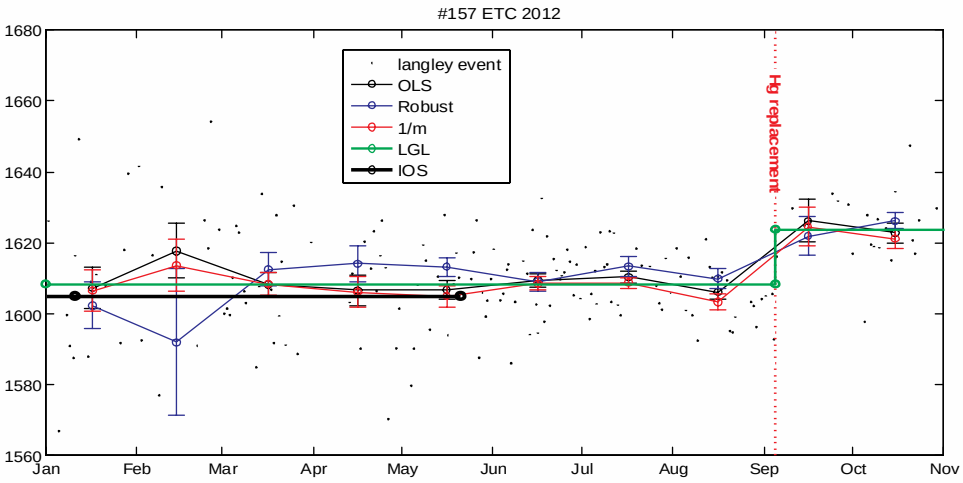

Figure 23: Langley analysis of the #157 during the 2012. The dots indicate the Langley events, the circles are the monthly mean with different regression methods: ***OLS*** *ordinary least square,* ***1/m*** *is the Dobson spectrometer regression and* ***Robust*** *is a robust estimation of the ETC. Finally the green line indicates the calibration adopted for this instrument* ***(LGL)*** *and the black line ,* ***(IOS)*** *the calibration transferred by IOS.*

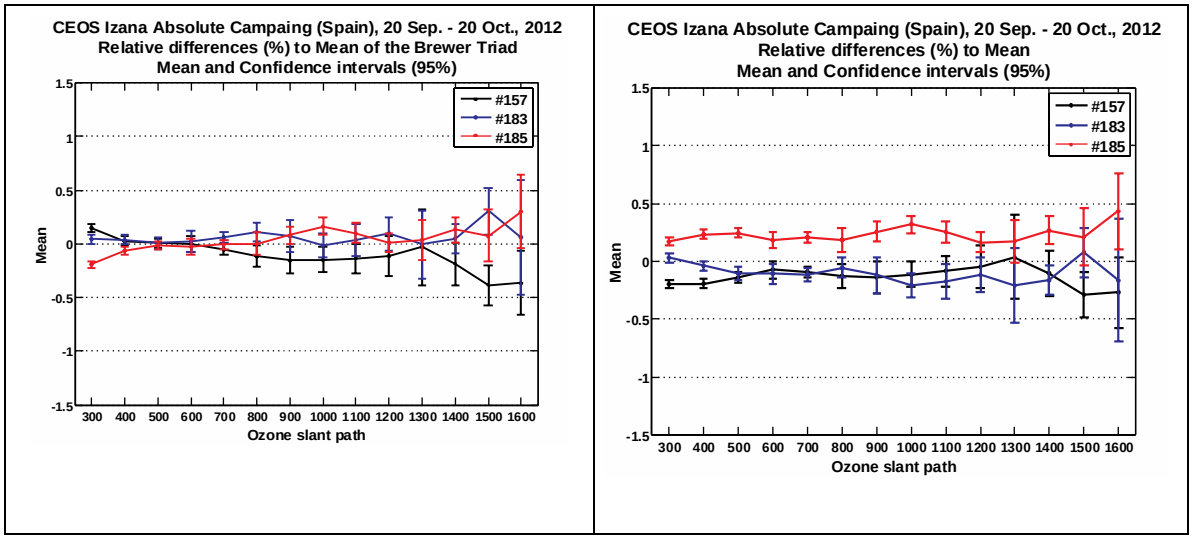

Figure 24 Ratio of simultaneous measurements of RBCC-E standard Brewers (serial no. #157, #183 and #185) to mean of all instruments against the ozone slant path grouped in 100 DU intervals with the original configuration from IOS (left panel) and the configuration obtained from the Langley analysis (right panel)

2.1.2.5 Evaluation of the use of five ozone absorption cross sections on Brewer and Dobson

On this work we evaluate five ozone cross-sections and the effect on the ozone calculation on Dobson and Brewer instruments. The ozone cross section used for the Brewer and Dobson network is from Bass & Paur (Bass and Paur, 1985), as recommended by the International ozone commission (www.esrl.noaa.gov/gmd/ozwv/dobson/papers/coeffs.html). The Dobson absorption

coefficients calculation is described by Komhyr et al., 1993 and re-evaluated by Bernhard et al., 2005. Our Dobson calculations are compared with their results, referred hereinafter as Komhyr93 and Bernhard05. The brewer calculation follow the operative procedure (Groebner et al., 1998; Kerr, 2002) used by the RBCC-E staff at the calibration campaigns. The ozone absorption coefficient is determined by the wavelength calibration, which provides the values for the operative wavelengths as well as the instrument's slit function. The Bass & Paur (B&P) ozone cross section at -45C is then convolved with this slit function. In contrast with the Dobson, where a unique absorption coefficient is used for the full network, every brewer has slightly different operative wavelengths and in consequence slightly different ozone absorption coefficient.

2.1.2.6 Ozone absorption cross sections calculations

There are three versions of B&P ozone cross section used in this study, denoted as Brewer, IGACOQ4 and Bernhard:

- **Brewer**: Brewer B&P is the file used by the RBCC-E and the Brewer network to derive the ozone absorption coefficient. We assume it as equivalent to the Bass & Paur publication (Bass and Paur, 1985) without any other adjustment. The plot of this set for six different temperatures agrees with the Figure 2 of the Bass & Paur paper, but we restrict the wavelength range to brewer instrument range (297-332 nm). ***This file is not available on the IGACO web page.***
- **IGAGOQ4:** There are two different sets available at the IGACO web page, one with the individual temperatures and the other with the quadratic coefficients on the file "Bp.par". The six individual temperatures of the individual files do not agree with B&P paper and do not include -45ºC, which is used on Brewer calculations. In this work we use the quadratic coefficients set, to be consistent with the Komhyr determination (Komhyr et al., 1993) of Bass & Paur. Following the instructions of the program from the web page to get the -45 temperature, the Brewer file at -45 and the IGACO at -45 are similar but not equal. The Brewer file is noisier
- **Bernhard (B&P B):** In order to compare with Bernhard calculations (Bernhard et al., 2005), we use the same set as in his calculations at -46.3 Cº.

In addition we use two high-resolution ozone absorption coefficients:

- **Daumont, Brion & Malicet (DBM),** (Daumont et al., 1992)**,** (Brion et al., 1993)**,** (Malicet et al., 1995) from the IGACO web page
- **University of Bremen (IUP):** Serdyuchenko et al. (2011, 2012)**.**

For consistency, the units of all of this sets, the wavelengths, were referred to air, using Bernhard tool on "Libradtran" package, and using the -45C temperature for brewer and -46.3C for Dobson calculations. When these temperatures were not available on the cross section set a linear interpolation were used. The units are (atm cm-1), using for the Loschmidt's number a value of 2.69e-19.

The ozone absorption coefficient is determined by the Brewer operational method (Groebner et al., 1998; Kerr, 2002), which is essentially the same as the ozone absorption "approximation" used by Bernhard05

$$\alpha = \frac{\int S(\lambda,\lambda') * \alpha(\lambda)\, d\lambda}{\int S(\lambda,\lambda')\, d\lambda}$$

Where S is the normalized slit function and α is the ozone cross-section at the defined temperature. The integral is calculated in sums and the slit measurements are linearly interpolated to the ozone cross-section resolution.

There are two slits sets used on Dobson instrument, measured (Dobson 083), and the trapezoid parameterization from the values from Table 1 of Bernhard05. For the Brewer we use also a parameterization for the slits. a truncated isosceles triangle with central wavelength and Full Width at Half Maximum (FWHM) determined from the wavelength calibration.

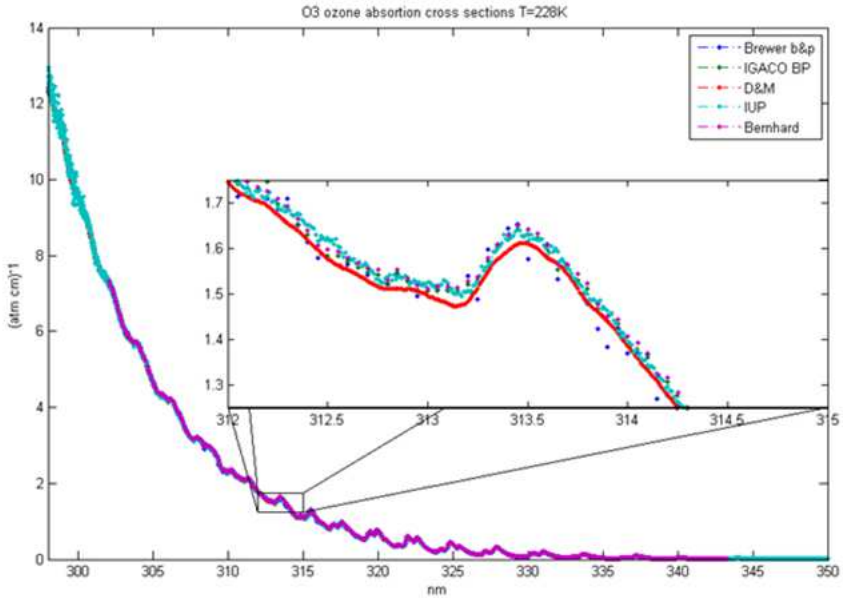

Figure 25:The five ozone cross section at -45ºC used on this work, Bass & Paur (Brewer), Bass &Paur (IGACO4), DBM Daumont, Malicet and Brion (IGACO4) the new set from Bremen University (IUP) and the set of B&P used for Bernhard 2005

	Measured slit				Parameterized slit									
	Brewer b&p	**IGACO B&P**	**DMB**	**IUP**	**Brewer b&p (*)**	**IGACO BP(*)**	**DMB(*)**	**IUP(*)**	**B&P B05 (*)**	**Komhyr approx.**	**Komhyr**	**Komhyr adj.**	**Bernhard approx.**	**Bernhard**
A1	1.9012	1.9001	1.8952	1.8970	1.9033	1.9022	1.8973	1.8993	1.9148	1.9170	1.9150		1.9150	1.9140
A2	0.1091	0.1090	0.1072	0.1071	0.1157	0.1155	0.1139	0.1139	0.1167	0.1150	0.1090		0.1150	0.1100
A pair	1.7921	1.7912	1.7881	1.7899	1.7876	1.7867	1.7834	1.7854	1.7981	1.8020	1.8060	1.8060	1.8000	1.8050
B1					1.2321	1.2326	1.2329	1.2325	1.2415	1.2440	1.2390		1.2410	1.2420
B2					0.0650	0.0647	0.0633	0.0632	0.0654	0.0650	0.0620		0.0650	0.0630
B pair						1.1679	1.1696	1.1693	1.1761	1.1790	1.1770	1.1920	1.1760	1.1800
C1	0.8620	0.8616	0.8557	0.8620	0.8614	0.8611	0.8551	0.8615	0.8676	0.8700	0.8730		0.8680	0.8710
C2		0.0378	0.0375	0.0375		0.0393	0.0388	0.0388	0.0398	0.0390	0.0400		0.0400	0.0390
C pair		0.8238	0.8182	0.8245		0.8218	0.8163	0.8227	0.8277	0.8310	0.8330	0.8330	0.8280	0.8320
D1	0.3820	0.3821	0.3757	0.3792	0.3801	0.3803	0.3738	0.3773	0.3837	0.3790	0.3840		0.3840	0.3870
D2		0.0095	0.0097	0.0099		0.0105	0.0105	0.0107	0.0104	0.0100	0.0170		0.0100	0.0100
D pair		0.3726	0.3660	0.3693		0.3698	0.3633	0.3666	0.3733	0.3690	0.3670	0.3740	0.3730	0.3770
AD		1.4186	1.4220	1.4205		1.4169	1.4201	1.4188	1.4248	1.4330	1.4390	1.4320	1.4270	1.4280
BD						0.7981	0.8063	0.8027	0.8028	0.8110	0.8100	0.8180	0.8030	0.8030
CD		0.4512	0.4522	0.4552		0.4519	0.4530	0.4561	0.4545	0.4620	0.4660	0.4590	0.4550	0.4550

Table 7: Summary for Dobson absorption ozone coefficient calculations for the five ozone cross sections (see text for details), using measured slit functions and parameterized slit functions (with an asterisk on the name) note that measured slit B is not available. Values from Komhyr and Bernard are also displayed for comparison. The calculations using B&P cross sections by Bernhard 2005 (B&P B05) is also calculated for parameterized slit

	IGACO BP	**D&M**	**IUP**	**IGACO BP(*)**	**D&M(*)**	**IUP(*)**	**B&P B**	**Komhyr approx**	**Komhyr**	**Bernhard approx**	**Bernhard**
AD	0.991	0.993	0.992	0.989	0.992	0.991	0.995	1.001	1.005	0.997	0.997
BD				0.976	0.986	0.981	0.981	0.991	0.990	0.982	0.982
CD	0.983	0.985	0.992	0.985	0.987	0.994	0.990	1.007	1.015	0.991	0.991

Table 8: Ratio of ozone absorption coefficient to Komhyr adjusted.

2.1.2.7 Dobson calculations

The Dobson calculations are summarized in Table 7. The comparison with the values of Komhyr (Figure 26), which are the values currently used in the Dobson network, shows that our calculations are 1% lower on AD pair using the different ozone cross sections. On CD pair the differences are larger, around 1.5%, for B&P and DMB, with the values of UIP 0.5% higher. The measurements using the parameterized slits are slightly lower than using the measured ones.

The Bernhard B&P cross section, available only for -46.3 Cº, was only calculated for the trapezoid approximation to assess the validity of the method, whereas the four remaining cross sections were calculated using both measured and parameterized slits. For easy comparison, Komhyr93 and Bernhard05 calculations are also displayed in Table 8.

The validity of the calculation can be checked when we use the same ozone cross section and the same slit parameterization as Bernhard 2005. The comparison is showed in **¡Error! No se encuentra el origen de la referencia.** for individual Dobson wavelengths. The agreement is very good for the short wavelengths, which correspond with narrow slits, but not so good on the longer wavelengths with wider slits. The ratios of the longer wavelengths slits are up to 4% different but the absolute value of the cross section is low and the effect on the pair ratios is very low, on pair wavelengths and double pair we get a maximum difference of 0.15**%. (**¡Error! No se encuentra el origen de la referencia.**)**

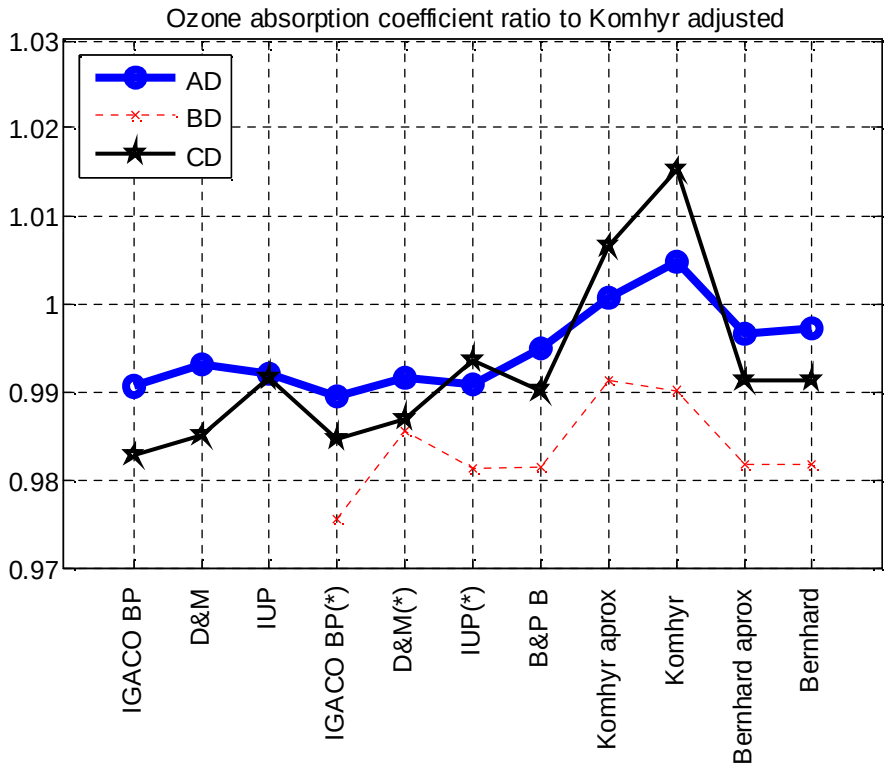

Figure 26 Double pair absorption coefficients ratios against Komhyr adjusted, the set used in the actuality on Dobson network. Asterisk indicates the calculations performed with parameterized slits.

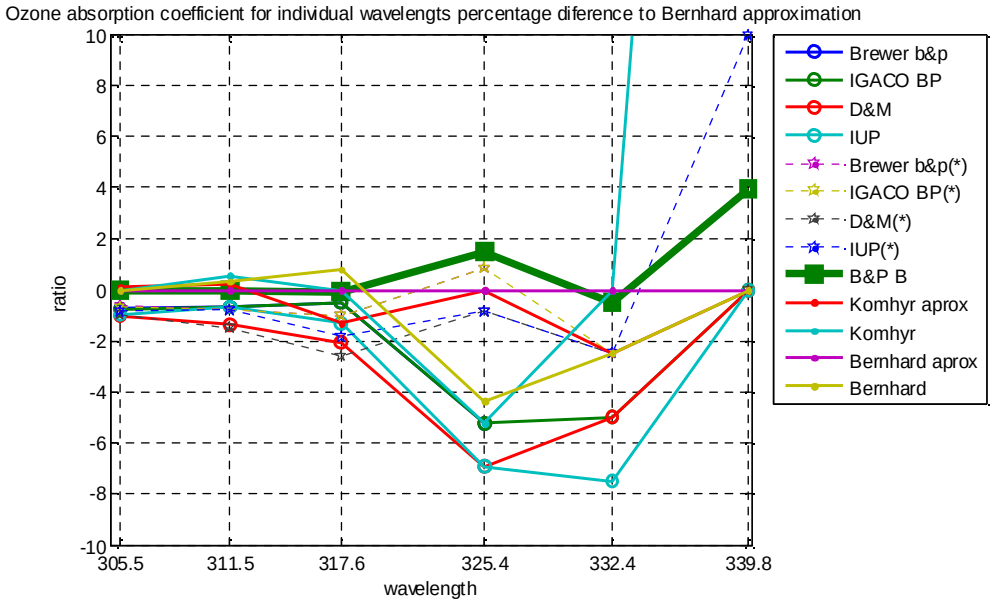

Figure 27: Ozone absorption coefficient ratio to Bernhard 2005 approximation for individual wavelengths.

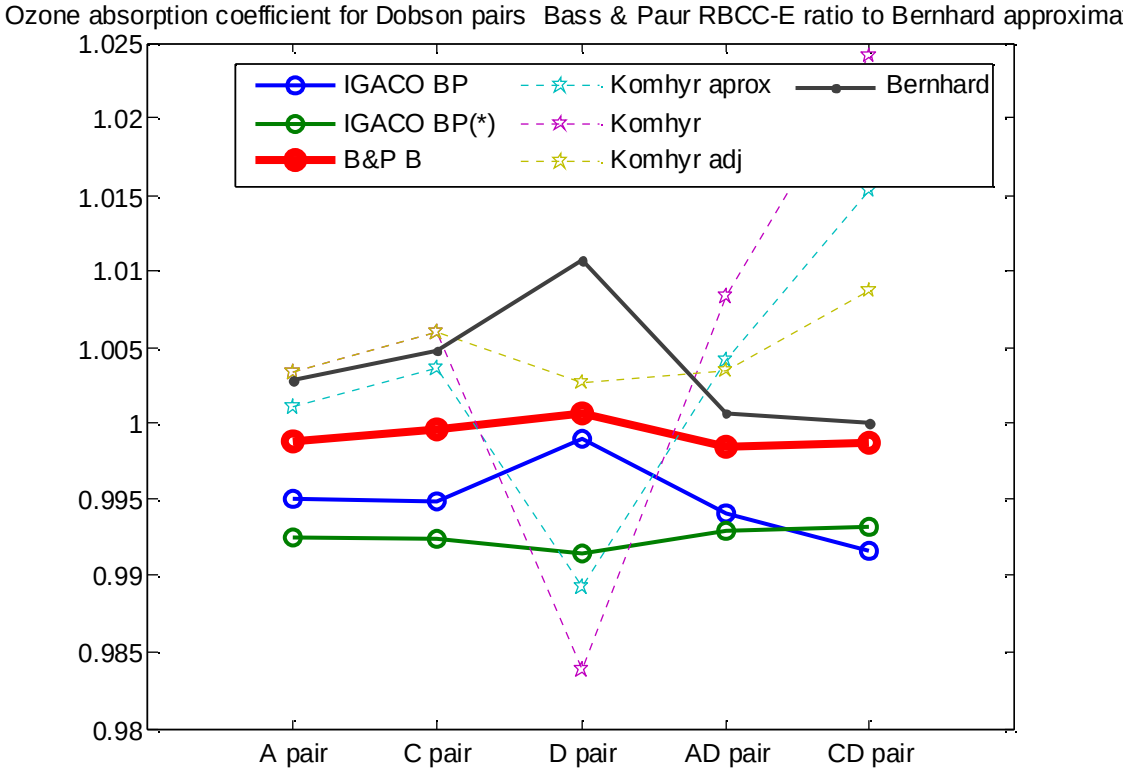

Figure 28: Ozone absorption coefficient ratio to Bernhard 2005 approximation for Dobson pairs and double pairs.

2.1.2.8 Brewer calculations

For the Brewer calculations we use 48 dispersion test performed on 16 instruments during the last RBCC-E campaign held at El Arenosillo (Huelva, Spain), see **¡Error! No se encuentra el origen de la referencia.**, using the standard procedure as described by (Groebner et al., 1998). The statistics are presented in **¡Error! No se encuentra el origen de la referencia.** and confirm the results for DMB presented at ASCO meetings. Surprisingly the use of the B&P file for IGACO produces higher ozone measurements (1%) than the operational procedure. The results for Bremen (UIP) measurements are very similar to operative set, 0.5% lower ozone.
For this campaign the maximum difference between Brewers is around 0.5%, which is the maximum error we introduce if we use a common factor to correct the ozone record.

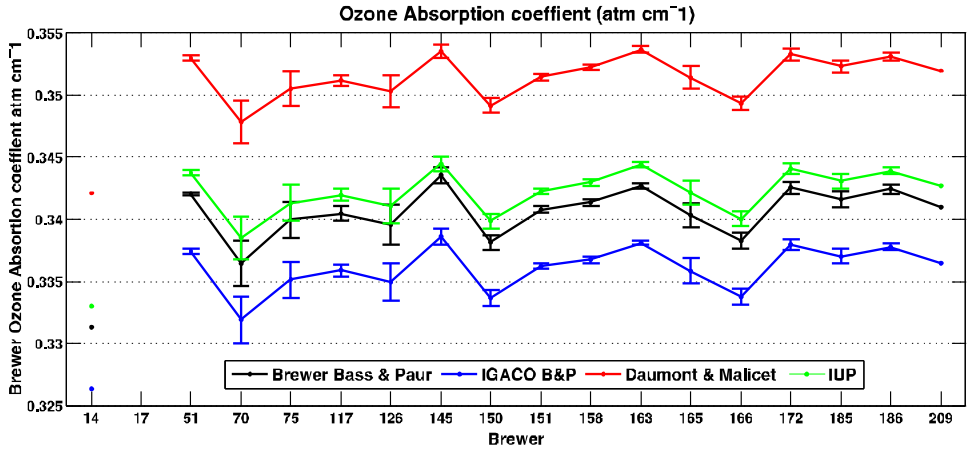

Figure 29: Brewer Ozone absorption coefficient for the instruments at Huelva 2011 campaign, mean and standard error.

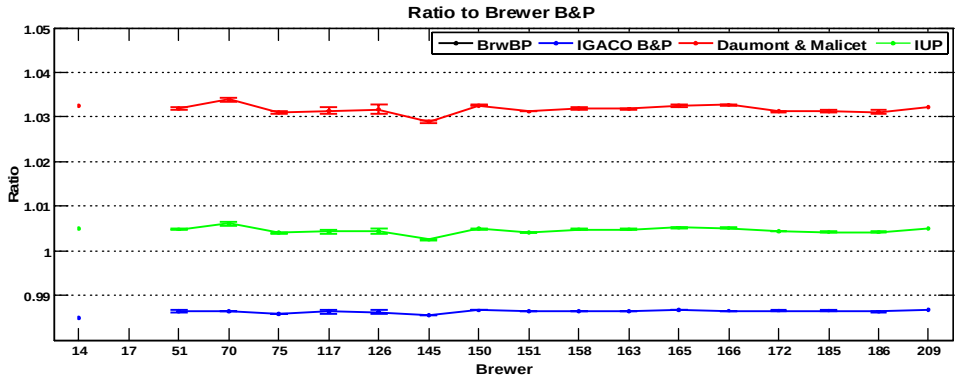

Figure 30 Ratio to Brewer operational B&P absorption coefficient against IGACO B&P (blue circles), Daumont, Malicet & Brion (red circles) and Bremen ozone cross section.

	IGACO	DMB	IUP
Mean	0.987	1.032	1.005
Standard deviation	0.001	0.001	0.001
Range	0.003	0.005	0.004

Table 9: Statistics of 48 wavelengths calibrations during Huelva 2011 campaign of the Ratio of the ozone absorption coefficient used on Brewer (Bass & Paur -45C) to the calculated with B&P file at -45C from IGACO web page (IGACO), Daumont, Malicet and Brion (DMB) also from IGACO web page and University of Bremen cross-sections (UIP).

2.1.2.9 Application to Izaña 2012 dataset

We can evaluate the effect of the ozone cross sections used in this study on the Brewer Dobson comparison using the synchronized measurements data set of the Langley Campaign. The effect on the ozone calculated by Dobson and Brewer instrument of change from ozone cross-section α to α' is simply the ratio between the old and new absorption coefficients, $O'_3 = O_3 * \alpha'/\alpha$. The factors applied to the synchronized observations of Dobson and Brewer are shown in Table 10). The effect on ozone ratios after the application of these factors is shown in Figure 31. The use of the IGAGCO ozone cross sections do not change the Brewer Dobson comparison, but slightly increase the Dobson CD/AD double pair difference. The DBM increase the difference between the instruments from 1.5 % of the operative algorithm to 2% and 3% on the case of CD pair and AD pair respectively. Finally the UIP reduces significantly the differences between Brewer-Dobson and maintain the differences between CD/AD pairs of the operative set.

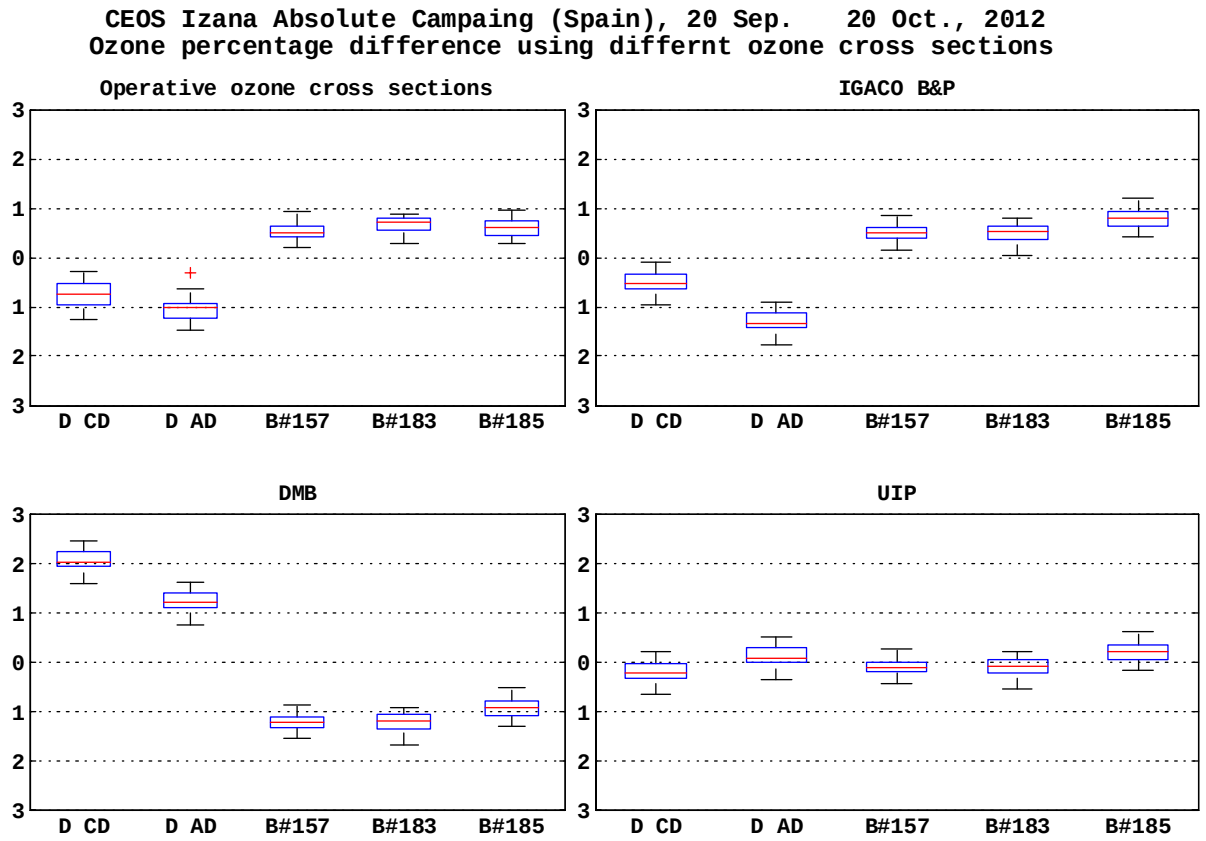

Figure 31 Boxplot of the percentage differences vs. the mean of Dobson and Brewer instruments with four cross sections: 1) Operative ozone cross section, (Bass & Paur) 2) Bass & Paur from quadratic coefficients 3) Daumont Malicet and Brion (DBM) and 4) University of Bremen (UIP:

	IGACO	DMB	UIP
Brewer	1.013	0.969	0.995
Dobson CD	1.017	1.015	1.008
Dobson AD	1.009	1.007	1.011

Table 10 : Factors applied to the Dobson and Brewer ozone calculations from the operational value Bass& Paur to the Bass & Paur IGACOQ version Daumont Malicet and Brion (DMB) also from IGACO web page and University of Bremen cross-sections (UIP).

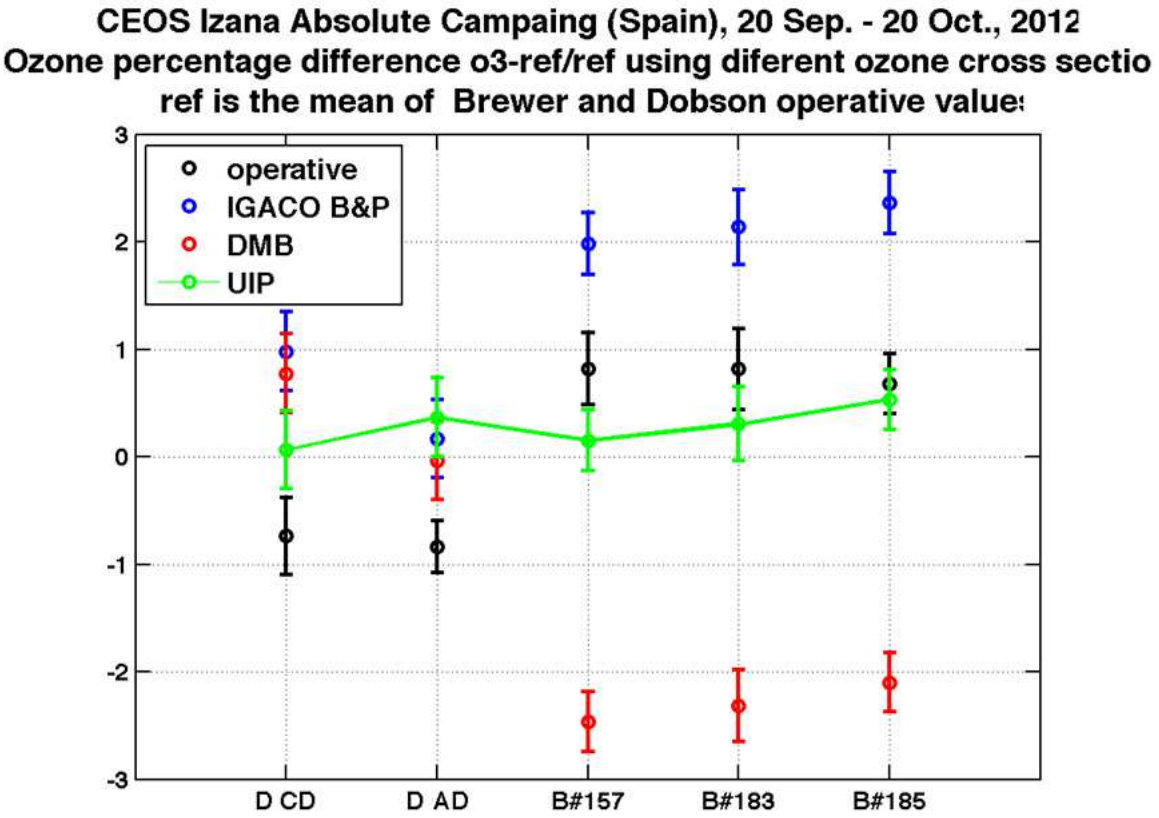

Figure 32. Mean an standard error of the the percentage differences o3-ref /ref where the reference is the mean of Dobson AD and CD pair and the three Brewer instruments evaluated with the operational cross section (Bass & Paur). The ozone o3 is calculated with four different cross sections: 1) Operative ozone cross section, (Bass & Paur) 2) Bass & Paur at -45C from quadratic coefficients 3) Daumont Malicet and Brion (DBM) and 4) University of Bremen (UIP:

2.2 UV-Vis MAXDOAS activities

2.2.1 HCHO slant column intercomparison and sensitivity study

The intercomparison of HCHO slant column measurements already described in the previous annual report of this project has been extended and finalised in the course of 2012, resulting in a paper published in AMTD (Pinardi et al., 2012). The CINDI HCHO intercomparison exercise involved nine atmospheric research groups having simultaneously operated MAXDOAS instruments of various designs during a few weeks in summer 2009. All data sets were evaluated using common retrieval parameters and the resulting HCHO differential slant columns (DSCDs) were found to be highly consistent, the mean difference between instruments generally not exceeding 15% or 7.5×10^{15} molec/cm^2, for all viewing elevation angles.

Furthermore a sensitivity analysis was performed to investigate the uncertainties of the HCHO slant column retrieval when varying key input parameters such as the molecular absorption cross-sections, correction terms for the Ring effect or the width and position of the fitting interval. This study, which is further detailed below, has led to the identification of potentially important sources of errors associated to cross-correlation effects involving the Ring effect, O_4, HCHO and BrO cross-sections and the DOAS closure polynomial. As a result, a

set of updated recommendations was formulated for HCHO slant column retrieval in the 336.5-359 nm wavelength range. To conclude the study an error budget has been proposed which makes a separation between systematic and random uncertainties. The total systematic errors are estimated to be of the order of 20% and is dominated by uncertainties on absorption cross-sections and related spectral cross-correlation effects. For a typical integration time of one minute, random uncertainties range between 5% and 30% depending on the noise level of individual instruments.

The sensitivity study concentrated on evaluating the sensitivity of HCHO results to possible changes in the retrieval settings. This was conducted using representative spectra from the BIRA instrument. Results highlight possible optimizations in the HCHO slant column retrieval parameters and lead to the recommendation of new analysis settings.

Closure polynomial and Ring effect

When performing a DOAS retrieval, an important free parameter is the degree of the polynomial function that is used to account for the smooth part of the attenuation spectrum. To avoid oscillations that may correlate with trace gas absorption features, the degree of this polynomial is generally restricted to values less than 5. For the baseline retrievals, a 3rd order polynomial was selected. However during our sensitivity tests we noticed that any changes to these polynomial settings had a strong impact on the diurnal behaviour of the HCHO DSCD, especially for high elevation angles. This raised two questions: (1) why such a dependence on the polynomial order, and (2) which one of the tested settings is the most satisfactory? In order address the second question, we investigated the consistency of vertical columns estimates (VCDs) as follows. In first approximation, the HCHO VCD can be derived from measured SCDs in two different simple ways: first from the difference between 30° elevation off-axis and zenith observations using the so-called geometrical approximation (Hönninger et al., 2004) and second, from direct conversion of the zenith-sky observations using appropriate AMFs. For the present analysis zenith-sky HCHO AMFs were calculated using the UVspec/DISORT model (Hendrick et al., 2006) at the wavelength of 346 nm and for a typical HCHO profile peaking in the boundary layer.

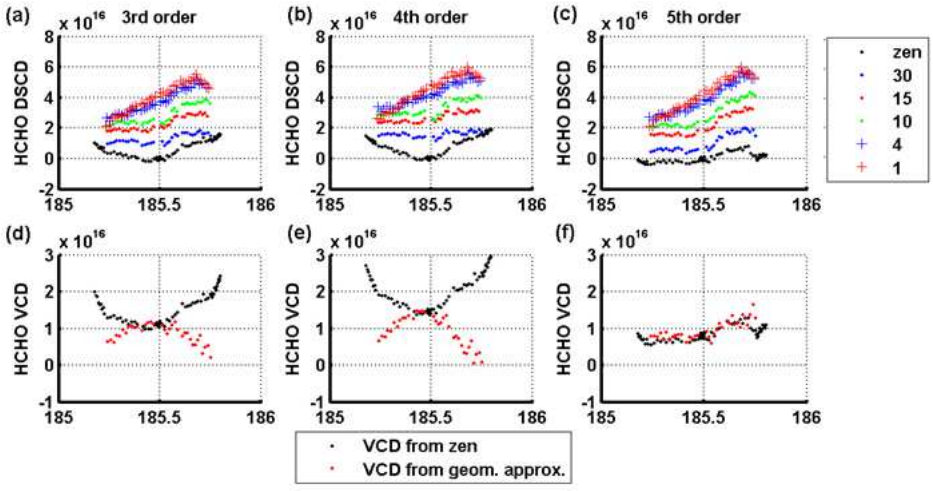

Figure 33. Effect of the choice of the polynomial order used in the DOAS fit. (a), (b), (c): impact in term of HCHO DSCD columns for the different elevation angles; (d), (e), (f) impact on the corresponding HCHO VCD columns obtained using two different methods. Only the 5th order case leads to geophysically consistent results (see text).

The HCHO content in the noon reference spectrum was derived using the geometrical approximation, so that both VCD evaluations (geometrical approximation and zenith-sky conversion) were constrained to agree at

the time of the noon reference spectrum. The resulting time-series of retrieved HCHO VCDs are displayed in for the same three polynomial settings.

As can be seen only the third case, i.e. the DOAS evaluation using a 5th order polynomial, leads to consistent retrievals of HCHO VCDs using both geometrical approximation and zenith-sky conversion. Although these results strengthen our confidence in the corresponding HCHO SCDs, the question remains: what is causing the observed dependence on the polynomial order? The curvature of the zenith-sky daily variation observed when using polynomials of order 3 and 4 (black dots in the first two upper plots) is striking and suggests an interference problem involving another absorber.

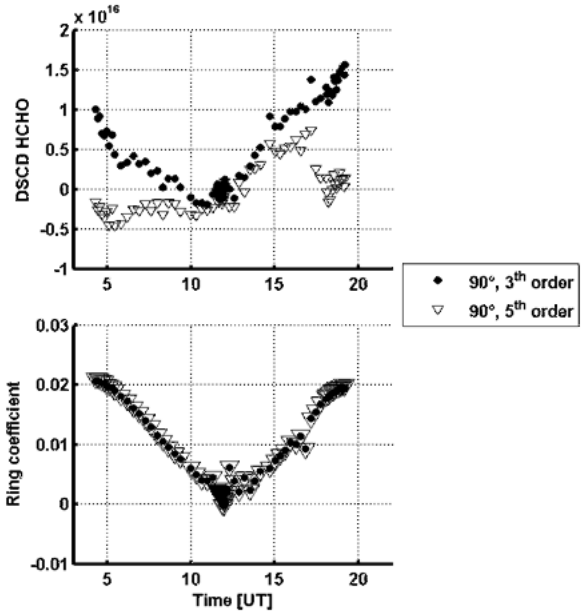

Figure 34. Daily variation of the zenith HCHO DSCD columns and of the Ring coefficients for retrievals with a 3rd and 5th order polynomial. A similar variation is observed for HCHO and Ring when a 3rd order polynomial is used in the DOAS retrieval.

As can be seen in Figure 34, the Ring effect clearly displays a similar curved pattern. Additional tests also show that none of the other parameters involved in the HCHO retrieval produces a similar shape. The Ring effect is a well-known phenomenon responsible of a filling-in of the solar and telluric lines in sky light spectra (e.g. Wagner et al., 2009 and references therein). This effect is large in comparison to the faint absorption features of HCHO and it can therefore produce interferences if not well corrected in the DOAS evaluation. To investigate further the sensitivity of our HCHO DSCDs to uncertainties in the Ring effect, additional test analyses were performed using different alternative sources for the Ring cross-sections.

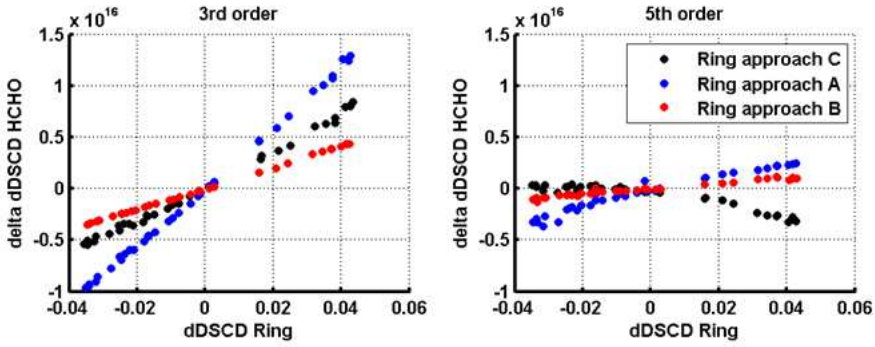

Figure 35. Sensitivity of HCHO dDSCD to changes in the Ring cross-section used in the DOAS fitting procedure, expressed as the difference to the baseline scenario, for data recorded on 4th July 2009. The two panels present the results for different orders of the polynomial used in the DOAS fit.

Figure 35 shows the relation between changes in HCHO DSCDs and corresponding changes in the Ring fit coefficients when using different Ring cross-sections. One can see that HCHO DSCD changes (dDSCDs) are linearly related to changes in the Ring fit coefficients. Comparing the retrieval cases using respectively a third and a 5th order polynomials, it is also clear that the interference between HCHO and the Ring effect is much stronger when a 3rd order polynomial is used. This suggests that, for our analysis conditions, the use of a third order polynomial introduces a misfit that activates the correlation between Ring and HCHO differential absorption features.

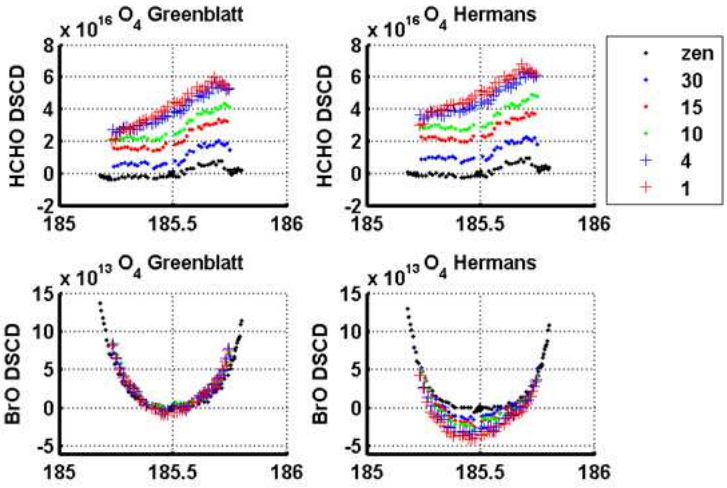

Figure 36. Effect of the choice of the O_4 cross-section used in the DOAS fit, on HCHO and BrO DSCD columns. Results (a) and (c) are obtained with the Greenblatt et al. (1990) cross-sections while (b) and (d) are obtained using the Hermans et al. (2003) cross-sections.

O_4 absorption cross-section

Another important interfering species in the HCHO fitting interval is the collisional dimer of molecular oxygen (O_4), of which the absorption cross-sections are still poorly characterized due the difficulty of measuring them in laboratory under pressures and temperatures representative of atmospheric conditions. Figure 36 shows the HCHO and BrO DSCD columns, as retrieved from MAXDOAS measurements using the Hermans et al. (2003) and the Greenblatt et al. (1990) O_4 cross-sections. As can be seen, the Hermans dataset (our ini-

tial baseline for the intercomparison exercise) leads to larger HCHO columns but also to a larger spread in the BrO DSCDs retrieved at different viewing elevations, a feature not expected for a stratospheric absorber like BrO. In contrast, the BrO DSCDs derived using the Greenblatt O_4 cross-section appear to be more consistent. Like for the case of the polynomial discussed before, one concludes that a misfit to the O_4 absorption (larger in this case using the Hermans et al. data set) activates a correlation between HCHO and BrO DSCDs.

DOAS fitting interval

The HCHO fitting interval used for MAXDOAS HCHO retrieval extends from 336.5 to 359 nm. This wavelength region, which includes three strong absorption bands of HCHO, has generally been recommended in the literature. However it is known that the absorption structures of HCHO and BrO are to some extent correlated in this wavelength interval. Figure 37(b) graphically displays the correlation matrix of the different absorption cross-sections used in the HCHO fit. As can be seen, HCHO and BrO present the largest coefficient of correlation (around 0.55), which can be easily explained by the similarities of their differential absorption cross-sections (see Figure 37(a)).

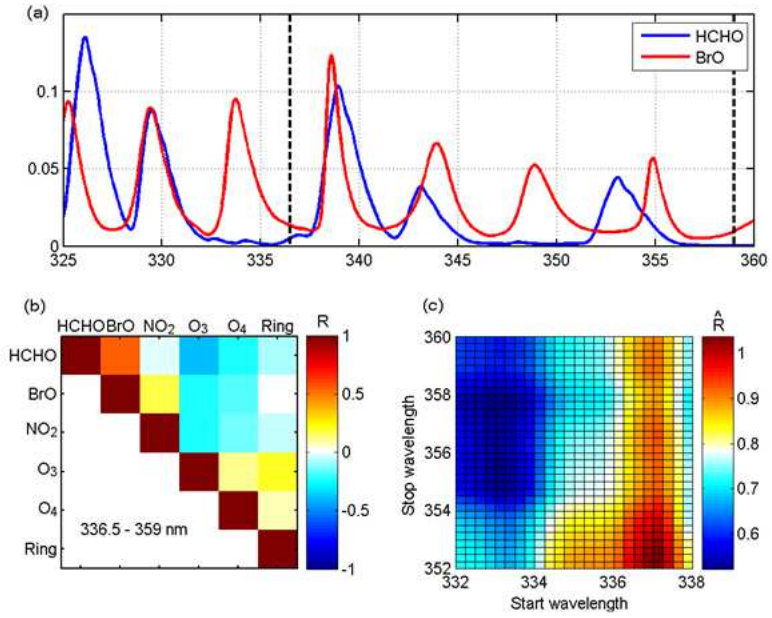

Figure 37. (a) HCHO and BrO absorption cross-sections in the 325-360 nm wavelength range convolved at the resolution of the BIRA instrument (0.38 nm FWHM) and normalized in arbitrary units. (b) Correlation matrix of the absorption cross-sections used for HCHO DOAS retrievals in the 336.5-359 nm interval. (c) Overall correlation (expressed as the root-mean-square of the non-diagonal elements of the correlation matrix) for different wavelength intervals in the 332-360 nm wavelength range.

In comparison, other species are less correlated, however the coefficient of correlation between HCHO and O_3 is not completely negligible and this is also true for other combinations involving O_3, O_4, BrO, NO_2 and Ring. One may expect such correlations to be dependent on the wavelength interval considered for the analysis. Therefore in an attempt to identify the settings that would minimize the correlation matrix, calculations were performed for a range of fitting intervals starting between 332 and 338 nm and ending between 352 and 360 nm by steps of 0.25 nm, in a similar way than what done in Vogel et al. (2012). For each case, the root-mean-square of the non-diagonal elements of the correlation matrix was reported in Figure 37(c). Smaller correlations are clearly found for fitting intervals starting at short wavelengths. From visual inspection of Figure 37(c), one can conclude that the 333-358 nm wavelength range presents a local minimum of correlation which can be explained by the addition of one band of BrO at 334 nm in a region free of HCHO absorption.

To further explore the potential of this extended fitting interval on our HCHO MAXDOAS retrievals, additional sensitivity tests were performed. Results however show again large instabilities with respect to the Ring effect interference. This is illustrated in Figure 38(a,b,c) where the HCHO DSCD retrieved in the 333-358 nm interval is displayed for different elevation angles and for different choices of the Ring cross-sections. As can be seen, the diurnal behaviour of the retrieved HCHO DSCD depends a lot on the source of the Ring cross-section used in the DOAS fit, and the corresponding HCHO VCDs calculated using the two methods introduced before are generally inconsistent. These results suggest that the extended fitting interval that minimizes the BrO-HCHO interference is also more sensitive to Ring effect misfits. Therefore any attempt to use this interval should be made with great care.

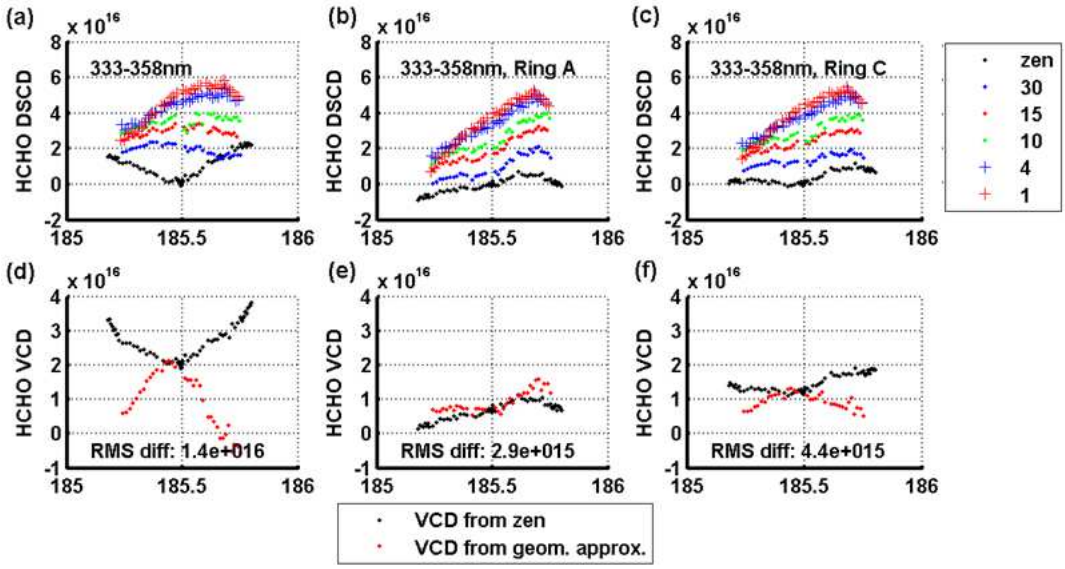

Figure 38. Same as Figure 33, but for an analysis in the 333-358 nm wavelength region, and for different choices of the Ring cross-sections.

Random uncertainties

Random errors in DOAS experiments are primarily related to the measurement noise. Assuming that the errors from individual detector pixels are uncorrelated and that the DOAS fit residuals are dominated by instrumental noise, the random contribution to the SCD error can be derived from the DOAS least-squares fit error propagation. Any deviation with respect to these assumptions generally results in an overestimation of the random error, so one can consider to a first approximation that the DOAS DSCD error constitutes an upper limit of the true random error. In order to better compare the actual performances of the different instruments, the DSCD error are further normalised to a common integration time of 1 minute. As can be seen in Figure 39(c), the scientific-grade instruments all display similar noise levels. The NASA and Mainz instruments which use small and uncooled detectors have larger errors as to be expected and JAMSTEC appears to be the noisiest system operated during the CINDI campaign.

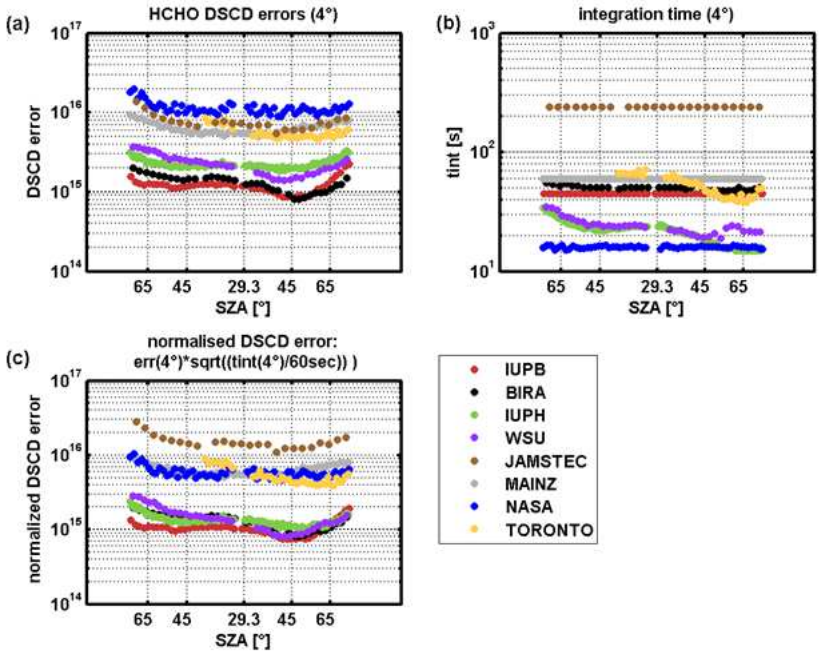

Figure 39. Comparison of HCHO DSCD errors retrieved by each participating group for the case of 4° elevation, based on measurements from 4 July 2009. (a) DSCD errors from DOAS evaluations, (b) corresponding integration times, (c) DSCD errors normalized by their integration times.

Systematic uncertainties and total error budget

Several important sources of systematic uncertainty have been discussed as part of the sensitivity analysis, leading to new recommended HCHO retrieval settings minimizing interference effects (Pinardi et al., 2012). Additional uncertainties have been treated with the aim to conclude on a comprehensive error budget considering the impact of systematic errors on absorption cross-sections, wavelength calibration and slit function.

Based on these results an overall assessment of the total uncertainties on HCHO dDSCDs has been made which is summarized in Figure 40 for typical conditions (elevation angle of 4° and HCHO dDSCD of 3.8×10^{16} molec/cm^2). Assuming that the different effects are sufficiently uncorrelated with each other, we can sum all deviations in quadrature to obtain an estimate of overall systematic uncertainty, which is represented by the black line in Figure 40. On this basis, we estimate the total systematic uncertainties on HCHO dDSCDs to be of approximately 20% for measurements at 4° elevation, with a weak dependence on the SZA. Since some of the effects considered in this study are likely to be partly correlated, these values could be considered as upper limits, however despite our efforts to include the most important sources of uncertainties in our sensitivity analysis, the need for possible additional terms cannot be excluded a-priori. Therefore, arguably, the uncertainties reported here are to be interpreted as realistic conservative values.

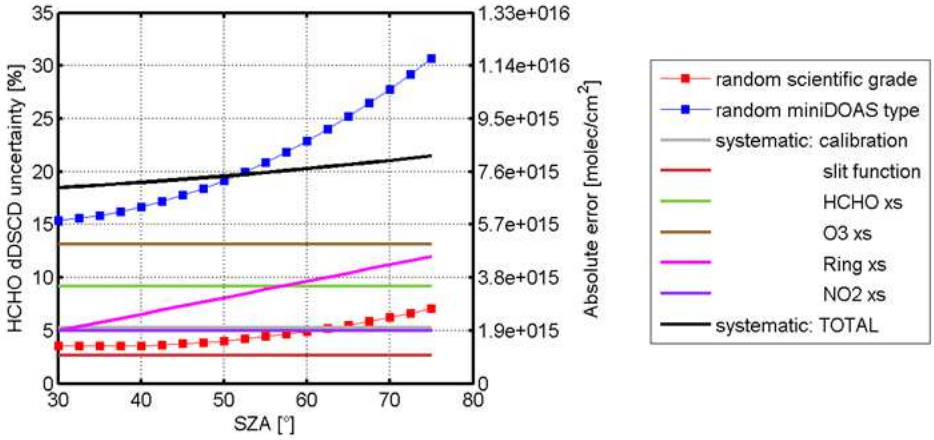

Figure 40. Summary assessment of the error budget on HCHO dDSCD at 4° elevation, as a function of the SZA. Random uncertainties are typical of low-noise scientific grade instruments and of mini-DOAS types of instruments for a typical integration time of 1 minute.

2.2.2 Aerosol Profiling during CINDI

During the CINDI campaign, a number of aerosol measuring systems were deployed as summarized in Table 11. These data have been used to study the consistency of MAXDOAS retrievals of aerosol extinction profilesand integrated AOD values, performed by 5 CINDI participants.

Institute	Instrument	Quantities
RIVM	Backscatter Lidar	Backscatter profiles
KNMI	Vaisala CT75 Ceilometer	Backscatter profiles
RIVM	CAELI Raman Lidar	Backscatter and extinction profiles
PSI	Humidity controlled Nephelometer	Surface extinction coefficient
TNO	Multi Angle Absorption Photometer	Black carbon
TNO	CIMEL Sun Photometer	AOT

Table 11. Aerosol instrumentation deployed during CINDI

Unfortunately Raman Lidar extinction profiles were not delivered yet, therefore simple backscatter aerosol profile made by the RIVM instrument have been used for a qualitative comparison with extinction profiles derived from MAXDOAS instruments. In order to allow for meaningful interpretation of the data, the Lidar data (Ceilometer) were degraded at the resolution of the MAXDOAS retrievals. This was performed by first averaging the Lidar measurements in layers of 200 m thickness and then further applying the MAXDOAS averaging kernels, as illustrated in Figure 41. Lidar measurements vertical smoothed in this way were subse-

quently compared to MAXDOAS measurements from 5 participating groups. Results for a few selected days are represented in Figure 42, Figure 43 and Figure 44. Likewise, integrated AOD values derived at 477 nm by the BIRA, IUPHD, KNMI, MPI-Mainz and JAMSTEC MAXDOAS instruments are compared to sunphotometer data in Figure 45. Note that for some instruments, a conversion to AOD value at 477 nm had to be performed, using Angstrom coefficient values provided by the syn photometer instrument.

From the various comparisons performed, the following conclusions can be drawn:

- The vertical structure of boundary layer as retrieved from MAX-DOAS is in good qualitative agreement with backscatter profiles from Ceilometer, especially for BIRA and IUPHD instruments and aerosol retrieval schemes
- The AOD is in good agreement with Sun Photometer for most groups
- The comparison of data at 477 nm with measurements at other wavelengths (e.g. MPI, 360 nm) is problematic. No sun Photometer data were available during CINDI at wavelengths below 440 nm.
- The systematically higher surface extinction obtained with MAXDOAS instruments in comparison to Wet Nephelometers in the afternoon remains unresolved. Discrepancies can be huge and still need to be understood.
- Each of the algorithms and different approaches developed by the different CINDI participants has its individual advantages/shortcomings (in terms of vertical resolution, robustness, etc). More work is needed to converge towards a harmonised algorithm for MAXDOAS aerosol processing.

The write-up of a publication on the MAXDOAS aerosol intercomparison during CINDI is in progress and will be completed in the course of 2013.

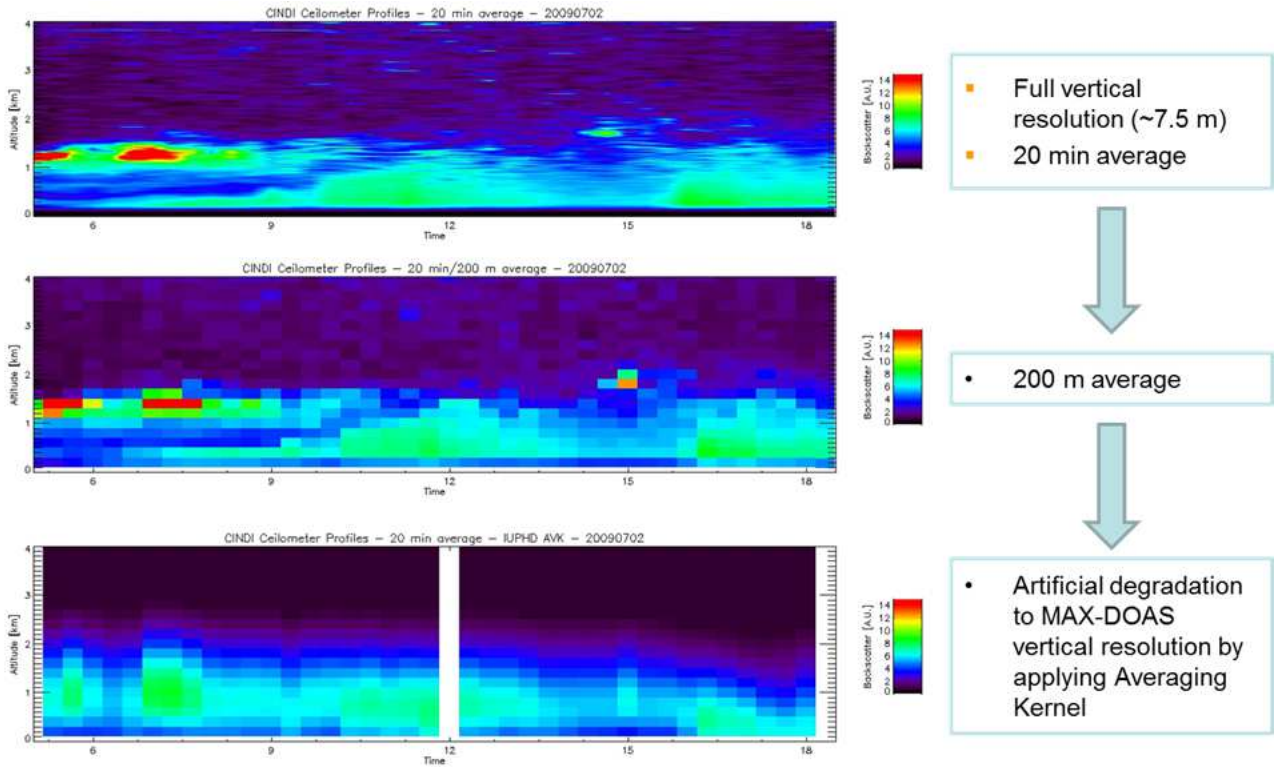

Figure 41. Treatment of Lidar backscatter profiles to allow their compairison with MAXDOAS profiles

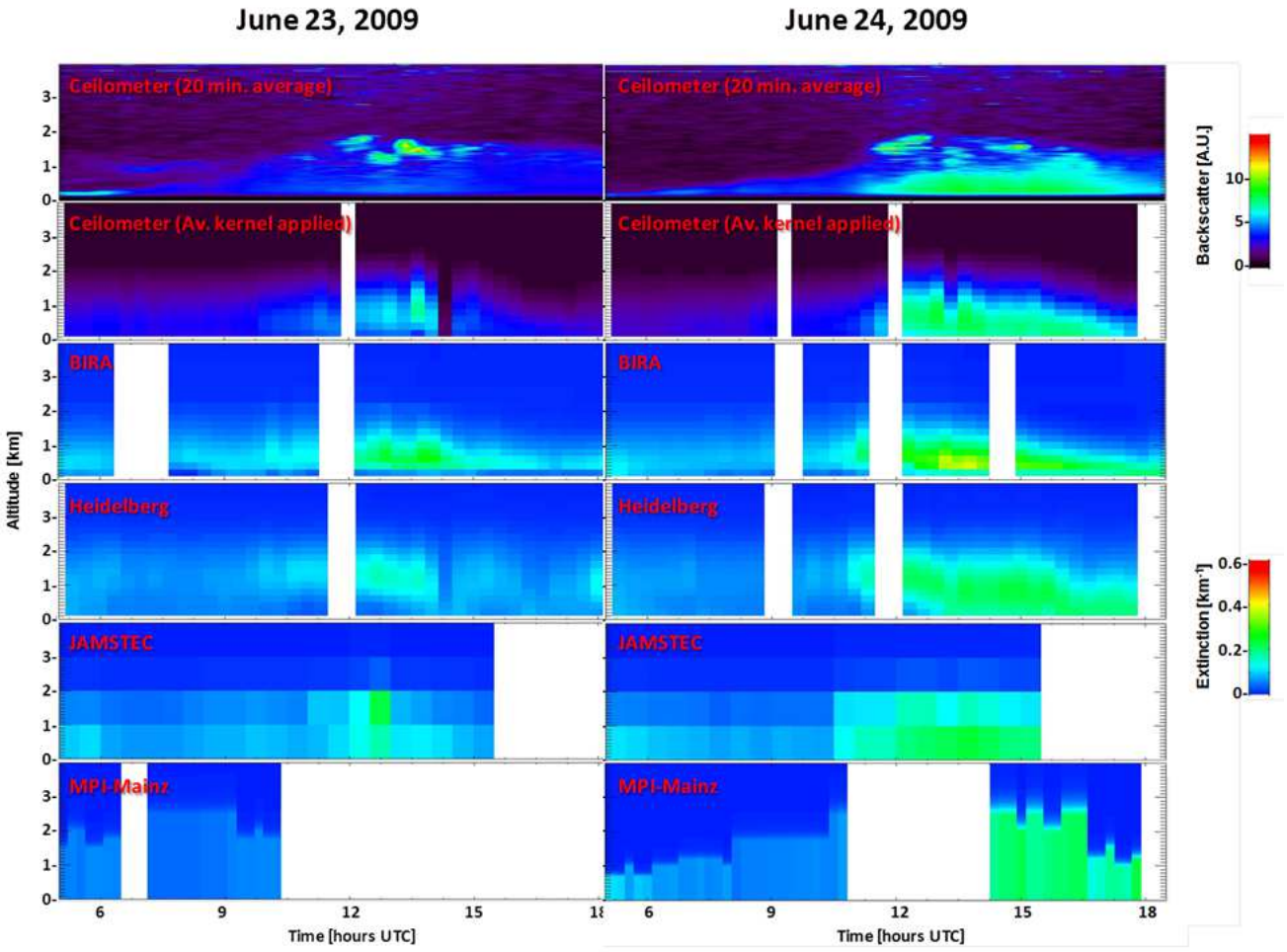

Figure 42. Comparison of backscatter aerosol profile from RIVM ceilometer an d aerosol extinction profiles derived from BIRA, Heidelberg, JAMSTEC and MPI-Mainz MAXDOAS instruments during the CINDI campaign on June 23 and 24, 2009.

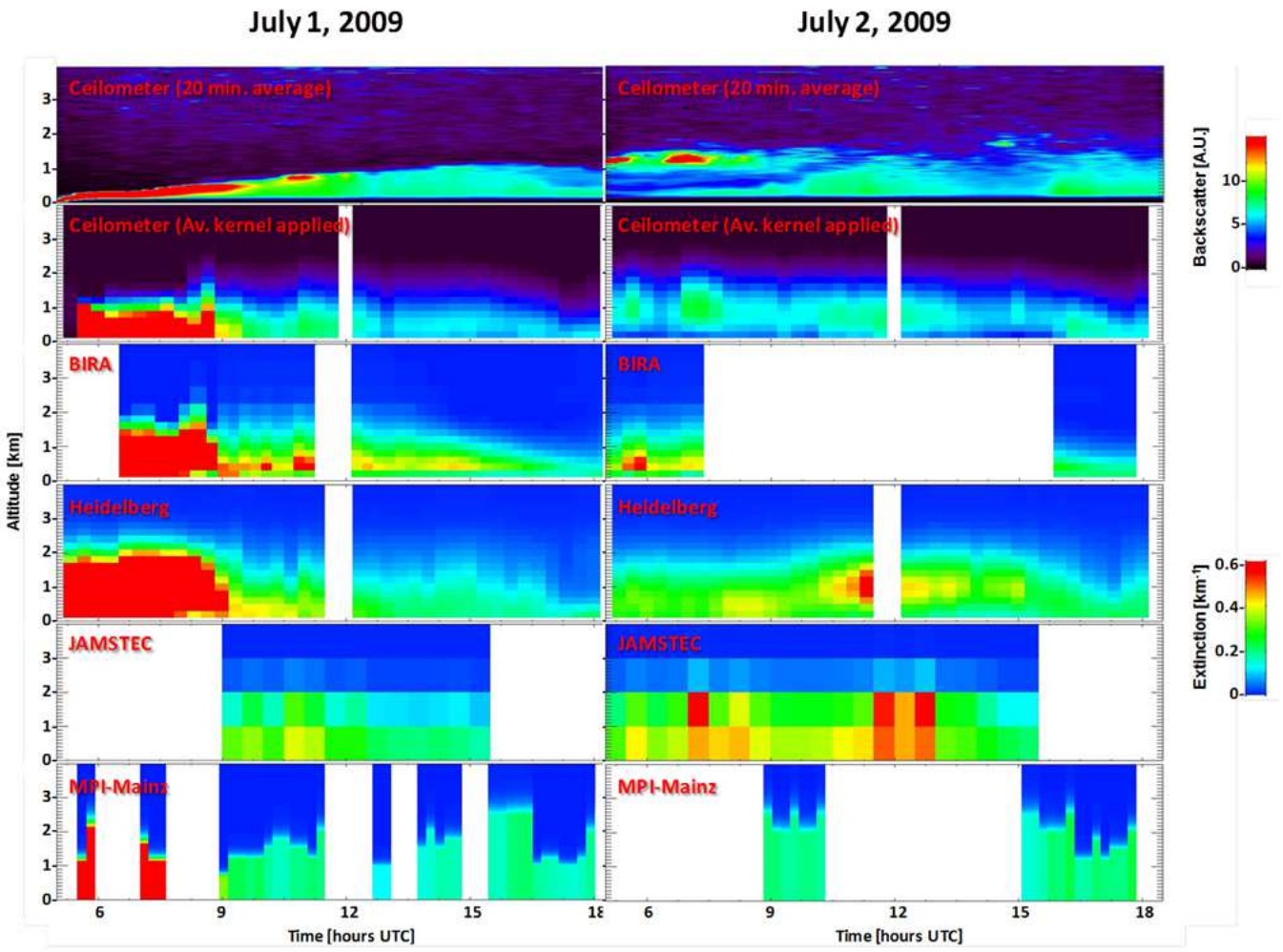

Figure 43. Comparison of backscatter aerosol profile from RIVM ceilometer an d aerosol extinction profiles derived from BIRA, Heidelberg, JAMSTEC and MPI-Mainz MAXDOAS instruments during the CINDI campaign on July 1 and 2, 2009.

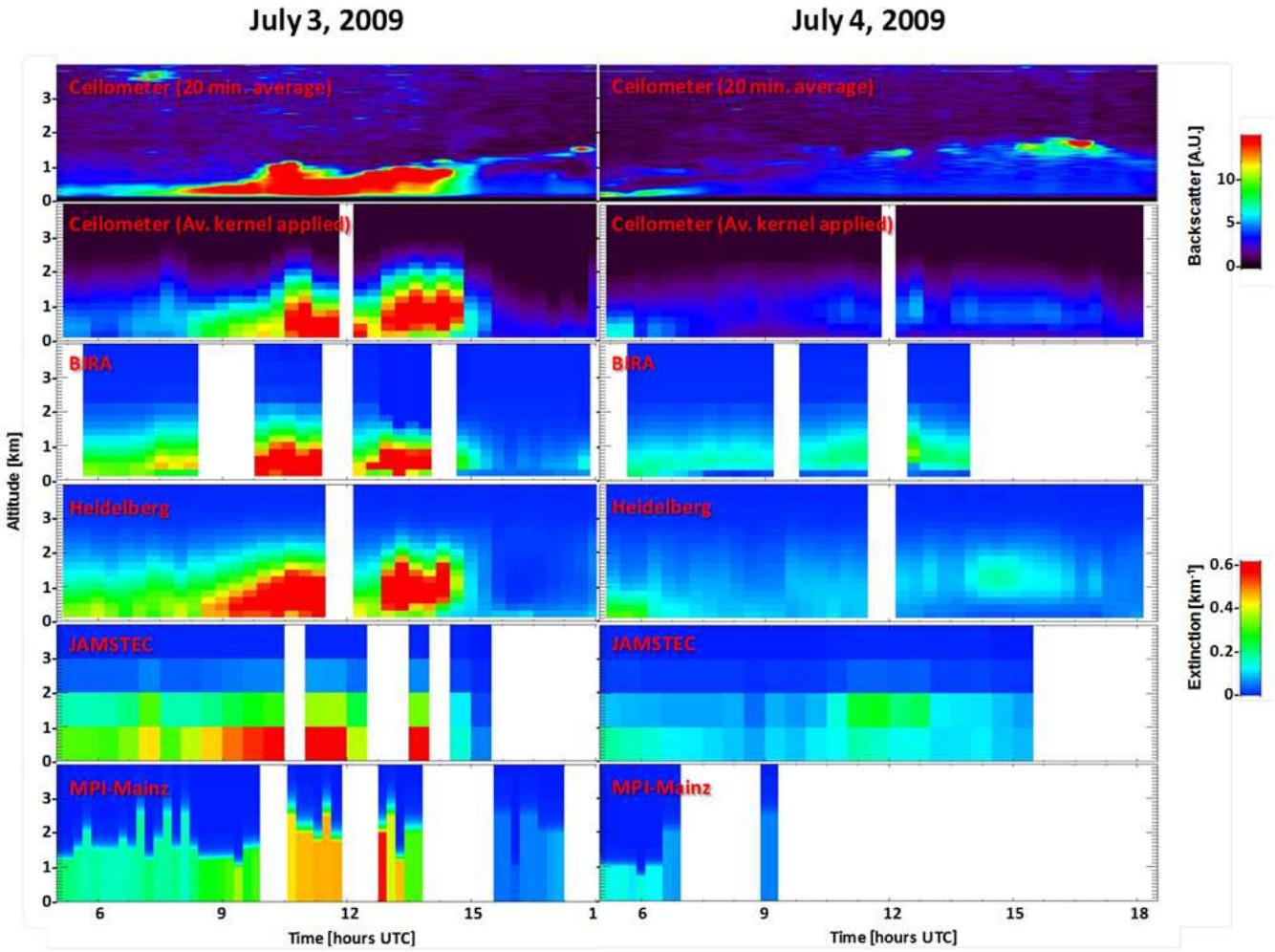

Figure 44. Comparison of backscatter aerosol profile from RIVM ceilometer an d aerosol extinction profiles derived from BIRA, Heidelberg, JAMSTEC and MPI-Mainz MAXDOAS instruments during the CINDI campaign on July 3 and 4, 2009.

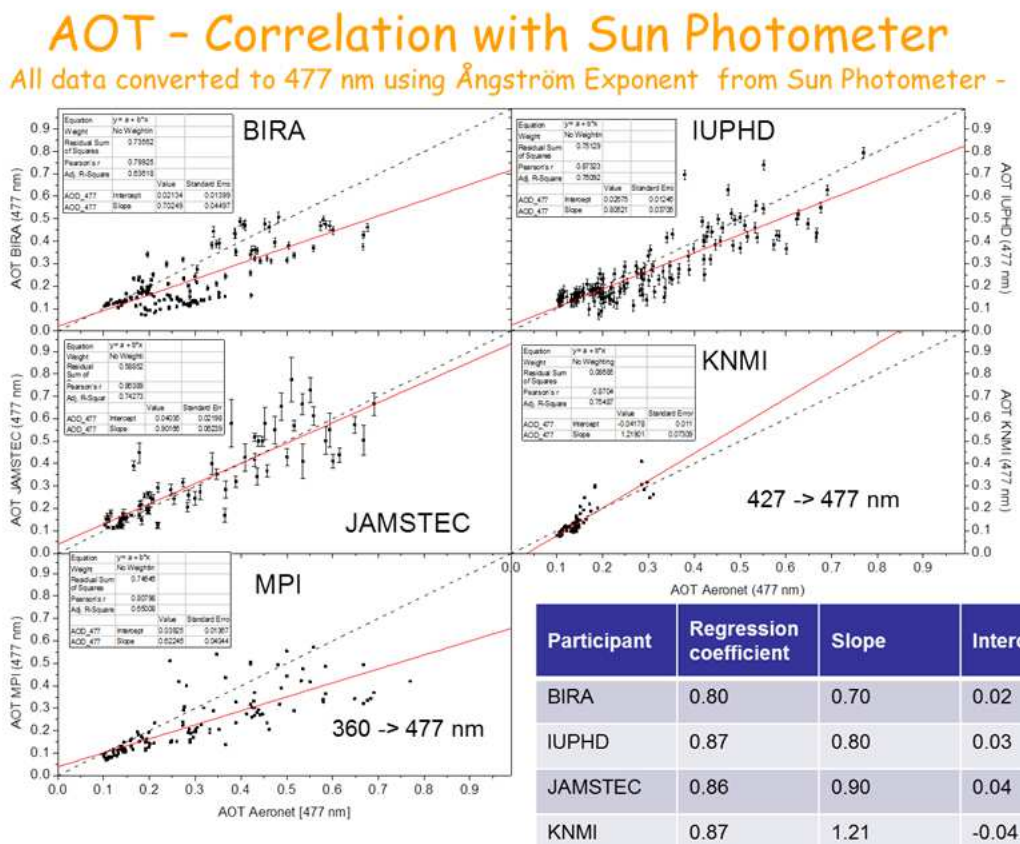

Participant	Regression coefficient	Slope	Intercept
BIRA	0.80	0.70	0.02
IUPHD	0.87	0.80	0.03
JAMSTEC	0.86	0.90	0.04
KNMI	0.87	1.21	-0.04
MPI	0.81	0.62	0.04

Figure 45. Comparison of aerosol optical depths (AOD) measured at 477 nm during the CINDI campaign with a sun-photometer and determined from MAXDOAS O_4 measurements by BIRA, Heidelberg, JAMSTEC, MPI-Mainz and KNMI.

2.2.3 Mobile-DOAS measurements during CINDI

A mobile-DOAS instrument was operated during the CINDI campaign for investigating the importance of horizontal gradients in NO_2 column around the Cabauw site. The instrument follows the MAX-DOAS principle but uses two spectrometers measuring scattered light spectra in parallel at different elevation angles. This reduces the problem of inhomogeneities in the trace gases previously observed from mobile MAX-DOAS instruments (e.g. Wagner et al., 2010). To retrieve the vertical tropospheric columns, previous mobile DOAS studies (Wagner et al., 2010; Ibrahim et al., 2010; Shaiganfar et al., 2011) assume that the light path can be approximated from the observation geometry -the so called geometrical approximation- leading to errors of up to 50%. In this study (Merlaud et al., 2013), we use a more accurate parameterization of the tropospheric AMF with explicit dependences on the solar and viewing geometries, which reduces uncertainties down to 20%. Figure 46 presents the observation geometry of the Mobile-DOAS instrument. The scattered light spectra are recorded simultaneously in the zenith direction and 30° elevation above the horizon, following the MAX-DOAS approach. The system is based on two similar compact Avantes spectrometers operated in parallel. The entry slit of each spectrometers is 50 micrometers, the focal length 75 mm and the grating is a 600 l/mm, blazed at 300 nm. The CCD detector is a Sony 2048 linear array. An optical head mounted on the car window holds the two telescopes with fused silica collimating lenses of focal

length 8.7 mm, leading to a field of view of 2.6°. The spectrometers are controlled by a laptop and a GPS antenna is used for georeferencing the measurements. The whole set-up is powered by the car battery 12V through an inverter.

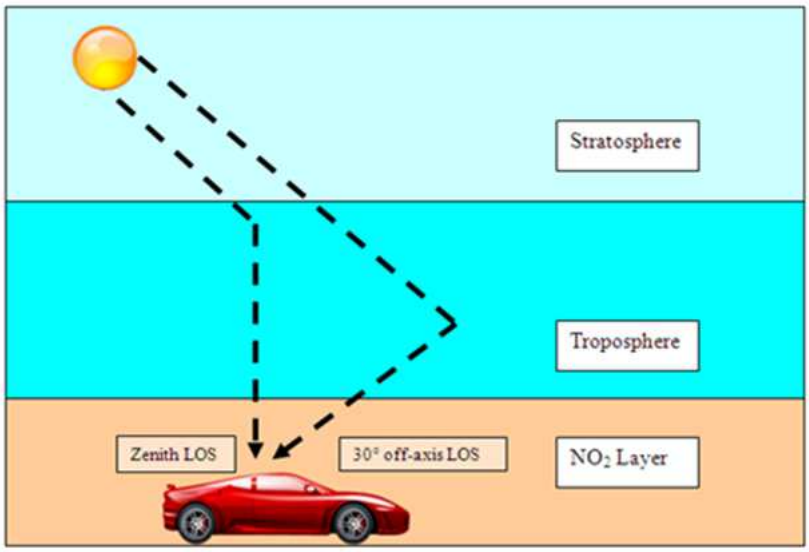

Figure 46. Principle of the mobile-DOAS instrument operated by BIRA during CINDI

The BIRA-IASB mobileDOAS was operated after the intercomparison on the local roads around Cabauw and on the highways between Utrecht and Rotterdam. The motivation, beside testing the newly developped instrument, was to study the variability of the NO_2 field inside one OMI pixel (13 x 24 km^2). Unfortunately, for the best measurements days, when the MobileDOAS and OMI measurements are coincident, the latter are affected by the row anomaly. The mobile-DOAS dataset collected during CINDI is thus not optimal for such a comparison, nevertheless it reveals accurately the NO_2 horizontal gradients around the CESAR site.

As an exemple, Figure 47 and Figure 48 present NO_2 tropospheric columns measured in the afternoon of 14 July 2009, between CESAR and Utrecht. Figure 48 also shows the vertical column derived from the static MAXDOAS at 13:04, when the mobileDOAS was still at the CESAR site. A description of the MAX-DOAS instrument is given in (Clémer et al., 2010). The two measurements are very close, around 310^{15} molec/cm^2 which gives confidence in the NO_2 loading derived from the MobileDOAS instrument along the other part of the track. The situation represented on this figure illustrates the typical situation for NO_2 measurements in a sub-urban site like Cabauw. Moderate gradients are found in the near vicinity of the site while much stronger variations are observed when coming closer to the Utrecht agglomeration and its NOx sources.

Mobile measurements are complementary to MAXDOAS measurements at fixed location. In order to get access a more comprehensive (ideally 3D) representation of the NO_2 distribution, more measurements are needed using a combination of ground-based systems complemented by aircraft profiling and 2D imaging systems. Such deployment will be considered for future campaigns.

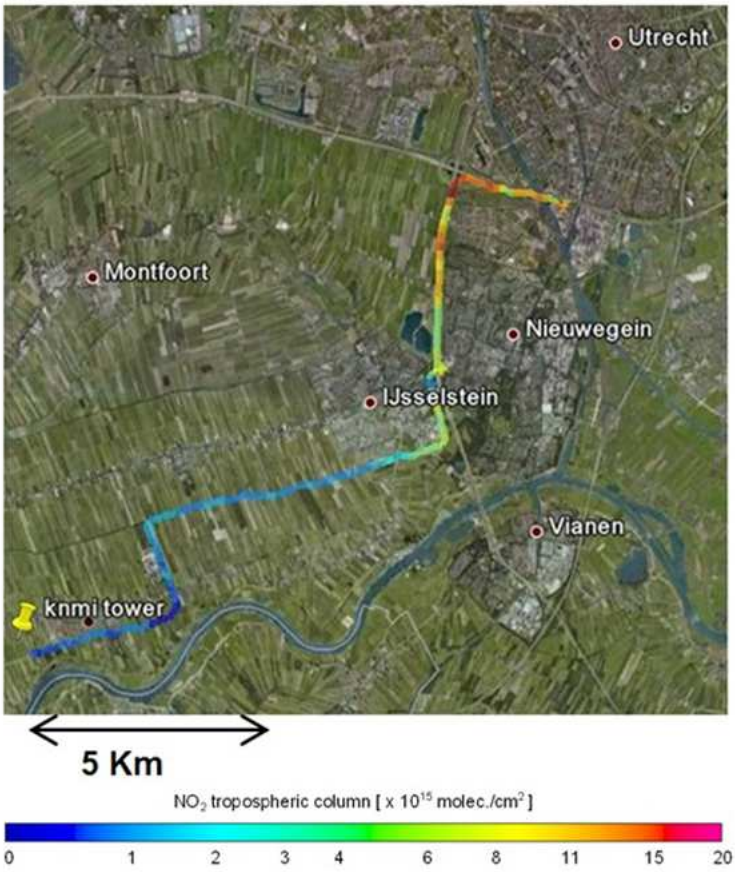

Figure 47. Mobile-DOAS measurements on 14 July 2009 measured on the way from Cabauw to Utrecht.

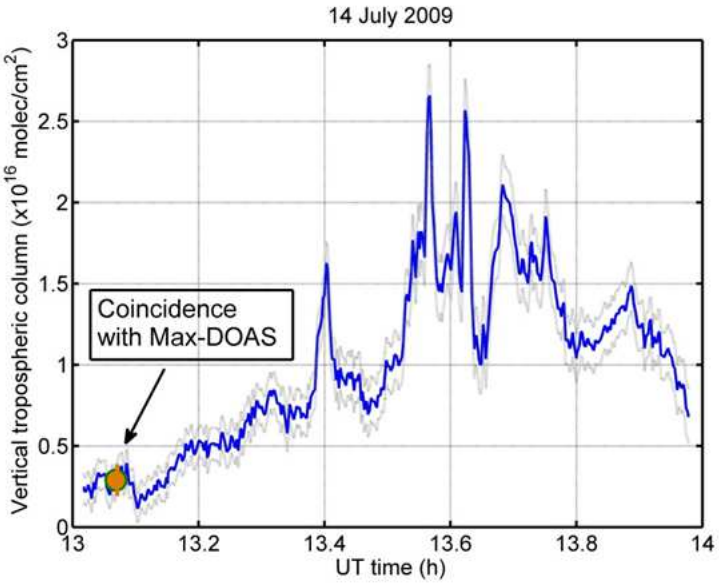

Figure 48. Mobile-DOAS measurements on 14 July 2009 from Cabauw to Utrecht. Time series of tropospheric NO_2 columns and comparison with reference MAXDOAS measurements at the Cabauw site.

2.3 EARLINET intercalibration activities

The AQUILI12 (L'Aquila Lidar Intercomparison 2012) intercomparison measurement campaign was performed with the lidar system in L'Aquila from 10 to 15 September 2012 using the reference lidar system POLIS from Munich (Germany). Three measurements were planned, with three Italian lidar stations: Lecce, Napoli and L'Aquila, but only the measurement campaign in L'Aquila was carried out, because of unexpected failure of Napoli and Lecce systems. The Lecce system was affected by a serious loss of energy, while the Napoli system suffered from an electronic break down and stopped to run. Both systems were not in conditions suitable to perform measurement campaigns and were shipped for repairing. The AQUILI12 intercomparison was performed in different atmospheric conditions. In the comparison, 7 aerosol backscatter and 5 aerosol extinction profiles were compared. During the comparison, several discrepancies arose, in particular at low range. The failure reasons were individuated and removed.

2.3.1 Participants to the LIDAR intercomparison AQUILI2012.

- SLAQ - CETEMPS/Univ. L'Aquila, AQ, (Vincenzo Rizi and Marco Iarlori)
- POLIS Meteorologisches Institut der Universität München, Munich, POLIS, (Volker Freudenthaler)

The system's technical details can be found in Appendix A; in **¡Error! No se encuentra el origen de la referencia.** the LIDARs main sub-systems (telescopes, detectors, etc.) are shown.

Figure 49. The AQ and POLIS LIDAR systems.

2.3.2 Location of the experiment.

The AQUILI2012 experiments were carried at latitude 42°22'6.00"N, longitude 13°21'1.70"E, altitude 656m a.s.l., in the Osservatorio Atmosferico laboratories of CETEMPS, Dipartimento di Scienze Fisiche e Chimiche, Università Degli Studi dell'Aquila, Italy (**¡Error! No se encuentra el origen de la referencia.**) .

Figure 50. The location of AQUILI2012 .

2.3.3 Strategy of the experiment.

In the previous inter-comparison campaigns of different LIDAR systems, the comparison of range corrected signals instead of LIDAR products like backscatter or extinction coefficients was adopted, in order to avoid the influence of different algorithms used for the analysis of the LIDAR signals.
But during AQUILI12 experiment, the pointing direction of POLIS had to be tilted relative to AQ LIDAR (zenith directed) to measure through the same roof window (Figure 51), and hence the inter-comparison of the final aerosol optical products, i.e., the vertical profiles of the backscatter and extinction coefficients, has to be used.

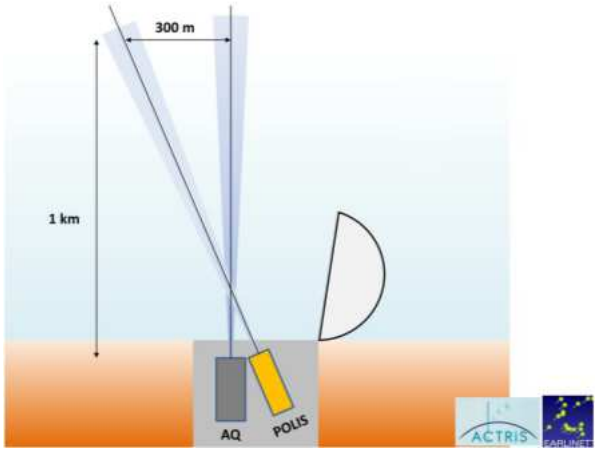

Figure 51. Relative tilt of the field of view of POLIS with respect to AQ.

2.3.4 Measurements.

It was possible to compare **7** β_a (aerosol backscatter) and **5** α_a (aerosol extinction) profiles, collected in different periods and meteorological situations:

<u>10/09/2012 (clear, after strong storm)</u>
Periods
19:44-20:16 UTC (α_a and β_a profiles)
[used atmosphere: GFS/NCEP of 11/09/2012 00:00 UTC]
20:16-20:47 UTC (α_a and β_a profiles)
[used atmosphere: GFS/NCEP of 11/09/2012 00:00 UTC]

<u>11/09/2012 (clear)</u>
Periods
09:25-09:56 (β_a profile) - 09:56-10:27 (β_a profile)
[used atmosphere: GFS/NCEP of 11/09/2012 09:00 UTC]
18:25-18:57 UTC (α_a and β_a profiles)
[used atmosphere: GFS/NCEP of 12/09/2012 00:00 UTC]
18:57-19:28 UTC (α_a and β_a)
[used atmosphere: GFS/NCEP of 12/09/2012 00:00 UTC]

<u>15/09/2012 (scattered clouds, clear)</u>
22:31-23:39 UTC (α_a and β_a)
[used atmosphere: GFS/NCEP of 16/09/2012 00:00 UTC]

The next Figures report a resume of all the measurements:

10.09.2012

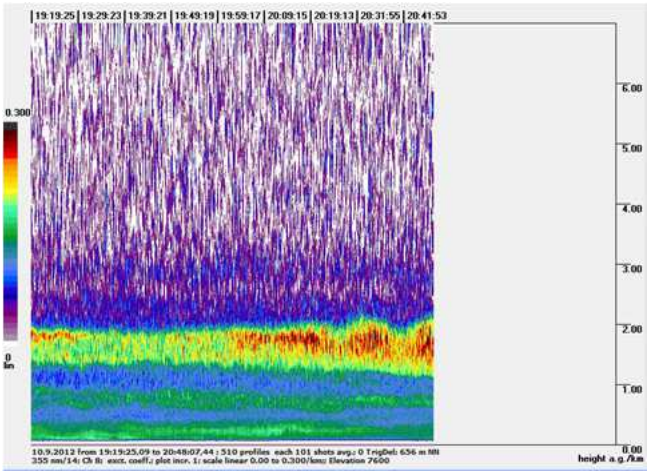

Figure 52. Overview quicklook POLIS 355 nm extinction coefficients [1/km] (Klett, lidar ratio assumed 55 sr) on 10.09.12 – 19:19-20:48 UTC. Situation: clear after strong storm.

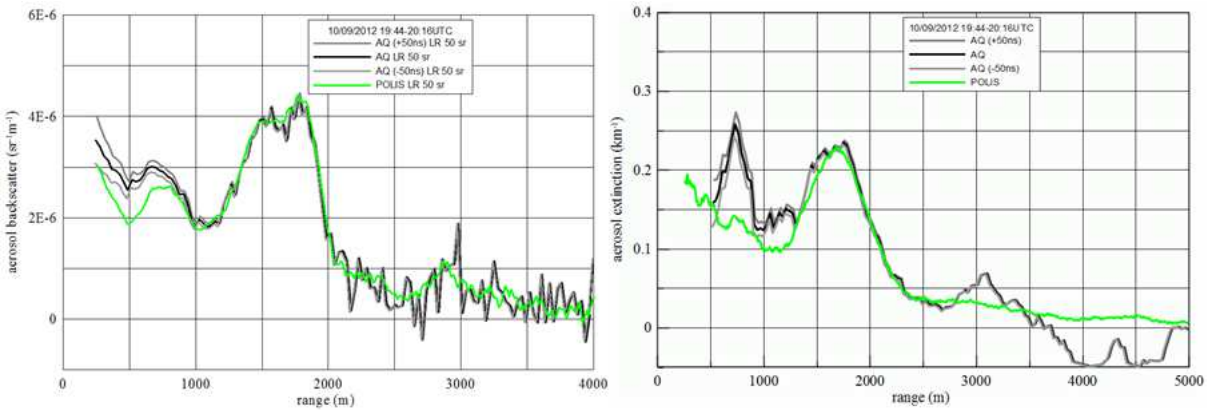

Figure 53. Intercomparison of backscatter (left) and Raman extinction coefficients (right) of lidar systems POLIS (355/387 nm) and SLAQ (351/382 nm) in L'Aquila/Italy on 10.09.12 - 19:44-20:16 UTC. Used Radiosonde: GFS 11.09.12 - 00:00 UTC.

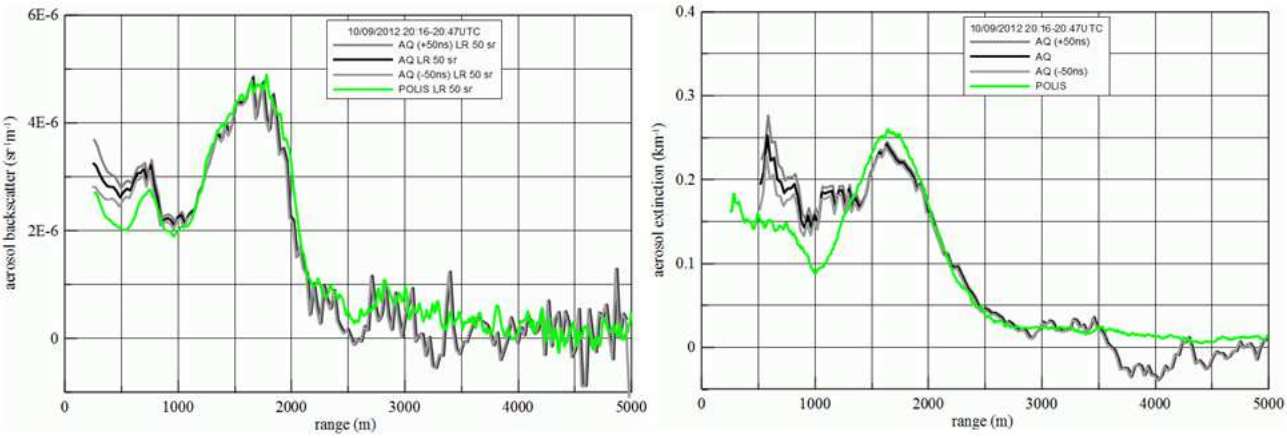

Figure 54. Intercomparison of backscatter (left) and Raman extinction coefficients (right) of lidar systems POLIS (355/387 nm) and SLAQ (351/382 nm) in L'Aquila/Italy on 10.09.12 - 20:16-20:47 UTC. Used Radiosonde: GFS 11.09.12 - 00:00 UTC.

11.09.2012

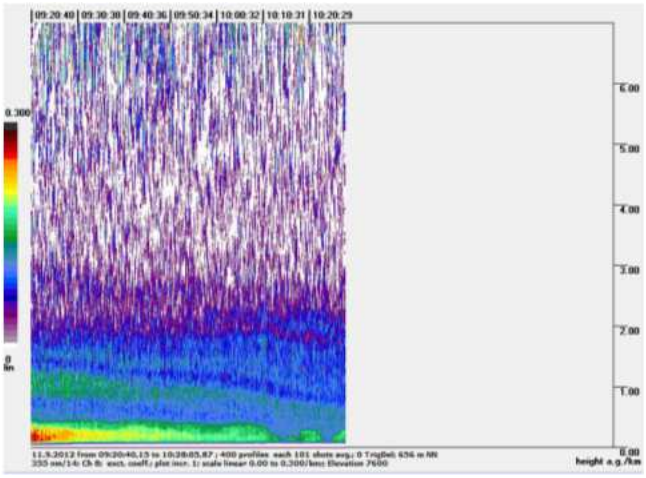

Figure 55. Overview quicklook POLIS 355 nm extinction coefficients [1/km] (Klett, lidar ratio assumed 55 sr) on 11.09.12 – 09:20-10:28 UTC. Situation: clear.

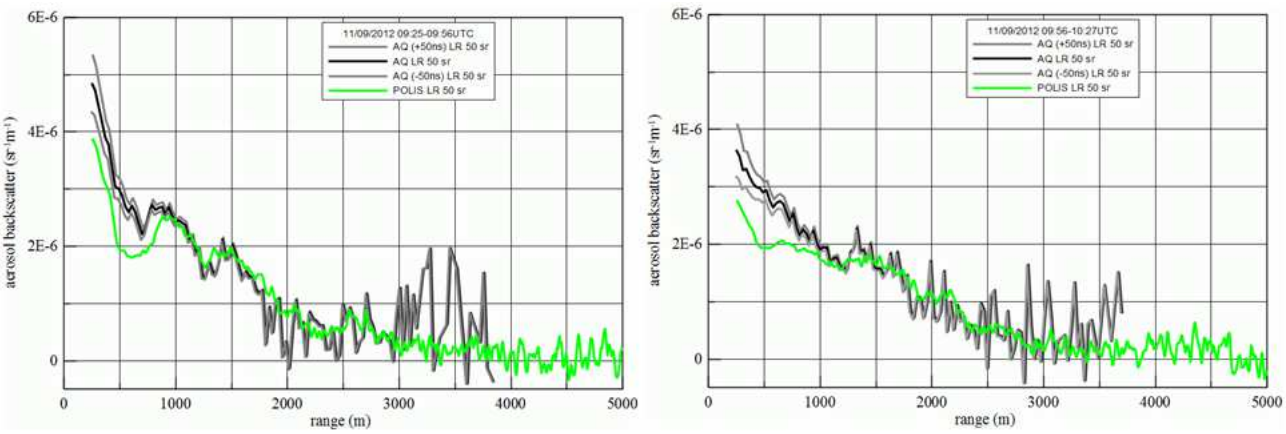

Figure 56. Intercomparison of backscatter coefficients of lidar systems POLIS (355 nm) and SLAQ (351 nm) in L'Aquila/Italy on 10.09.12 - 09:25-09:56 UTC (left) and 09:56-10:27 UTC (right). Used Radiosonde: GFS 11.09.12 - 09:00 UTC.

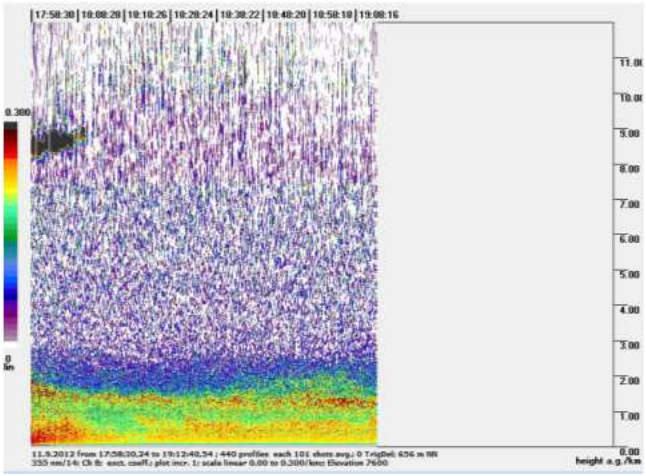

Figure 57. Overview quicklook POLIS 355 nm extinction coefficients [1/km] (Klett, lidar ratio assumed 55 sr) on 11.09.12 – 17:58-19:12 UTC. Situation: clear.

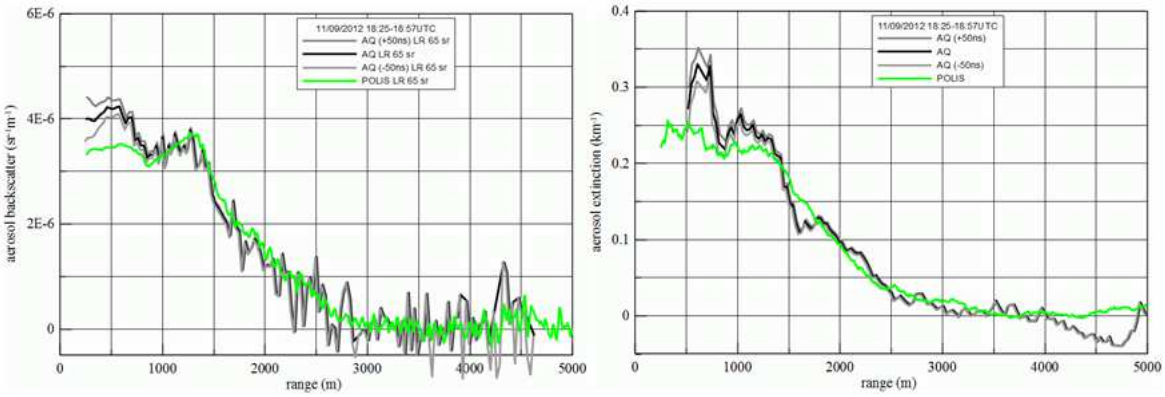

Figure 58. Intercomparison of backscatter (left) and Raman extinction coefficients (right) of lidar systems POLIS (355/387 nm) and SLAQ (351/382 nm) in L'Aquila/Italy on 11.09.12 - 18:25-18:57 UTC. Used Radiosonde: GFS 12.09.12 - 00:00 UTC .

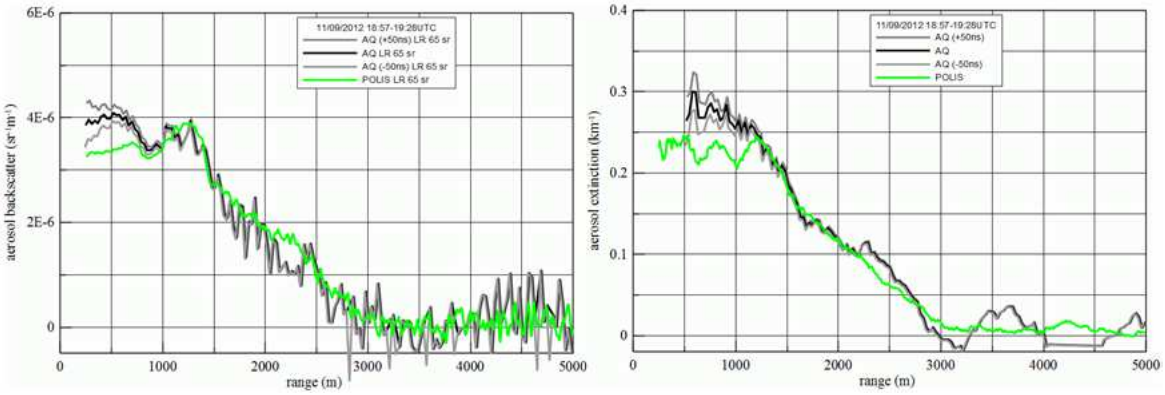

Figure 59. Intercomparison of backscatter (left) and Raman extinction coefficients (right) of lidar systems POLIS (355/387 nm) and SLAQ (351/382 nm) in L'Aquila/Italy on 11.09.12 - 18:57-19:28 UTC. Used Radiosonde: GFS 12.09.12 - 00:00 UTC .

15.09.12

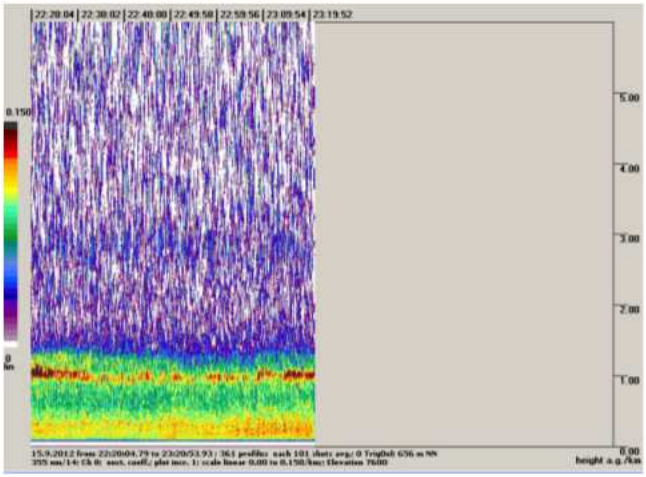

Figure 60. Overview quicklook POLIS 355 nm extinction coefficients [1/km] (Klett, lidar ratio assumed 55 sr) on 15.09.12 – 22:20-23:20 UTC. Situation: scattered clouds, clear.

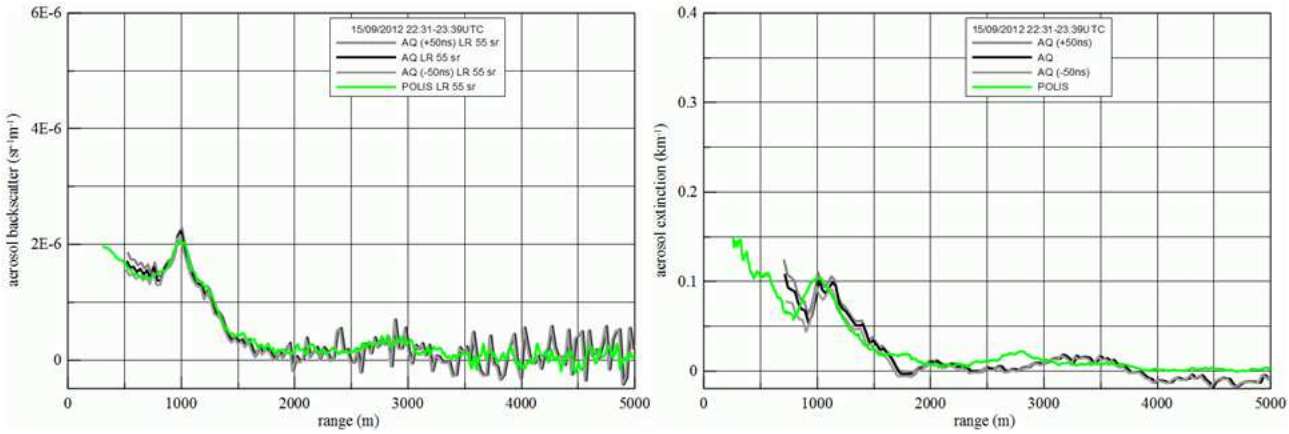

Figure 61. Intercomparison of backscatter (left) and Raman extinction coefficients (right) of lidar systems POLIS (355/387 nm) and SLAQ (351/382 nm) in L'Aquila/Italy on 15.09.12 - 22:31-23:39 UTC. Used Radiosonde: GFS 16.09.12 - 00:00 UTC.

2.3.5 Comments and conclusions

In general, the comparisons of the vertical profiles of the aerosol backscatter and extinction coefficients were quite good; anyway several discrepancies arose, in particular at low range. In the measurement periods of 10/09 and 11/09, the AQ and POLIS profiles of βa were coincident above 0.7 km range, αa profiles are similar above 1.2 km (see corresponding Figures). The reasons of the low level discrepancies were probably due to misalignment of the AQ system, and marginally to electronic noise, and to the different algorithms used for data retrieval (AQ and POLIS use their own software for the estimations of βa and αa profiles, anyway these programs have been quality checked within EARLINET).

From 12/09 to 14/09, it has been checked the alignment of the AQ LIDAR (there was no chances to run the LIDARs, because of low level clouds and rain), in particular the performances of the receiving telescope and its alignment (Figure 62) have been evaluated using a CCD camera positioned in the focus of the telescope.

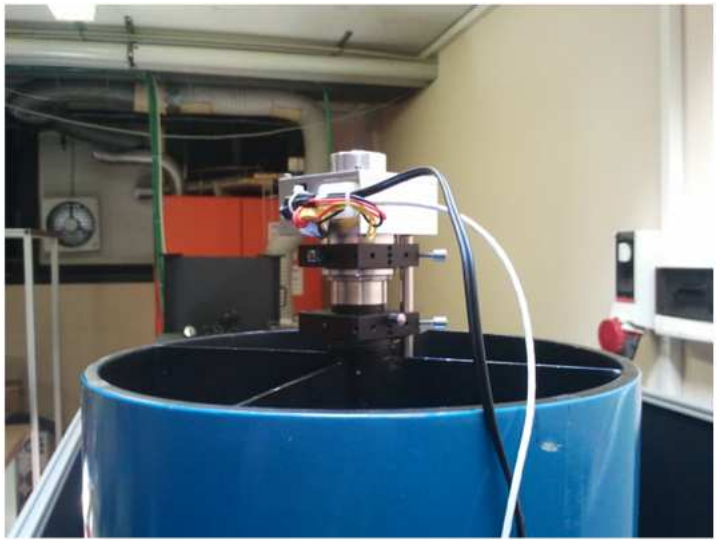

Figure 62. The AQ receiving telescope and the CCD camera mounted on it for the alignment check.

The expected optical image of the laser beam in the atmosphere was simulated using Zemax© optical software (Figure 63), it has been taken in account the relative position of the laser beam and receiving telescope, the laser beam divergence, the geometry and quality of the telescope mirror (parabolic), and the collecting area (a circle of about 5mm in diameter) were the optical fiber that transport the LIDAR returns to the receiver box (a combination of dichroic beam splitters, interference filters) containing the detectors (photomultipliers) is positioned with its collecting lens. This image is reported in Figure 63, it should be noted that, according to the design, the AQ telescope, perfectly aligned, can collect LIDAR returns, i.e. the full laser beam image impinges on the collecting area) without any optical modulation (overlap function) from above 250m range.

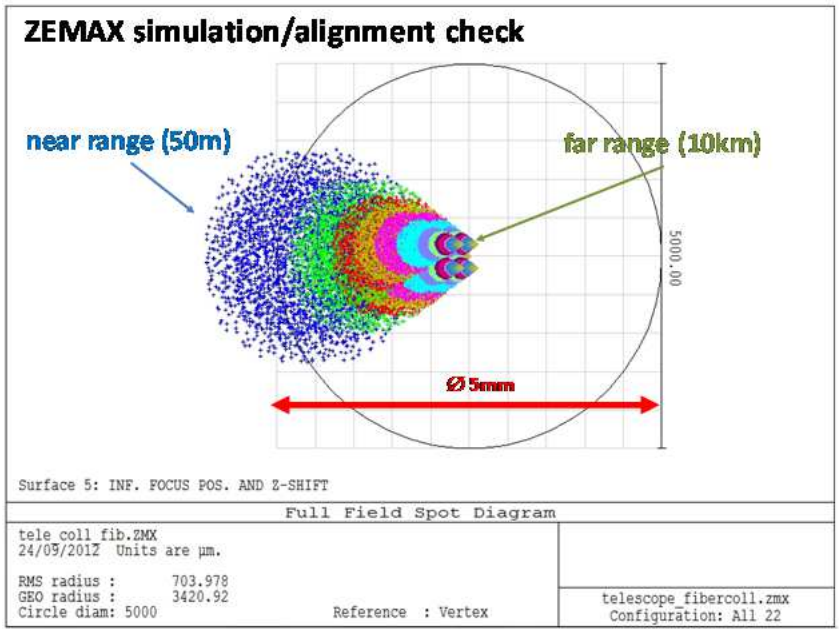

Figure 63. The results of the Zemax© simulation of the laser beam images returned from different distances in the focus position of the AQ receiving telescope. The different colors refer to laser beam images from different altitudes (from 50m to 10km).

The laser beam images observed with the CCD are shown in Figure 64, it is quite evident that the AQ receiving telescope is well aligned, and the image dimensions are as expected.

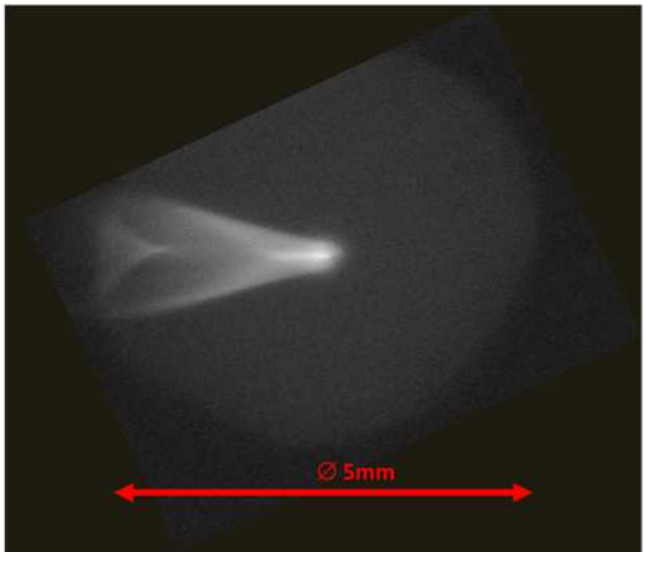

Figure 64. The laser beam image in the focus position of AQ telescope as captured by the CCD camera.

On the other hand, after the alignment check, the measurements carried in 15/09 show better coincidences between β_a and α_a profiles, see Figure 61. The aerosol backscatter and extinction coefficients are coincident, within the error bars (not shown in the Figures) from above 0.5km and 0.7km, respectively.

In summary the "messages to be taken home" are:

- the alignment procedures of a single LIDAR system can be improved within this kind of inter-comparisons;
- the POLIS LIDAR system acting as the "reference LIDAR" can also offer other tools for checking the hardware performances of the other systems (i.e., plug and play CCD camera).
- the β_a and α_a profiles obtained by the two independent LIDAR systems involved in AQUILI2012 are coincident within ± 10%, at least, after a careful check of the alignment and of the hardware performances.

2.3.6 Implementation of the optical products retrieval in the centralized calculus system

In addition, the automated and centralized calculus system was implemented and used in order to obtain and compare not only the pre-processed lidar range corrected signals, but only the optical products (aerosol and extinction backscatter coefficient) from the data measured during the several intercomparison campaigns.

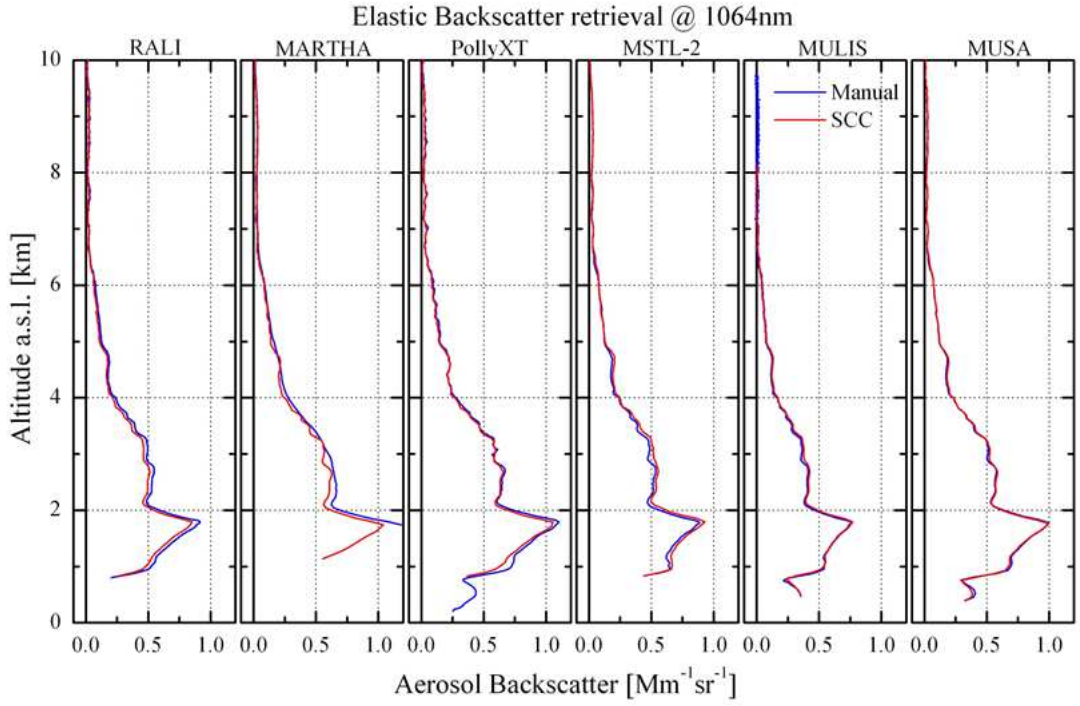

Figure 65. Example of retrieval of aerosol backscatter coefficient at 1064 nm, using the Single Calculus Chain developed within EARLINET on the data measured by several lidar systems during EARLI09.

Figure 65**¡Error! No se encuentra el origen de la referencia.** shows an example of retrieval of aerosol backscatter coefficient at 1064 nm, while Figure 66 shows an example of retrieval of aerosol extinction coefficient at 355 nm, both obtained using data from intercomparison campaign EARLI09 held in Leipzig on May 2009, but the retrieval will be extended to the data of all the intercomparison measurement campaigns.

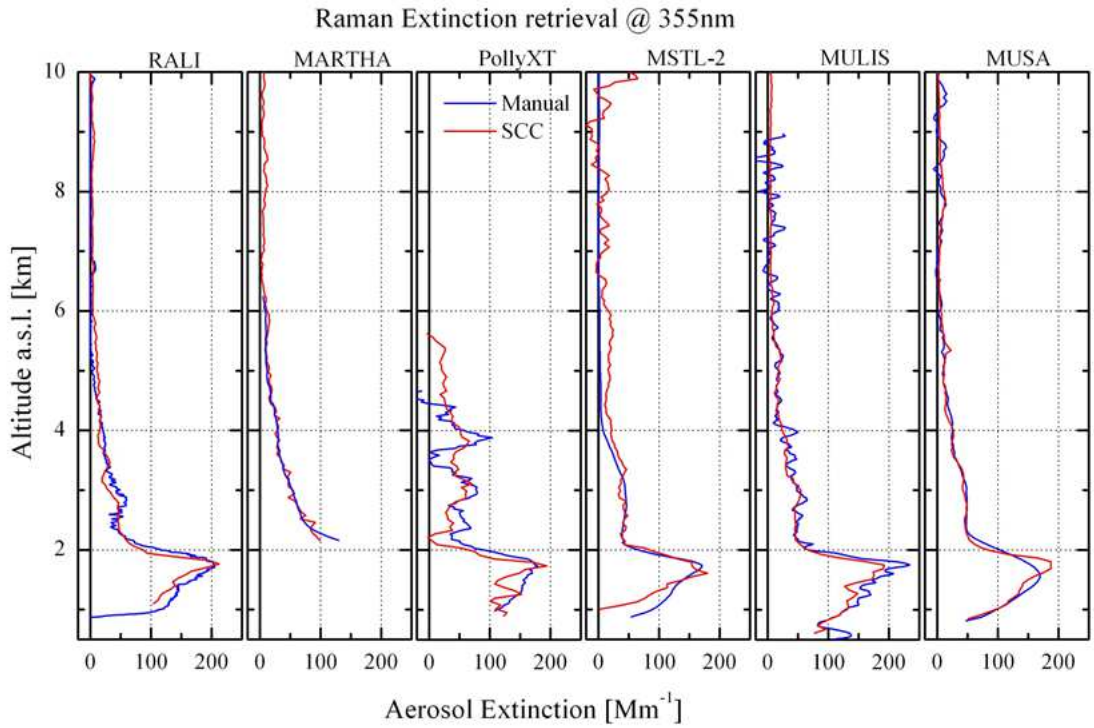

Figure 66. Example of retrieval of aerosol backscatter extinction at 355 nm, using the Single Calculus Chain developed within EARLINET on the data measured by several lidar systems during EARLI09.

3 Conclusions of the CEOS ICal project and outlook

3.1 Dobson calibrations

Seven ESA funded campaigns and four regular RDCC-E intercomparisons (DWD funding) have been carried out since 2009. The locations of these campaigns represent a wide range of atmospheric conditions, which allows the characterization of the properties of the Dobson instrument and their differences to the Brewer spectrophotometer.

The location from North to South:

Sodankylä:	Low altitude with normal turbidity, large SZA and high ozone
Hradec Kralove:	Low altitude with enhanced turbidity, entire range of SZA and “normal” ozone
MOHp:	High altitude with reduced turbidity, entire range of SZA and “normal” ozone
Arosa:	Very high altitude with low turbidity, entire range of SZA and “normal” ozone
El Arenosillo:	Low altitude with normal turbidity, entire range of SZA and somewhat lower ozone
Izaña:	Very high altitude and very low turbidity, entire range of SZA, lower and constant ozone
Irene:	High altitude, southern hemisphere, moderate turbidity, entire range of SZA, less ozone

The general finding is that the standard Dobson with its current calibration level (traced back to the World Primary Standard D083) measures about 1% lower ozone than the standard Brewer. Larger differences at low sun, high ozone and high turbidity can be predominantly explained by the various temperature dependencies of the instrumentally specific absorption coefficients (Kerr, 2002), different calculation of μ using different heights of the ozone layer and different straylight sensitivity. The effects of the first two reasons can easily be corrected in a general manner, whereas the third issue needs some intense investigation of the properties of each specific instrument.

A very important, special finding is that Izaña is an appropriate location for the performance of absolute calibration of both types of spectrophotometers using the Langley Plot method. The obtained results are comparable with the Mauna Loa calibrations of the World Primary Standard D083.

The preparation of two publications is considered:

- Comparison of Standard Dobsons and Brewers (RDCC-E and RBCC-E) and explanation of the principal differences, progress depending on new absorption coefficients.
- Suitability of the Izaña facility for Dobson Langley campaigns in comparison with Mauna Loa results (RDCC-E, WDCC and RBCC-E).

These results in principle confirm the capability and qualification of the Dobson spectrophotometer to produce high quality ozone data sets. These data sets are appropriate for reliable analyses of the status of the ozone layer and its trend as well as for Cal/Val activities related to satellite-borne ozone measuring instruments.

Unfortunately the intended transition from the Bass-Paur ozone cross sections/absorption coefficients to a newer, better and hopefully more consistent data set (originally proposed were Daumont-Brion-Malicet DBM cross sections) was not carried out yet. New findings of the RBCC-E (Alberto Redondas) led to the conclusion to shift this introduction until further investigations were finished, which data set of cross sections provides better and more consistent absorption coefficients for all types of instruments in use to monitor the ozone layer. After the successful introduction of new coefficients all comparisons between Dobson and Brewer have to be reprocessed either to confirm the old results or to find out new features. The application of

improvements in the algorithms (e.g. temperature corrections) does not make sense, before the introduction of the new coefficients is completed.

In addition cuts of budgets, staff reductions and recently/future retirements of experts endanger both the global ozone monitoring network and the Dobson calibration system. One focus of the future activities in the ozone community should be to maintain the function of the global networks of ozone monitoring and of instruments' service and calibration. The concentration and focus on potential super sites to enable the optimal use of the available resources should be discussed.

3.2 Brewer calibrations

During the project seven Brewer calibration campaigns were organized and 65 calibrations were performed to 40 instruments. Three types of campaigns were conducted:

- Absolute calibration campaigns at Izaña focusing on the calibration check of reference Brewer and Dobson through Langley method.
- Nordic calibration campaigns focusing on the study of the stray light effect at high ozone and zenith angle conditions
- Routine calibration campaigns at Arosa and Huelva with the main objective to transfer the calibration of the regional Center to the network instruments.

In these campaigns the calibration scale has been transferred from the RBCC-E triad at Izaña Atmospheric Research Centre to the participants. A significant improvement on the reference triad characterization and maintenance has been obtained including the development of operational procedures and the public diffusion of the status of the reference. We can estimate a long-term precision of 0.25% for the European Reference Triad. The observations from all campaigns have been submitted to the CEOS Cal-Val Database.

In cooperation with Tom McElroy and Volodya Savastiouk a calibration checklist was developed with the objective to describe the Brewer calibration for operators, data users and database managers. These reports are publicly available and they were distributed during the calibration campaigns.

The status of the network as revealed during the calibration campaigns is that all of the operative instruments are on the +/-2% range, 80% of the Brewer instruments are inside 1% range and 2/3 shows a perfect agreement of +/- 0.5% after two years calibration period. The reference instruments, i.e. the Brewers that are used to transfer calibration, show an agreement around 0.5%.

A significant improvement has been brought to the instrument characterization and calibration. This includes studies of the filter attenuation issue, ozone absorption coefficient and stray light.

Attenuation filter
The Brewer uses attenuation filters to adapt the light intensity. The Brewer algorithm assumes "neutral filter" but in real instruments this is not true and can produce an error up to 2% (20% in one extreme case) on the recorded ozone. A methodology for detecting, characterizing and correcting the attenuation filter response has been developed.

Ozone absorption coefficients
The calibration of the Brewer determines two constants: the Extraterrestrial constant (ETC) and the ozone absorption coefficient (O3ABS). The ETC is transferred for the reference instrument and the O3ABS can be calculated from the dispersion test (one parameter calibration) or transferred from a reference instrument (two parameter calibration). The recommended method is the one-parameter calibration but a significant number of

instruments use the two-parameter calibration. A mismatch of the O3Abs produces a slope on the relative differences as function of slant path; this slope can compensate nonlinearities of the instruments like the filter attenuation. We found that both methods will give the same results, within the precision of the Brewer instrument. The comparison of both calibration methods can give us an indication of the quality of the instrument. Based on that we can divide the Brewer instruments in two classes:

Class I instrument where the calculated and transferred O3ABS are within the wavelength precision of the instrument, and Class II where they are outside:
Class I: ETC (+/- 5 units 0.4% , o3abs +/- 1 step 0.3%)
Class II : ETC (+/- 10 units 0.8%, o3abs +/- 2 step 0.6%)

Stray light
During the calibration campaigns, measurements of the slit function have been performed and these data have been used to model the Stray Light determination. In particular the FMI Brewers were characterized during the Nordic campaign and the counterpart Izaña campaign. The model detects the underestimation of the ozone but the reconstructed DS response for the ozone slits used for the model Brewer Stray Light are likely to differ from the real ones. In the continuation project the real DS responses for the ozone slits has to be measured. The stray light can also be introduced in the calibration against a double spectrometer, and an empirical correction has been developed and the parameters of the correction are determined on the calibration procedure.

Evaluation of the differences Brewer/Dobson
The comparisons of Brewer from RBCC-E and Dobson 64 from RDCC-E shows an disagreement of about 1.5% in the different common calibrations performed during the project. Two Langley campaigns were performed at Izaña, during which the Langley methodology has been evaluated. We found that if we apply it there is no significant change if we use the Dobson methodology on the Brewer. On the other hand the spread of the results on both instruments is related which can be due to the atmospheric variability and is not necessarily to instrument performance.

Ozone cross-sections
As a part of this study, four different ozone cross sections were evaluated for use with Dobson and Brewer instruments. These are the Bass & Paur “operative” cross sections used by Brewer and Dobson, the quadratic adjustment of Bass & Paur (IGACOQ4), the high resolution cross section of Daumont, Brion & Malicet (DBM), (Daumont et al., 1992), (Brion et al., 1993), (Malicet et al., 1995) and the cross-section data set recently developed by the university of Bremen (IUP, Serdyuchenko et al., 2011, 2012). Whereas on the case of the Dobson the calculated ozone change is of +1% with very little variation depending on which dataset is used on the case of the Brewer the changes are substantial in the case of DMB (-3.2%) and less important for IUP (-0.5%).

Applying this ozone cross section to the Brewer-Dobson dataset from the Langley campaigns, we found that the use of the IGACOQ4 cross sections does not change the Brewer Dobson comparison but slightly increases the Dobson CD/AD double pair difference. The DBM increases the difference between the instruments from 1.5 % for the operative algorithm to 2% and 3% on the case of CD pair and AD pairs respectively. Finally the UIP reduces significantly the difference between Dobson and Brewer, the difference between AD/CD pair is the same as the operative set. For the Izaña dataset, the use of IUP makes the ozone measurements from different instruments indistinguishable.

3.3 UV-Vis MAXDOAS intercomparisons

The CINDI campaign has been very successful in achieving its observational and scientific objectives. A large data set of continuous ground-based in-situ and remote sensing observations of nitrogen dioxide, aerosols and

other air pollution constituents has been collected under various meteorological conditions and under various air pollution loadings. The day-to-day variability of NO_2 for sunny days (nine days had at least 10 sunny hours) was mostly driven by wind direction, with cleaner air coming from northerly directions. The CINDI campaign also experienced periods of enhanced HCHO with warm winds coming over land. Detailed comparisons (still ongoing for some of them) performed with the CINDI data have shown that:

- MAX-DOAS slant column measurements of NO_2 and O_4 agree within 5–10% (Roscoe et al., 2010);
- MAX-DOAS slant column measurements for HCHO agree within 15% (Pinardi et al., 2012);
- tropospheric columns and surface values of NO_2 from MAX-DOAS NO_2 profile retrievals agree within 15% between different instruments, and within 25% with the NO_2 lidar data and in-situ NO_2 data obtained at different altitudes, except for the situation of very shallow boundary layers, where the MAX-DOAS algorithms underestimate the NO_2 values by up to 50% (Wittrock et al., to be submitted to AMT);
- MAX-DOAS aerosol optical depth are in good agreement with the AERONET measurements and aerosol extinction profiles are in good qualitative agreement with ceilometer data (Frieß et al., to be submitted to AMT),
- MAX-DOAS aerosol extinction values are generally well correlated with in-situ values at the surface, but a factor 1.5 to 3.4 larger (Zieger et al., 2011).
- MAX-DOAS data demonstrate a good potential to derive at least 8 independent atmospheric parameters, including NO_2, HCHO, glyoxal, SO_2, O_3, water vapour and aerosol at two wavelengths (Irie et al., 2011).

Other studies that are still being performed include the comparisons of tropospheric NO_2 columns from mobile DOAS systems (Merlaud et al., in progress) and from direct-sun, zenith-sky and MAXDOAS systems (Spinei et al., in progress), HCHO profiles, BrO slant columns (Puentedura et al., in progress) the spatial variability of NO_2 (Piters et al.), and the application to satellite data validation. The studies performed during the CINDI campaign have resulted in increased knowledge about the performance of ground-based remote sensing instruments regarding the accuracy with which NO_2 and aerosol information in terms of vertical profiles and tropospheric/total columns can be derived. The CINDI intercomparison results provided the necessary first steps towards harmonization of retrieval settings and observation methods, and in recommendations for building the networks of ground-based systems urgently needed for satellite data validation. Such efforts need to and will be further pursued in future projects and activities, among them the planned extension of this CEOS ICal project but also the already ongoing EU FP7 NORS project.

3.4 EARLINET intercomparisons

EARLINET, the European Aerosol Research Lidar NETwork, established in 2000, is the first coordinated lidar network for tropospheric aerosol study on the continental scale. The network activity is based on scheduled measurements, a rigorous quality assurance program addressing both instruments and evaluation algorithms, and a standardised data exchange format. At present, the network includes 27 lidar stations distributed over Europe.

The intercomparison program is of fundamental importance in order to assure the quality of the data provided, also in view of future ESA calibration/validation programs in the frame of satellite missions with onboard lidar systems. The intercomparison program is part of a wider strategy addressed to intercompare the systems at all levels: not only at instrument level, but also at algorithm level. It has been carried out during the FP6 EARLINET-ASOS and the FP7 ACTRIS projects. At present, EARLINET it is funded by the FP7 infrastructure project ACTRIS (1 April 2011 – 31 March 2015) that will support just partially the future intercomparison campaigns.

The strategy includes several steps:

a) development of instrumental standard tools for internal quality check of the performance of the instruments;
b) definition of standards (deviations, signal to noise, maximum and minimum range) to accept a system in terms of performances suitable for EARLINET QA data;
c) development of a common data pre-processing and processing calculus system (Single Calculus Chain) suitable for all the lidar systems, able to fast pre-process and process data and to fast reduce the data at the same resolution;
d) definition of the mobile reference lidar systems within EARLINET;
e) on site intercomparison of the lidar reference systems;
f) on site intercomparison of all the EARLINET lidar systems with the lidar reference systems.

Six intercomparison measurement campaigns were carried out in between 2009 and 2012:

1) EARLI09 (EArlinet Reference Lidar Intercomparison campaign, Leipzig, 5 May to 5 June 2009),
2) ALI09 (Alomar Lidar Intercomparison campaign, Alomar, Norway, 21 October to 5 November 2009),
3) SOLI10 (SOfia Lidar Intercomparison campaign, Sofia, Bulgaria, 9 to 14 October 2010),
4) ROLI10 (ROmanian Lidar Intercomparison campaign, Bucharest, Romania, 17 to 23 October 2010),
5) SPALI10 (SPAin Lidar Intercomparison campaign, Madrid, Spain, 18 October to 5 November 2010) and
6) AQUILI12 ((AQUIla Lidar Intercomparison campaign, L'Aquila, Italy, 10 – 15 September 2012).

The first measurement campaign (EARLI09) was addressed mainly to the intercomparison among the five reference lidar systems from Hamburg, Munich, Potenza and Minsk, but further six EARLINET stations joined the measurement campaign. It was sufficiently long to allow a good comparison among the reference lidar systems. This campaign was important also because it allowed to fix the standard procedure to carry out the instruments intercomparison.

The following intercomparison measurement campaigns allowed to check the performances of the systems and when they were not fully satisfactory, the reasons of the failure were understood and the way to solve them were defined.

All the Quality Assurance tests have been applied during the measurement campaigns for each single lidar instrument and have been used in order to solve specific problems before the actual intercomparison. The comparison has been carried out through the comparison of the range corrected raw lidar signals by pre-processing the raw data in an uniform way through an analysis tool developed in the frame of EARLINET (the Single Calculus Chain). The capability of this tool has been extended implementing the retrieval of optical products (vertical profiles backscatter and extinction coefficients). In fact, at present it is in progress the last part of the comparison protocol that is addressed to the comparison of the optical products.

All the measurement campaigns can be considered successfully accomplished. Technical problems, responsible of discrepancies, were individuated and solved. The intercomparison campaigns allowed to compare 21 lidar systems (18 from EARLINET).

- Concerning EARLI09 campaign, performed mainly among the reference systems, the deviations of the range corrected lidar signals respect to the average signal were, for all the systems, within 10% from the full overlap height up to at least 10km of height, an important result for the study of PBL and low troposphere.
- Concerning the other measurement campaigns, all the measurements from the involved lidar systems showed a deviation within 10% respect to the corresponding lidar reference system, from the full overlap height to the up to at least 10km of height.

The intercomparison of Lecce and Napoli systems (Italy), planned in 2012, have been moved to spring 2013 because of systems failure. The Lecce system was interested by a serious loss of energy, while the Napoli

system was affected by electronic break down and stopped to run. Both systems were not in conditions suitable to perform measurement campaigns and were shipped for repairing.

In the next two years, campaigns are planned for the remaining EARLINET systems (Clermont-Ferrand, Palaiseau, Neuchatel, Payerne, Gebze, Cork, Linköping, Belsk, Thessaloniki, Athens) and in the next future for the instruments of new EARLINET stations.

Concerning publications in journal papers, an EARLINET special issue on AMT is open, where the results of the intercomparison campaigns will be presented in an EARLINET joint paper.

EARLINET provides long-term, quality-assured aerosol data on a continental scale and thus offers a unique opportunity for the validation and full exploitation of the spaceborne missions. Because of its geographical distribution over Europe, EARLINET allows us to investigate a large variety of different aerosol situations with respect to layering, aerosol type, mixing state, and properties in the free troposphere and the local planetary boundary layer. With a network on a continental scale it is not only possible to directly validate space-borne backscatter, extinction, and depolarization-ratio profiles, but also to study the representativeness of the limited number of satellite lidar cross sections along an orbit against long term network observations. In this context, the quality assurance program of EARLINET play a crucial role in the measurement strategy of EARLINET.

The intercomparison campaigns allowed to fix standards for data, in terms of standard deviation respect to reference lidar signals and products, and to define and assess methodological procedures for intercomparison. The intercomparison activity will be prosecuted because it is fundamental to guarantee the data quality of the network, especially for the EARLINET systems not yet intercompared or that will receive important upgrades, and for new systems that are joining the network.

These intercomparison measurement campaigns were possible thanks to the fundamental financial support from ESA, because the funds from the EARLINET-ASOS project, and from ACTRIS project after the end of the EARLINET-ASOS project, were not sufficient to cover all the expenses. Therefore, the prosecution of the intercomparison activity will depend on the availability of funds in the next future.

4 References

Brion, J., A. Chakir, D. Daumont, J. Malicet, C. Parisse, High-resolution laboratory absorption cross section of O3: Temperature effect, Chem. Phys. Lett., 213, 610-612, 1993.

Clémer, K., Van Roozendael, M., Fayt, C., Hendrick, F., Hermans, C., Pinardi, G., Spurr, R., Wang, P., and De Mazière, M.: Multiple wavelength retrieval of tropospheric aerosol optical properties from MAXDOAS measurements in Beijing, Atmos. Meas. Tech., 3, doi:10.5194/amt-3-863-2010, 2010.

Daumont, M., Brion, J., Charbonnier, J., and Malicet, J.: Ozone UV spectroscopy, I: Absorption cross-sections at room temperature, J. Atmos. Chem., 15, 145–155, 1992.

Hermans, C., A.C. Vandaele, S. Fally, M. Carleer, R. Colin, B. Coquart, A. Jenouvrier, M.-F. Mérienne: Absorption cross-section of the collision-induced bands of oxygen from the UV to the NIR, in: Proceedings of the NATO Advanced Research Workshop, Weakly Interacting Molecular Pairs: Unconventional Absorbers of Radiation in the Atmosphere, Fontevraud, France, 24 April-2May 2002, eds C. Camy-Peyret and A.A. Vigasin, Kluwer Academic Publishers, Boston, NATO Science Series IV Earth and Environmental Sciences, vol 27, pp 193-202, 2003.

Greenblatt, G. D., J. J. Orlando, J. B. Burkholder, and A. R. Ravishankara: Absorption measurements of oxygen between 330 and 1140 nm, J. Geophys. Res., 95, 18,577–18,582, 1990.

Hendrick, F., Van Roozendael, M., Kylling, A., Petritoli, A., Rozanov, A., Sanghavi, S., Schofield, R., von Friedeburg, C., Wagner, T.,Wittrock, F., Fonteyn, D., and De Mazière, M.: Intercomparison exercise between different radiative transfer models used for the interpretation of ground-based zenith-sky and multiaxis DOAS observations, Atmos. Chem. Phys., 6, 93–108, http://www.atmos-chem-phys.net/6/93/2006/, 2006.

Hönninger, G., von Friedeburg, C., and Platt, U.: Multi axis differential optical absorption spectroscopy (MAX-DOAS), Atmos. Chem. Phys., 4, 231–254, doi:10.5194/acp-4-231-2004, 2004.

Ibrahim, O., Shaiganfar, R., Sinreich, R., Stein, T., Platt, U., and Wagner, T.: Car MAX-DOAS measurements around entire cities: quantification of NOx emissions from the cities of Mannheim and Ludwigshafen (Germany), Atmos. Meas. Tech., 3, 709721, doi:10.5194/amt-3-709-2010, 2010.

Irie, H., Takashima, H., Kanaya, Y., Boersma, K. F., Gast, L., Wittrock, F., Brunner, D., Zhou, Y., and Van Roozendael, M.: Eight-component retrievals from ground-based MAX-DOAS observations, Atmos. Meas. Tech.., 4, 1027-1044 doi:10.5194/amt-4-1027-2011, 2011.

Karppinen T., Redondas, A., Garcia, R.D., Lakkala, K., McElroy C.T. and Kyrö, E.: Correcting Stray Light in single-monochromator Brewer spectrophotometers, Manuscript submitted for publication, 2012.

Kerr, J. B., C. T. McElroy, and R. A. Olafson.: Measurements of ozone with the brewer ozone spectrophotometer. Quadrennial International Ozone Symposium, Boulder, CO; International Organization; 4-9 Aug.1980: 74-79, 1981.

Kerr, J.B.: Mew methodology for deriving total ozone and other atmospheric variables from Brewer spectrophotomer direct sun spectra, J. Geophys. Res., 107, No. D23, 4731, 10.1029/2001JD001227, 2002.

Köhler, U., Evans, R., Miyagawa, K., Easson, J., Coetzee, G., Sanchez, R., Vanicek, K. and Stanek, M.: Global Dobson Calibration System – Basic requirement for high quality monitoring of the ozone layer, Poster for the XXII Quadrennial Ozone Symposium, Toronto, 2012a.

Köhler, U., Redondas, A., Kyrö, E.: Regional Calibration Centers for Dobson and Brewer in Europe – A joint venture for highest quality in monitoring the ozone layer, Poster for the XXII Quadrennial Ozone Symposium, Toronto, 2012b.

Malicet, J., Daumont, D., Charbonnier, J., Parisse, C., Chakir, A., and Brion, J.: Ozone UV spectroscopy. II. Absorption crosssections and temperature dependence, J. Atmos. Chem., 21, 263–273, 1995.

Pinardi, G., M. Van Roozendael, N. Abuhassan, C. Adams, A. Cede, K. Clémer, C. Fayt, U. Frieß, M. Gil, J. Herman, C. Hermans, F. Hendrick, H. Irie, A. Merlaud, M. Navarro Comas, E. Peters, A. J. M. Piters, O. Puentedura, A. Richter, A. Schönhardt, R. Shaiganfar, E. Spinei, K. Strong, H. Takashima, M. Vrekoussis, T. Wagner, F. Wittrock, and S. Yilmaz, MAXDOAS formaldehyde slant column measurements during CINDI: intercomparison and analysis improvement, Atmos. Meas. Tech. Discuss., 5, 6679-6732, 2012.

Roscoe, H.K, M. Van Roozendael, C. Fayt, A. du Piesanie, N. Abuhassan, C. Adams, M. Akrami, A. Cede, J. Chong, K. Clemer, U. Friess, M. Gil Ojeda, F. Goutail, R. Graves, A. Griesfeller, K. Grossmann, G. Hemerijckx, F. Hendrick, J. Herman, C. Hermans, H. Irie, P.V. Johnston, Y. Kanaya, K. Kreher, R. Leigh, A. Merlaud, G.H. Mount, M. Navarro, H. Oetjen, A. Pazmino, M. Perez-Camacho, E. Peters, G. Pinardi, O. Puentedura, A. Richter, A. Schoenhardt, R. Shaiganfar, E. Spinei, K. Strong, H. Takashima, T. Vlemmix, M. Vrekoussis, T. Wagner, F. Wittrock, M. Yela, S. Yilmaz, F. Boersma, J. Hains, M. Kroon, A. Piters, Y.J. Kim: Intercomparison of slant column measurements of NO_2 and O_4 by MaxDOAS and zenith-sky UV and visible spectrometers, Atm. Meas. Tech. 3, 1629-1646, 2010.

Serdyuchenko, A., V. Gorshelev, M. Weber, W. Chehade and J. P. Burrows, New broadband high-resolution ozone absorption cross-sections, Spectroscopy Europe, 23(6), 14, 2011.

Serdyuchenko, A., V. Gorshelev, M. Weber, W. Chehade and J. P. Burrows, High spectral resolution ozone absorption cross-sections: Part II. Temperature dependence, JQSRT, 2012.

Shaiganfar, R., Beirle, S., Sharma, M., Chauhan, A., Singh, R. P., and Wagner, T.: Estimation of NOx emissions from Delhi using Car MAXDOAS observations and comparison with OMI satellite data, Atmos. Chem. Phys., 11, doi:10.5194/acp-11-10871-2011, 2011.

Vogel, L., Sihler, H., Lampel, J., Wagner, T., and U. Platt, Retrieval interval mapping, a tool to optimize the spectral retrieval range in differential optical absorption spectroscopy, Atmos. Meas. Tech. Discuss., 5, 4195-4247, 2012.

Wagner, T., Ibrahim, O., Shaiganfar, R., and Platt, U.: Mobile MAXDOAS observations of tropospheric trace gases, Atmos. Meas. Tech., 3, 2010.